

SPARC

— Secure Pathways —
for Resilient Communications



7-8 GHz Point-to-Point Testing

October 2024

7-8 GHz Point-to-Point Testing

October 2024

This work was conducted by the Idaho National Laboratory (INL) for the Department of Energy (DOE) Office of Electricity (OE) Secure Pathways for Resilient Communications (SPaRC) program.



OE Project Sponsor:	David Wells
INL Project Lead:	Robert Comstock
INL Project Co-Lead:	David Wallis
INL Technical Advisor:	Nicholas Kaminski
INL Lead Engineer:	Azim Muqtadir
INL Relationship Manager:	Brad Nelson

INL is a U.S. Department of Energy National Laboratory operated by Battelle Energy Alliance, LLC.

Contents

Executive Summary	6
1 Introduction	8
1.1 Key Takeaways	8
1.2 Project Motivation	8
1.3 Overview	9
1.4 Testing Context	10
1.5 Testing Concept	10
1.6 Testing Structure	12
1.6.1 Simulation Studies	12
1.6.2 Open-Range Testing	12
2 Test Items and Equipment	13
2.1 P2P Link	13
2.1.1 P2P Equipment	13
2.1.2 P2P Link Parameters	13
2.1.3 P2P Operational Paradigms	14
2.2 Interference Waveforms	15
2.2.1 Interference Types	16
2.2.2 Equipment	18
2.2.3 Interference Generation Method	19
2.2.4 Interference Parameters	20
2.2.5 Interference Power Levels	20
2.3 Spectrum Monitoring	21
2.3.1 Spectrum Monitoring Equipment	21
2.3.2 Spectrum Monitoring Parameters	21
2.4 Locations	22
2.4.1 Filmore Location	22
2.4.2 Haul Location	22
2.4.3 Interferer Location 1	23
2.4.4 Interferer Location 2	23
2.4.5 Interferer Location 3	23
2.4.6 Interferer Location 4	23
3 Simulation Study for Site Selection	25
3.1 Tools Used	25
3.2 Methodology	25
3.2.1 Overall Approach	25
3.2.2 Identifying Candidate Locations	26
3.2.3 Determining P2P Endpoints	26
3.2.4 Determining Interferer Locations	27
3.2.5 Simulating Propagation Paths	27
3.3 Results	28

3.3.1	Candidate Locations	28
3.3.2	P2P Locations	30
3.3.3	Interferer Locations	34
3.4	Conclusions	40
4	Simulation Study for Parameter Selection	41
4.1	Tools Used	41
4.2	Methodology	41
4.2.1	Overall Approach	41
4.2.2	P2P Modeling	42
4.2.3	Interferer Modeling	43
4.3	Results	45
4.3.1	P2P Results	45
4.3.2	Interferer Results	46
4.4	Conclusions	50
5	Initial Testing of Components	51
5.1	Tools Used	51
5.2	Locations	51
5.2.1	Transmit	51
5.2.2	Receive	52
5.2.3	Path Parameters	52
5.3	Supporting Analysis	52
5.3.1	Defining P2P Power Levels	52
5.3.2	Defining Interferer Power Levels	55
5.4	Methodology	55
5.4.1	Overall Approach	56
5.4.2	Data Examined	56
5.4.3	Phase 1: Examination of Received Power Level	57
5.4.4	Phase 2: Evaluation of P2P Link	58
5.4.5	Phase 3: Exploration of Interference	58
5.5	Results	59
5.5.1	Phase 1: Examination of Received Power Level	59
5.5.2	Phase 2: Evaluation of P2P Link	59
5.5.3	Phase 3: Exploration of Interference	59
5.6	Conclusions	59
6	Open-Range Testing	60
6.1	Tools Used	60
6.2	Methodology	60
6.2.1	Overall Approach	60
6.2.2	Data Examined	60
6.2.3	Test Sequence	62
6.2.4	Test Sets	63
6.2.5	Test Cases	64
6.2.6	Power Ratio Analysis	64
6.3	Results	67
6.3.1	Baseline Results	67
6.3.2	Interference Thresholds	71
6.3.3	Interferer Locations	74
6.3.4	Unexpected Results	79
6.4	Conclusions	81

7	Simulation to Interpolate Results	82
7.1	Tools Used	82
7.2	Methodology	82
7.2.1	Modeling Impactful Locations	82
7.2.2	Selecting Received Interference Thresholds	83
7.3	Results	83
7.3.1	Low-Rate Paradigm	83
7.3.2	Mid-Rate Paradigm	85
7.3.3	High-Rate Paradigm	88
7.4	Conclusions	90
8	Discussion of Results	91
8.1	Summary of Results	91
8.2	Technical Limitations	92
8.3	Major Trends	93
8.4	Lessons Learned	94
9	Conclusions	95
9.1	Project Goals	95
9.2	Operational Considerations	95
9.3	Operational Implications	96
9.4	Next Steps	97
A	References	98
B	Mathematical Notation	99
C	Procedures	100
C.1	Data Collection	100
C.1.1	Sequences	100
C.1.2	Scripts	104

Executive Summary

Wireless spectrum is a limiting resource for continued economic growth in the United States. As discussed in the recent National Spectrum Strategy (NSS), wireless spectrum underpins several aspects of the U.S. economy and the demand for additional spectrum is driving the need for realizing spectrum sharing to enable continued development. At the same time, wireless spectrum is an essential foundation of critical energy infrastructure, including electric, oil, and natural gas resources. In particular, wireless point-to-point (P2P) links (a.k.a microwave links) are the backbone of vast infrastructure networks that enable the flow of sensor and control information needed to manage critical energy sector infrastructure in the United States. These links will only become more important as the energy sector incorporates more diverse sensing and more efficient control mechanisms, which increases system complexity and data volume requiring more resilient communications. Therefore, the continued economic development of the U.S. depends on determining novel approaches to spectrum management that balance both broad access for advanced wireless technologies and resilience for critical infrastructure.

Here, we support balancing the competing needs outlined above by providing scientifically grounded data on potential interference to critical energy sector P2P links in a co-mingled sharing scenario. We focus on over-the-air testing of commercial off-the-shelf transmitting equipment to ensure that our project captures the large variety of factors that influence the impact of interference in real-world settings. First and foremost, our efforts demonstrate that co-mingled spectrum sharing generates interference that renders critical P2P links inoperable when the approach to sharing prioritizes broad access to spectrum. Secondly, we note that simulation based examinations of interference are prone to errors leading to either under estimation or over estimation of interference impacts. Thus, simulation centric approaches are limited in their ability to balance protection of critical links against utilization of potential spectrum. Finally, our results show that effective management of spectrum sharing must extend beyond reported interference events. The identification and attribution of interference is impractical for two major reasons: (1) the large variety of environmental, geographical, and electromagnetic factors that influence communications performance and (2) limitations of metrics in commercially available equipment to monitor links. This study examines commercial off-the-shelf P2P equipment to identify potential issues in co-mingled spectrum sharing that goes beyond limitations in simulation and improves the identification of interference.

This project is an exploratory examination of co-mingled spectrum sharing in the 7 GHz band (7125 - 8400 MHz) and the potentially associated interference. This work is largely inspired by the recent opening of the 6 GHz band (5925 - 7125 MHz) to unlicensed, co-mingled sharing. In the case of the 6 GHz band, the Federal Communications Commission (FCC) primarily considers simulation centric approaches to understand potential interference which generally minimize the concerns of the critical infrastructure community.^{1 2} We believe that an approach that validates simulation with over-the-air testing provides a holistic picture of the nuances of spectrum sharing. This builds a solid foundation for policy makers to represent the needs of all spectrum stakeholders. Therefore, we focus on open-range, over-the-air testing as the central component of our data collection. This allows us to characterize the conditions necessary for representative interferers to impact critical energy sector P2P links. We transparently describe our approach, our results including data, and the conclusions that we draw in our main report. Together, this work is intended as a foundation to facilitate policy makers taking a data driven approach to designing spectrum sharing strategies in the 7 GHz band that extracts maximum utility from the spectrum while continuing to support the resilient operation of critical energy sector infrastructure.

¹ *FCC 20-51: Report and Order and Further Notice of Proposed Rulemaking.* Tech. rep. Federal Communication Commission, 2020.

² *FCC CIRC2310-04: Second Report and Order, Second Further Notice of Proposed Rulemaking, and Memorandum Opinion and Order on Remand.* Tech. rep. Federal Communication Commission, 2023.

Acronyms

AWGN	additive white Gaussian noise
BER	bit error rate
CBRS	Citizens Broadband Radio Service
CW	continuous wave
DER	distributed energy resource
DOE	Department of Energy
DOE-OE	Department of Energy, Office of Electricity
EIRP	effective isotropic radiated power
FCC	Federal Communications Commission
GPS	global positioning system
IMOM	Improved Many-on-Many
INL	Idaho National Laboratory
ISR	interference to signal ratio
NSS	National Spectrum Strategy
NTIA	National Telecommunications and Information Administration
OE	Office of Electricity
P2P	point-to-point
PAPR	peak to average power ratio
PMA	Power Marketing Administration
PoE	power over Ethernet
RF	radio frequency
RPE	radiation pattern envelope
RSL	received signal level
SCADA	supervisory control and data acquisition
SDR	software defined radio
SNR	signal to noise ratio
SPaRC	Secure Pathways for Resilient Communications
UE	user equipment

1 Introduction

This document comprehensively discusses the examination of potential interference impacts to point-to-point (P2P) links operating in the 7-8 GHz band conducted by the Idaho National Laboratory (INL) for the Department of Energy (DOE) Office of Electricity (OE). Here, we cover the approach to this examination, our results, the impact of these results, and the reasoning behind each of these.

1.1 Key Takeaways

This section summarizes the major results of our testing and provides pointers to more detailed discussions. Our major findings are as follows:

- Under the scenarios we tested, we found interference to our microwave link that would be detrimental to grid operations. For example, Wi-Fi signals with power levels approximately 100 times lower than the microwave signals at the receiver cause the microwave link to be inoperable (see Section 6.3.2).
- Traditional methods of analysis that focus on simulation miss important aspects of interference. Over-the-air testing shows that simulation can be an order of magnitude off when estimating the interference levels that impact microwave links. Efficient spectrum policy needs to validate simulation with over-the-air testing (see Section 6.4).
- Relying on reports from the field of interference for spectrum management generate a false sense of success. Current equipment metrics do not provide enough clarity for when or how much interference impacts operations (see Section 8.3). In our testing, the bit error rate metric resets to show zero errors once the link has failed (see Section 6.3.4.1).
- Spectrum sharing is feasible when based on a disciplined, scientific and data driven methodology.

1.2 Project Motivation

Microwave technology is vital to the reliability, resilience and security of the nation's electric power and other critical infrastructure. Disruptive interference to microwave systems used for critical infrastructure poses a significant risk to our nation's security.

Microwave technology has played a significant role in the electric utility industry, particularly in the context of electric grid control and communication since the 1950s. From the 1950s through the 1990s, microwave communications evolved to become an integral part of electric grid management, supporting supervisory control and data acquisition (SCADA) and teleprotection systems which rapidly isolate faults to protect grid infrastructure. In the 1990s, the rise of smart grid technologies increased the demand for robust communications systems supporting advanced applications. Due to this demand, microwave usage increased to support continuous grid operations between remote grid components and central control centers. Over the last two decades, real-time data analytics further emphasized the importance of reliable microwave communications channels, especially for remote or rugged area where physical cabling is impractical.

Prior to the 2020s, electric utilities and other critical infrastructure providers relied on dedicated (licensed) spectrum in the 5.925-7.125 GHz band to protect against potential interference. In 2020, the Federal Communications Commission (FCC) repurposed the 5.925-7.125 GHz spectrum for unlicensed users allowing for Wi-Fi and other users to utilize this band applying modeling and simulation for evaluating potential

interference. To our knowledge, limited scientific, empirical, over-the-air field testing was conducted prior to the implementation of the repurposing. This FCC repurposing has increased the risk of interference to the critical infrastructure provider.

The National Telecommunications and Information Administration (NTIA) is now studying 3.5-24 GHz but specifically the 7.125-8.400 GHz band to expand its usability. To provide more scientific, empirical data for this evaluation, the Department of Energy, Office of Electricity (DOE-OE) requested INL to conduct a transparent modeling, simulation, and over-the-air interference evaluation of a representative electric utility system utilizing long distance microwave communications. With the given representative system, DOE-OE requested INL to evaluate interference thresholds for Wi-Fi and cellular (i.e., 5G) devices.

1.3 Overview

Wireless spectrum is a limiting resource for continued economic growth in the United States. As discussed in the recent National Spectrum Strategy (NSS), wireless spectrum underpins several aspects of the U.S. economy and the demand for additional spectrum is driving the need for realizing spectrum sharing to enable continued development. At the same time, wireless spectrum is an essential foundation of critical energy infrastructure, including electric, oil, and natural gas resources. In particular, wireless P2P links (a.k.a. microwave links) are the backbone of vast infrastructure networks that enable the flow of sensor and control information needed to manage critical energy sector infrastructure in the United States. These links will only become more important as the energy sector incorporates more diverse sensing and more efficient control mechanisms, which increases system complexity and data volume requiring more resilient communications. Therefore, the continued economic development of the U.S. depends on determining novel approaches to spectrum management that balance both broad access for advanced wireless technologies and resilience for critical infrastructure.

Here, we support balancing the competing needs outlined above by providing scientifically grounded data on potential interference to critical energy sector P2P links in a co-mingled sharing scenario. We focus on over-the-air testing of commercial off-the-shelf transmitting equipment to ensure that our project captures the large variety of factors that influence the impact of interference in real-world settings. First and foremost, our efforts demonstrate that co-mingled spectrum sharing generates interference that renders critical P2P links inoperable when the approach to sharing prioritizes broad access to spectrum. Secondly, we note that simulation based examinations of interference are prone to errors leading to either under estimation or over estimation of interference impacts. Thus, simulation centric approaches are limited in their ability to balance protection of critical links against utilization of potential spectrum. Finally, our results show that effective management of spectrum sharing must extend beyond reported interference events. The identification and attribution of interference is impractical for two major reasons: (1) the large variety of environmental, geographical, and electromagnetic factors that influence communications performance and (2) limitations of metrics in commercially available equipment to monitor links. This study examines commercial off-the-shelf P2P equipment to identify potential issues in co-mingled spectrum sharing that goes beyond limitations in simulation and improves the identification of interference.

This project is an exploratory examination of co-mingled spectrum sharing in the 7 GHz band (7125 - 8400 MHz) and the potentially associated interference. This work is largely inspired by the recent opening of the 6 GHz band (5925 - 7125 MHz) to unlicensed, co-mingled sharing. In the case of the 6 GHz band, the FCC primarily considers simulation centric approaches to understand potential interference which generally minimize the concerns of the critical infrastructure community [6, 7]. We believe that an approach that validates simulation with over-the-air testing provides a holistic picture of the nuances of spectrum sharing. This builds a solid foundation for policy makers to represent the needs of all spectrum stakeholders. Therefore, we focus on open-range, over-the-air testing as the central component of our data collection. This allows us to characterize the conditions necessary for representative interferers to impact critical energy sector P2P links. We transparently describe our approach, our results including data, and the conclusions that we draw in our main report. Together, this work is intended as a foundation to facilitate policy makers taking a data driven approach to designing spectrum sharing strategies in the 7 GHz band that extracts maximum utility from the spectrum while continuing to support the resilient operation of critical energy sector infrastructure.

1.4 Testing Context

P2P links are a critical foundation of electric utilities, serving as the lifeline for transmitting critical data and control signals across vast power networks. These communication links ensure the seamless integration and coordination of various components within the electrical grid, facilitating real-time monitoring, control, and maintenance activities that are vital for stable and efficient power delivery. P2P links are indispensable for modern electric utilities. They underpin the operational efficiency, reliability, and security of the electrical grid, enabling utilities to meet the growing demands of the energy landscape while ensuring the continuous and safe delivery of electricity to consumers.

Looking toward the future, we anticipate that P2P links will be increasingly important to the U.S. electric system. Resilient communications are a critical enabler for the ubiquitous sensors and robust actuation envisioned within the emerging smart grid [3]. Supporting these developing capabilities while maintaining existing operations requires a diversity of communications technologies with P2P links providing a critical capability [4]. P2P links are particularly important enablers for realizing distributed energy resources (DERs) and distributed substations [11]. As such, the robust operation of P2P links is now and will continue to be synonymous with the robust operation of electric systems.

At the same time, general demand for wireless communications is also growing rapidly. This trend is perhaps best encapsulated by the November 2023 NSS [10]. This strategy acknowledges (1) the general importance of wireless communications to modern society, (2) the rapid growth in demand for radio frequency (RF) spectrum, and (3) the inadequacy of current spectrum management approaches for meeting future demands. In pursuit of the reconciliation of these factors, the NSS proposes studying several bands for potential repurposing, to include co-mingled sharing. Of the bands proposed, the 7 GHz band (7125 - 8400 MHz) is the largest.

Considering the most recently established shared band, provides significant lessons for the balancing the needs to enable critical operation and to support continued economic development. In 2020, the FCC opened the 6 GHz band (5925 - 7125 MHz) to co-mingled, unlicensed spectrum sharing [6]. In both the initial report and order as well as the follow-up that expands access [7], the FCC notes that unlicensed access to the band was allowed largely on the basis of simulation studies. That is, while some minor open-range testing did occur, the FCC largely discounted these efforts. So far, this simulation approach is primarily focused on assess the probability that interference from an unlicensed user exceeds a pre-defined level and does not consider the reduction of P2P link resilience. Given that the electric system in the U.S. is becoming increasingly complex, these resilience degrading effects are increasingly important to the overall system stability [9].

To summarize, we stand at a position in which P2P links must provide increasing levels of performance and resilience while simultaneously coping with increased interference from co-mingled sharing. Further, the increasing complexity of the electric system leads to an increased impact of degradations in resilience. Therefore, we see the characterization of interference impacts on P2P links as critical for both the ongoing operation and future evolution of critical electric infrastructure.

1.5 Testing Concept

The overarching goal of this project is to characterize the conditions necessary for representative potential interference signals to impact incumbent electric utility P2P links operating in the 7-8 GHz band as well as explore the range of feasible impacts. Here, we take a forward leaning approach with the goal of informing spectrum policy decisions, before they occur, on the basis of a well-reasoned exploration of interference. Thus, our scenario is based on an exploratory examination of co-mingled spectrum sharing between P2P links and a set of potential interferers. We focus on developing scientifically grounded data that identifies and characterizes any potential interference impacts to P2P links. Ideally, this data provides a foundation for determining spectrum policy for the 7 GHz band that considers potential impacts to critical electric sector communications and shapes any spectrum sharing approaches appropriately. Note that in practice there is a broad range of what might constitute an impact to a P2P link from the perspectives of an electric utility. Here, we take a baseline approach that examines impact in terms of measurable communication performance of the link that provides a foundation for examination of other potential impacts. As such, this project takes a scientifically rigorous approach to establishing foundational data on the topic of interference impacts to

P2P links in the 7-8 GHz band.

Establishing foundational data in a forward leaning capacity requires us to make some predictions about future directions for the 7-8 GHz band. We take an approach driven by the current landscape of communications and informed by recent and emerging trends in spectrum policy to outline our testing approach. Given our focus on interference impacts to electric sector P2P links, we apply these considerations to selecting a meaningful set of potential interferers and outline the operations that P2P links in the 7 GHz band would support. Below, we first briefly describe how the trajectory of spectrum policy shapes our approach. Then, we discuss our selected set of potential interferers. Finally, we describe our approach to considering the electric sector operations that utilize, or would potentially utilize, P2P links in the 7 GHz band.

As discussed in Section 1.4, spectrum policy is increasingly trending toward spectrum sharing. Given that the NSS has already identified the 7-8 GHz for consideration of repurposing, we must strongly consider the possibility of co-mingled sharing in this band¹. The recent unlicensed model of co-mingled sharing in the 6 GHz band predicts one possible future for spectrum sharing in the 7 GHz band. Alternatively, the prior example of Citizens Broadband Radio Service (CBRS) establishes some precedent for a tiered access model for sharing. While both of these models introduce new potential interferers, the type of potential interferer and the rules governing the operation of potential interferers depends strongly on the sharing model. Here, we do not conjecture on the details of the model that may govern sharing in the 7 GHz band and simply consider an inclusive set of potential interferers.

Based on the trajectory of spectrum policy, we consider four potential interferers: (1) 5G, (2) Wi-Fi, (3) additive white Gaussian noise (AWGN), and (4) continuous wave (CW). We include 5G as the dominant cellular signal from the perspective of emerging spectrum demand, a highly likely signal in the case of a tiered sharing model, and a potential signal in the case of an unlicensed model utilizing the emerging 5G new radio unlicensed capability[2, 1]. We include Wi-Fi as a dominant signal in terms of adoption and use as well as a highly like signal in the case of an unlicensed sharing model. We include AWGN as a baseline wideband signal that loosely corresponds to generic digital signal spectrum profiles. We include CW as a baseline narrowband signal that loosely corresponds to generic analog voice spectrum profiles. Our two baseline signals provide a comparison point for the two commercial signals and highlight specific interference features.

Currently, P2P links operate in 7-8 GHz to support the electric system. In the U.S., these links are primarily operated by Power Marketing Administrations (PMAs). Bordering the U.S., several Canadian electric utilities operate P2P links in 7-8 GHz and are likely to be impacted by cross border interference related to any U.S. spectrum policy updates. Further, it is not inconceivable that commercial electric utilities within the U.S. begin to utilize the 7-8 GHz band as part of the repurposing of that band, although there are no current plans exploring this possibility. Therefore, our project considers the full compliment of electric utility operations leveraging P2P links. Given our focus on communication impacts and as a means to keep our project to a feasible scope, we group electric utility operations into P2P operational paradigms. These paradigms summarize the communication requirements that are emblematic of a broad set of electric utility use cases, but do not specifically correspond to the needs of any specific use of P2P links. As such, these operational P2P paradigms provide a representative collection of communication requirements that broadly span the full set of electric utility use of P2P links in a feasible size for testing.

We will consider the following paradigms for the P2P link:

- Maximum data rate regardless of latency: this operating paradigm is typical of bulk data transfer.
- Low data rate with low latency and deterministic latency profiles: this paradigm is typical of system control activities.
- Medium data rate with medium latency: this represents a balance between data rate and latency which would be indicative of average operation and provides a useful mid-point between the other two extremes.

Our project examines interference to P2P links nominally supporting an operation that falls into one of these paradigms, such as power distribution command and control or substation surveillance. We conduct

¹We note that that neither the NSS nor the associated implementation plan states that the 7-8 GHz band will be opened for co-mingled spectrum sharing; rather these documents simply describe a study the band that may recommend a spectrum sharing approach be proposed for this band.

over-the-air testing to develop scientifically rigorous data that outlines where the communications performance of these P2P links is degraded and the amount of degradation that occurs. This testing considers factors such as the pattern of directional antennas employed by P2P links and a broad range of potential interference power levels to best allow emerging spectrum policy to consider co-mingle spectrum sharing and the associated impacts on critical communication links.

1.6 Testing Structure

Our testing employs two methods: (1) simulation, and (2) open-range testing. This collection of methods is intended to produce defensible and empirical data on the potential impact of interference to P2P links in 7-8 GHz from representative interferers. Therefore, we view the simulation as supporting and supplementary to the open-range testing.

1.6.1 Simulation Studies

We employ simulation to achieve three overarching purposes. First, we leverage simulation as a planning support for the open-range testing. Second, we utilize simulation to reduce risks associated with open-range testing. Third, we interpolate the data collected during open-range testing.

The objectives related to planning for and reducing risk of open-range testing are the following:

1. Select sites for P2P endpoints and interferers.
2. Determine the range of link parameters of highest interest for testing.
 - (a) Characterize the expected margin of the P2P link.
 - (b) Identify interferer power ranges expected to impact to the P2P link.
 - (c) Estimate the expected impact of interferers on the P2P link.

The objective related to expanding the results beyond what can be studied in open-range testing are following:

1. Characterize expected interferer impacts for interferer locations beyond those tested.

We address these objectives across three simulation studies:

1. Simulation for Site Selection
2. Simulation for Link Parameter Exploration
3. Simulation to Expand Interference Impacts

1.6.2 Open-Range Testing

Open-range testing is the primary data collection method. The intent of this testing is to collect defensible, empirical, objective, quality data from a representative deployment of a P2P link in the presence of representative interference signals.

The objective of open-range testing centers on the production of representative data from real-world evaluation of links:

1. Characterize the impact of interference on P2P links.
2. Generate empirical data.
3. Evaluate the real-world attenuation associated with side or back lobe interference injection.

2 Test Items and Equipment

This section outlines the items that we examine in testing, the equipment used for these items, the configuration of this equipment, and the locations of this equipment.

2.1 P2P Link

This P2P represents the incumbent link the 7-8 GHz band that would need to be protected from interference generated by potential new entrant systems. For this test we have selected a link that is typical of existing P2P links in 7-8 GHz and would be representative of potential commercial P2P links should those be moved into 7-8 GHz.

We do not intend to conduct a complete performance evaluation of the P2P system. We will not examine the utility of this P2P system for any specific, deployed operational use case. We will also not examine ancillary considerations such as the security provided by this P2P system, even with regard to the impact of interference on security. Rather our intention is to provide a characterization of interference resilience for a representative link that can be instructive for a variety of deployed scenarios.

2.1.1 P2P Equipment

Table 2.1 lists the equipment that we use to realize the P2P link.

Table 2.1: P2P Link Equipment

Item Name	Manufacturer	Model	Qty	Description
P2P Terminal	Aviat	ATN-WTM4200	2	Radio terminal for P2P link (see Datasheet Supplement Section 1.1)
P2P Antenna	Aviat	AND-VHLP2-7W-GTU	2	0.6 m (2 ft) antenna for P2P link (see Datasheet Supplement Section 1.2)
P2P Data Driver	Dell	Precision 7530	2	Laptops to provide the data driver for the P2P link

2.1.2 P2P Link Parameters

Table 2.2 lists the P2P link parameters that span all considered scenarios. These parameters reflect the operation of the P2P terminals and provide a base for subsequent investigation.

Below we describe the selection of each P2P parameter:

- We set the center frequency to both (1) match a local operational P2P link exemplar and (2) avoid overlapping with other systems external to our testing. The P2P that we use in testing uses frequency separation to facilitate bidirectional transmission.
- We set the P2P bandwidth to reflect a typical value for P2P links while allowing us to focus on the overlapping interference case.

Table 2.2: P2P Link Parameters

Parameter	Units	Value
Center Frequency 1	MHz	7390
Center Frequency 2	MHz	7690
Rx Bandwidth	MHz	40
Rx Noise Figure	dB	7.0
Noise Floor	dBm	-91.0
Rx Saturation	dBm	-20.0
Tx Minimum Power	dBm	11.5
Antenna Gain	dBi	31.1
Polarization	N/A	Vertical

- We estimated the noise figure as a typical value for P2P links.
- We calculated the P2P noise floor as $N_{P2P} = -174 + 10 \log_{10}(B_{P2P} \times 10^6) + F_{P2P}$, where N_{P2P} is the P2P noise floor, B_{P2P} is the receive bandwidth in MHz, and F_{P2P} is the noise figure in dB.
- The receiver saturation level is taken from the Aviat ATN-WTM4200 datasheet.
- The minimum transmission power is taken from the Aviat ATN-WTM4200 datasheet.
- The antenna gain is taken from the Aviat AND-VHLP2-7W-GTU datasheet.
- We examine vertical polarization as the most common setting for rural P2P.

Additional parameters, such as transmit power and modulation, vary according to specific scenarios. We discuss the specific scenarios of our testing in the next sub-section.

2.1.3 P2P Operational Paradigms

We consider three operational paradigms for the P2P link:

1. Maximum data rate regardless of latency: this operating paradigms is typical of bulk data transfer or video streaming. We refer to this paradigm as the high-rate paradigm.
2. Low data rate with low latency and deterministic latency profiles: this paradigm is typical of system control activities. We refer to this paradigm as the low-rate paradigm.
3. Medium data rate with medium latency: this represents a balance between data rate and latency which would be indicative of average operation and provides a useful mid-point between the other two extremes. We refer to this paradigm as the mid-rate paradigm.

The Aviat ATN-WTM4200 datasheet defines 10 different possible rates for a 40 MHz channel in the 7 GHz band. Each of these rates is associated with a different modulation scheme, maximum transmission power, and minimum received signal threshold to achieve a bit error rate (BER) of 1×10^{-6} . Table 2.3 lists the rates and associated values. Note that the minimum received assumes a nominal noise environment.

For our purposes, we target the following rates for testing:

- The low-rate paradigm utilizes 52 Mbps (QPSK)
- The mid-rate paradigm utilizes 179 Mbps (64 QAM)
- The high-rate paradigm utilizes 368 Mbps (4096 QAM)

Table 2.4 lists the power parameters for each operational paradigm that we consider. Below we describe each column of Table 2.4:

Table 2.3: Rate Table for the P2P Link

Rate (Mbps)	Modulation	Max Tx Power (dBm)	Min Rx Power (dBm)
52 Mbps	QPSK	31.5	-89.5
121 Mbps	16 QAM	31.0	-81.0
137 Mbps	32 QAM	31.0	-79.0
179 Mbps	64 QAM	30.0	-75.5
211 Mbps	128 QAM	29.5	-73.0
241 Mbps	256 QAM	29.0	-70.0
276 Mbps	512 QAM	28.5	-66.5
311 Mbps	1024 QAM	27.5	-63.0
343 Mbps	2048 QAM	26.5	-59.5
368 Mbps	4096 QAM	25.5	-56.0

Table 2.4: P2P Paradigm Power Parameters

Paradigm	Min Rx Power (dBm)	Min Rx Power (Watts)	Min Rx SNR (dB)	Max Tx Power (dBm)	Max Tx Power (Watts)	Max EIRP (dBm)	Max EIRP (Watts)
Low-rate	-89.0	1.1×10^{-12}	1.5	31.5	1.4	62.6	1.8×10^3
Mid-rate	-75.5	2.8×10^{-11}	15.5	30.0	1.0	61.1	1.3×10^3
High-rate	-56.0	2.5×10^{-9}	35.0	25.5	0.35	56.6	4.6×10^2

- Paradigm: name of the operational paradigm considered
- Min Rx Power (dBm): the minimum received signal threshold to achieve a BER of 1×10^{-6} (copied from Table 2.3). The values in this column are in dBm.
- Min Rx Power (Watts): the minimum received signal threshold to achieve a BER of 1×10^{-6} . The values in this column are in Watts. These values are provided for convenience.
- Min Rx SNR (dB): the minimum received signal to noise ratio (SNR) to achieve a BER of 1×10^{-6} . These values are calculated as $S_{thres} = P_{P2P Rx Thres} - N_{P2P}$, where S_{thres} is the minimum received SNR to achieve a BER of 1×10^{-6} , $P_{P2P Rx Thres}$ is the minimum received power to achieve a BER of 1×10^{-6} , and N_{P2P} is the noise floor for the P2P link.
- Max TX Power (dBm): The maximum transmission power available (copied from Table 2.3). The values in this column are in dBm.
- Max Tx Power (Watts): The maximum transmission power available. The values in this column are in Watts. These values are provided for convenience.
- Max EIRP (dBm): The maximum effective isotropic radiated power (EIRP) available. These values are calculated as $P_{P2P EIRP} = P_{P2P Tx} + G_{P2P}$, where $P_{P2P EIRP}$ is the P2P EIRP, $P_{P2P Tx}$ is the maximum P2P transmission power, and G_{P2P} is the P2P antenna.
- Max EIRP (Watts): The maximum EIRP available. The values in this column are in Watts. These values are provided for convenience.

2.2 Interference Waveforms

The interference waveforms represent potential new entrants that might share the 7-8 GHz band. New entrants to any shared band must be managed to ensure that incumbents do not experience harmful interference. Our testing focuses on examining the impacts of potential interferers on P2P links to determine the conditions that lead to harmful interference.

Table 2.5: 5G Interferer Parameters

Parameter	Value
Native Frequency	2533.350 MHz
Bandwidth	40 MHz
Duty Cycle	8.27%

Note that our testing does not examine the performance of the interferers themselves. That is, we do not explore the potential utility that could be achieved by these interferers at any given location or transmit power level.

2.2.1 Interference Types

We consider four representative interferers: (1) 5G, (2) Wi-Fi, (3) AWGN, and (4) CW. Each of these represents an important class of potential new entrants should the 7-8 GHz band be shared. That is none of these interferers currently operate within the 7-8 GHz band, but these signals are largely representative of the types of interference that would be expected should the band be open to sharing. Here we outline each representative interferer; we cover the equipment used to realize these interferers and the parameters of the interference signals in subsequent sections.

2.2.1.1 5G Interferer

5G is the fifth and currently most recently deployed generation of cellular standards. This technology has significant commercial backing and drives a significant amount of spectrum demand. Currently, 5G primary operates in spectrum licensed for the use of 5G as either the primary or priority access spectrum user. The emerging 5G-NRU capability provides for unlicensed 5G operation but this has yet to see wide spread adoption. 5G does not currently operate in the 7-8 GHz band but is a likely new entrant.

We implement a standards compliant 5G interferer by utilizing a software defined radio (SDR) approach and the open-source 5GHOUL software¹. Our SDR provides a 5G base station (i.e., gNB) that interacts with a commercial-off-the-self user equipment (UE). This configuration produces a Release 17 standards compliant 5G signal that exhibits realistic behavior.

We drive data through the 5G connection to ensure that the signal is active. We accomplish this by establishing an UDP iperf session from the UE through our base station at 2 Mbits per second. This yields a 5G signal with an 8.27% duty cycle. This duty cycle is within the range of duty cycles observed in measurements of commercial 5G deployments [12].

Table 2.5 summarizes the parameters of the 5G interferer.

Figure 2.1 displays the spectrum of the 5G signal produced by the 5G interferer.

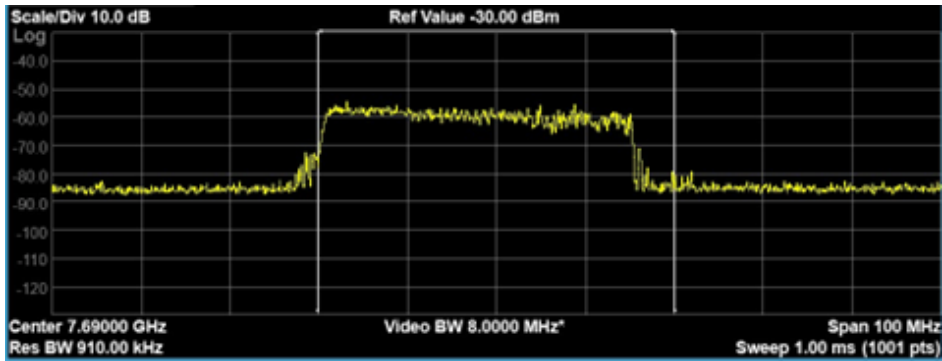


Figure 2.1: 5G Signal Spectrum

See Section C.1.1.4 for the detailed process of operating the 5G interferer.

¹<https://asset-group.github.io/disclosures/5ghoul/>

Table 2.6: Wi-Fi Interferer Parameters

Parameter	Value
Native Frequency	2437 MHz
Bandwidth	20 MHz
Duty Cycle	63.7%

Table 2.7: AWGN Interferer Parameters

Parameter	Value
Native Frequency	3000 MHz
Bandwidth	50 MHz
Duty Cycle	100%

2.2.1.2 Wi-Fi Interferer

Wi-Fi is a dominant technology for unlicensed spectrum based networking. This technology has recently been a significant part of the discussion around the unlicensed use of the 6 GHz band. We expect that Wi-Fi would be likely to leverage 7-8 GHz if the opportunity arose. Wi-Fi does not currently operate in the 7-8 GHz.

We implement our Wi-Fi interferer signal but simply employing a commercial-of-the-shelf Wi-Fi access point interacting with a commercial-of-the-shelf UE. We configure the access point to always utilize Wi-Fi channel 6 to ensure a consistent center frequency and bandwidth. We run 802.11ax (Wi-Fi 6) through this channel as an example of a modern Wi-Fi protocol.

We drive through the Wi-Fi utilizing a TCP iperf session that attempts to maximally utilize the available connection. This results in a Wi-Fi signal with a 63.7% duty cycle. This duty cycle is near the maximum level for Wi-Fi and thus represents a worst case interference [8].

Table 2.6 summarizes the parameters of the Wi-Fi interferer.

Figure 2.2 displays the spectrum of the Wi-Fi signal produced by the Wi-Fi interferer.

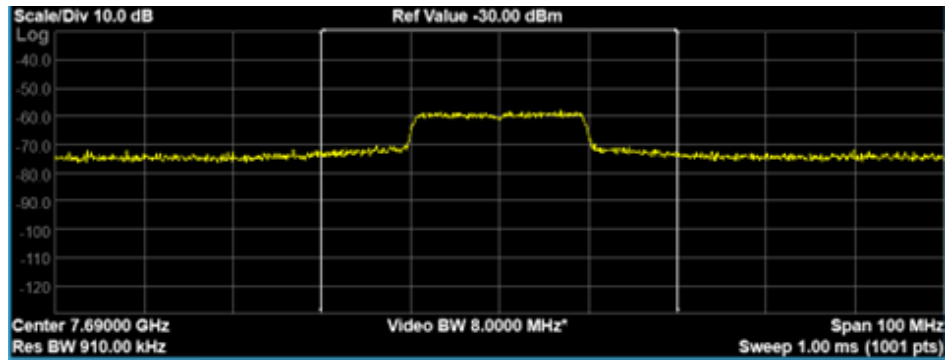


Figure 2.2: Wi-Fi Signal Spectrum

See Section C.1.1.5 for the detailed process of operating the Wi-Fi interferer.

2.2.1.3 AWGN Interferer

AWGN is a base-line signal that does not carry any data but provides a consistent interferer. Further the general qualities of the AWGN largely align with a generic digital signal that may be a new entrant to the 7-8 GHz band.

We implement our AWGN with a SDR and basic signal generation software.

Table 2.7 summarizes the parameters of the AWGN interferer.

Figure 2.3 displays the spectrum of the AWGN signal produced by the AWGN interferer.

Table 2.8: CW Interferer Parameters

Parameter	Value
Native Frequency	3000 MHz
Bandwidth	3 MHz
Duty Cycle	100%

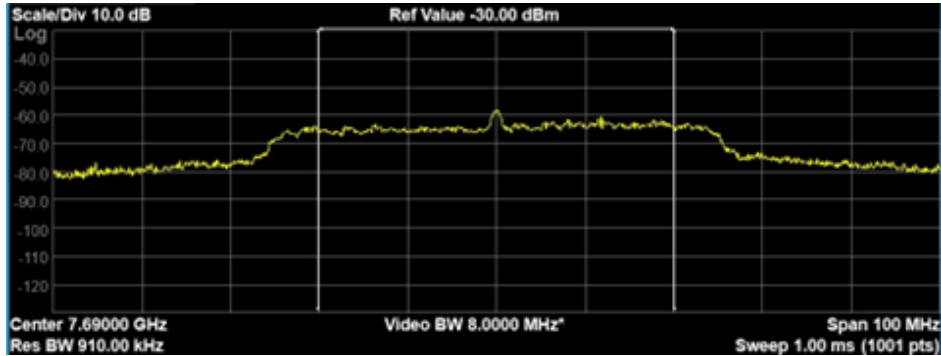


Figure 2.3: AWGN Signal Spectrum

See Section C.1.1.6 for the detailed process of operating the AWGN interferer.

2.2.1.4 CW Interferer

CW is a base-line signal that does not carry any data but provides a consistent interferer. This signal is a narrow-band tone that loosely mimics generic voice signals that may be new entrants to the 7-8 GHz band.

We implement our CW signal with a SDR and basic signal generation software.

Table 2.8 summarizes the parameters of the CW interferer.

Figure 2.4 displays the spectrum of the CW signal produced by the CW interferer.

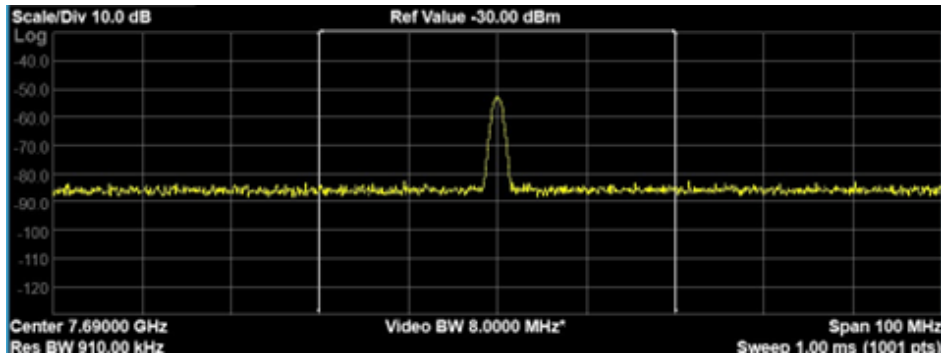


Figure 2.4: CW Signal Spectrum

See Section C.1.1.6 for the detailed process of operating the CW interferer.

2.2.2 Equipment

Table 2.9 lists the equipment that we use to realize the interferers. Note that this table includes the equipment necessary to generate an interference signal with realistic behavior, up-convert that signal to the 7-8 GHz band, amplify the signal to the desired power level, and transmit that signal. Given our focus on simply injecting interference onto a P2P in the 7 GHz band, we do not consider reception of interfering signals in 7 GHz. We discuss the approach to leveraging this equipment for generating these interference signals in Section 2.2.3.

Table 2.9: Interferer Equipment

Item Name	Manufacturer	Model	Qty	Description
SDR Front End	Ettus Research	USRP B210	1	Signal Source for 5G, AWGN, and CW interferers. (See Datasheet Supplement Section 2.1)
Wi-Fi Access Point	Cambium	XE3-4TN	1	Signal source for Wi-Fi interferer. (See Datasheet Supplement Section 2.2)
Interferer Controller	Dell	Precision 7530	1	Laptop to control interferer sources.
UE	Samsung	S22	1	User radio to drive 5G and Wi-Fi behavior.
2-way Splitter	Mini-Circuits	ZFSC-2-10G+	1	Splitter to support native behavior for 5G and Wi-Fi. (See Datasheet Supplement Section 2.3)
Interferer Behavior Antenna	Ettus Research	VERT2450	2	Antennas to support 5G behavior.
Mixer	Fairview	FMTX1051	1	Mixer to support interference up-conversion. (See Datasheet Supplement Section 2.4)
Signal Generator	Tektronix	TSG4100A	1	Signal generator to support interference up-conversion. (See Datasheet Supplement Section 2.5)
Filter	Pasternack	PE8741	1	Filter to support interference up-conversion. (See Datasheet Supplement Section 2.6)
Programmable Attenuator	Mini-Circuits	RC4DAT-8G-95	1	Variable attenuator to control interference power. (See Datasheet Supplement Section 2.7)
Interferer Amplifier 1	Mini-Circuits	ZVE-3W-183+	1	3W power amplifier. (See Datasheet Supplement Section 2.8)
Interferer Amplifier 2	RF Lambda	RFLUPA06G12GD	1	16 W power amplifier. (See Datasheet Supplement Section 2.9)
Interferer Antenna	Pasternack	PEWAN137-20	1	Horn antenna to support interference transmission. (See Datasheet Supplement Section 2.10)

2.2.3 Interference Generation Method

Our approach to generating interference comprises three phases: (1) signal generation, (2) up-conversion, and (3) amplification. The signal generation phase involves using signal sources to generate the various types of interference signals in convenient frequency ranges. The up-conversion phase shifts the interference signals to the center frequency of the target P2P receiver. The amplification phase allows us to control the EIRP of the transmitted interference signal. This approach allows us to generate interference signals at a range of transmit power levels while maintaining direct overlap with the targeted P2P receiver.

We employ both behavior preserving and non-behavior preserving signal generation. For both the 5G and Wi-Fi interference types, we generate a real-world interference signal that adheres to commercial standards with behavior driven by interaction with a commercial-off-the-shelf UE. In these cases, we employ a splitter to allow the UE to interact with our interference signal source in its native band while simultaneously up-converting the signal into 7-8 GHz. Figure 2.5 displays the process for behavior preserving interference generation. On the other hand, both the AWGN and CW interference types have no real behavior because

they are simply representative signals. Therefore, we simply generate and up-convert these signals without additional splitting, as displayed in Figure 2.6.

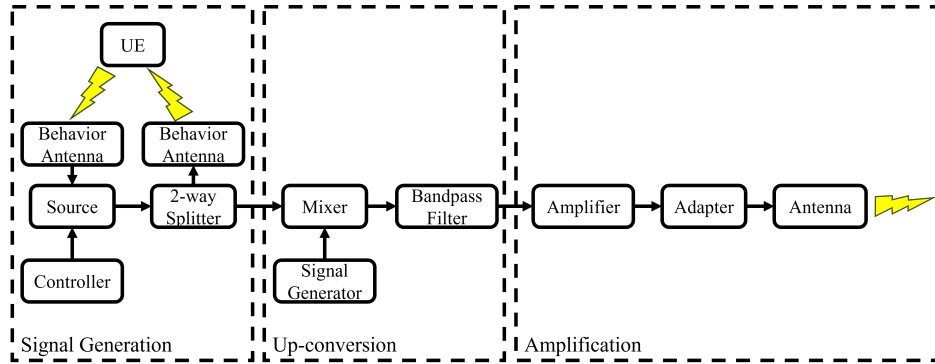


Figure 2.5: Behavior Preserving Interference Generation Process

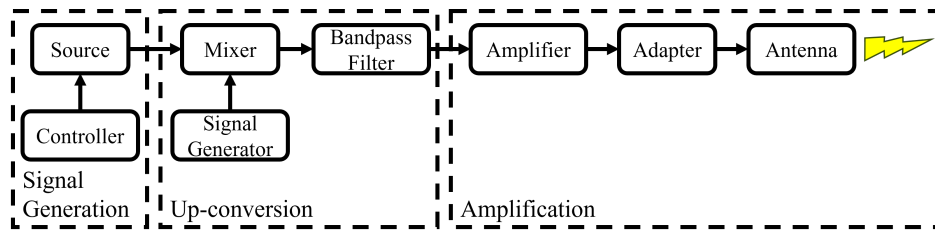


Figure 2.6: Non-Behavior Preserving Interference Generation Process

Our approach to the amplification phase is consistent across all interference types. In every case, we employ a fixed gain amplifier that feeds a directional antenna aimed directly at the targeted P2P receiver. We utilize a programmable attenuator to variable the input level to the amplifier. We employ two different amplifiers to access different ranges of power for our interference signals, as reflected in Table 2.9.

2.2.4 Interference Parameters

Table 2.10 lists the parameters that are common across all the interferers.

Table 2.10: Common Interference Parameters

Parameter	Units	Value
Antenna Gain	dBi	20.0
Amplifier 1 1 dB Compression Point	dBm	34.0
Amplifier 2 1 dB Compression Point	dBm	42.0

Below we describe each common interference parameter:

- The antenna gain is taken from the Pasternack PEWAN137-20 datasheet. A directional antenna allows us to produce controlled interference at a range of power levels.
- The amplifier 1 1 dB compression point is taken from the Mini-Circuits ZVE-3W-183+ datasheet.
- The amplifier 2 1 dB compression point is taken form the RF Lambda RFLUPA06G12GD datasheet.

2.2.5 Interference Power Levels

As discussed above in Section 2.2.3 we employ a fixed gain amplifier paired with a variable attenuator to control the transmitted interference power. Given this configuration, the achievable range of powers for each

Table 2.11: Interferer Transmit Power

Interferer Type	Max. Power (dBm)	Max. Power (Watts)
5G Amp 1	-3.6	4.4×10^{-4}
5G Amp 2	24.0	0.25
AWGN	12.2	1.7×10^{-2}
CW	7.2	5.3×10^{-3}
Wi-Fi	13.7	2.3×10^{-2}

interferer depends on the power level output by interferer signal source, the amount of attenuation applied, and the gain of the interferer amplifier used. Our attenuator provides attenuation up to 95 dB in 0.25 dB sets.

Table 2.11 shows the measured maximum transmit power for each interferer using interferer amplifier 1. Note that the measurements shown here provide the power at the interface to the interferer antenna, including the cabling necessary to connect to the antenna.

Given the relatively low power of the 5G power, we also assessed this interferer using the interferer amplifier 2.

2.3 Spectrum Monitoring

Spectrum monitoring is a supporting component of our test that is used to confirm the operating power levels for the P2P link and the interferer.

2.3.1 Spectrum Monitoring Equipment

Table 2.12 lists the equipment that we use for spectrum monitoring.

Table 2.12: Spectrum Monitoring Equipment

Item Name	Manufacturer	Model	Qty	Description
Spectrum Analyzer	Keysight	FieldFox N9915C	1	Portable wireless spectrum analyzer. (See Datasheet Supplement Section 3.1)
Monitoring Antenna	Pasternack	PEWAN137-20	1	Horn antenna to support spectrum monitoring. (See Datasheet Supplement Section 2.10)

2.3.2 Spectrum Monitoring Parameters

Table 2.13 lists the operational characteristics of the spectrum monitor. These parameters come from the FieldFox N9915C datasheet.

Table 2.13: Spectrum Monitoring Parameters

Parameter	Value
Minimum Frequency	3 kHz
Maximum Frequency	10 GHz
Power Level Accuracy	± 0.5 dB
Real-time Bandwidth	120 MHz
Resolution Bandwidth	1 Hz to 5 MHz

2.4 Locations

This section provides the locations used in testing. Figure 2.7 summarizes these locations and the subsequent material here provides further details. The process of selecting these locations is discussed further in Section 3.

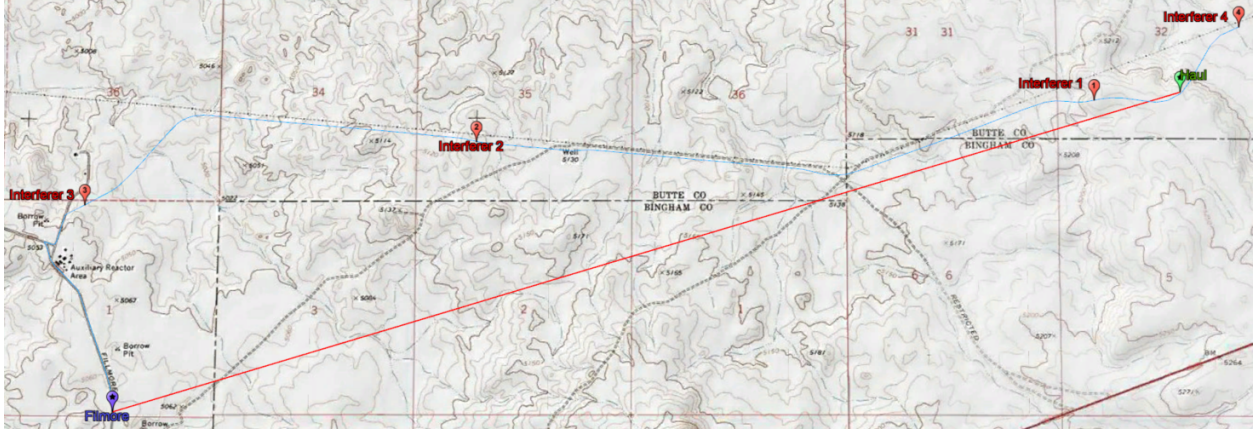


Figure 2.7: Locations for Testing

2.4.1 Filmore Location

The Filmore location provides one end of the P2P link. This location is 8.3 kilometers (5.2 miles) from the Haul location, which provides a reasonable length for a P2P link in the 7 GHz band (see Section 3). Table 2.14 provides additional details about this location.

Table 2.14: Filmore Location Details

Coordinates	43°31'18.63" N, 112°49'32.12" W
Decimal Degrees	43.521842, -112.825589
Antenna Height	32.3 m (106 ft)
Radio Type	P2P
Transmit Frequency	7390 MHz
Receive Frequency	7690 MHz

2.4.2 Haul Location

The Haul location provides one end of the P2P link. This location is 8.3 kilometers (5.2 miles) from the Filmore location, which provides a reasonable length for a P2P link in the 7 GHz band (see Section 3). Table 2.15 provides additional details about this location.

Table 2.15: Haul Location Details

Coordinates	43°32'35.49" N, 112°43'38.57" W
Decimal Degrees	43.54319167, -112.72738056
Antenna Height	18.3 m (60 ft)
Radio Type	P2P
Transmit Frequency	7690 MHz
Receive Frequency	7390 MHz

2.4.3 Interferer Location 1

This location allows for injecting interference into the main lobe of both P2P receivers. As such, this location provides a primary interference generation site for assessing the level of received interference power required to impact the P2P link between Filmore and Haul. Table 2.16 provides additional details about this location.

Table 2.16: Interferer Location 1 Details

Coordinates	43°32'33.52" N, 112°44'7.20" W
Decimal Degrees	43.542644, -112.735333
Antenna Height	9.1 m (30 ft)
Radio Type	Interferer

2.4.4 Interferer Location 2

This location allows for assessing interference generated from just off the central path of the P2P link. This location is still near the main lobe for both ends of the P2P link but not as central as location 1. As such, this is a supplementary location to location 1. Table 2.17 provides additional details about this location.

Table 2.17: Interferer Location 2 Details

Coordinates	43°32'23.55" N, 112°47'32.73" W
Decimal Degrees	43.539875, -112.792425
Antenna Height	9.1 m (30 ft)
Radio Type	Interferer

2.4.5 Interferer Location 3

This location primarily allows for assessing interference injection into the side lobe of the P2P receiver at the Filmore site. Secondly this provides an off-axis, longer range path to the P2P receiver at the Haul site. Table 2.18 provides additional details about this location.

Table 2.18: Interferer Location 3 Details

Coordinates	43°32'8.30" N, 112°49'43.17" W
Decimal Degrees	43.53563889, -112.82865833
Antenna Height	9.1 m (30 ft)
Radio Type	Interferer

2.4.6 Interferer Location 4

This location primarily allows for assessing interference injection into the backlobe of the P2P receiver at the Haul site. This location should be blocked by terrain from the Filmore site (see Section 3). Table 2.19 provides additional details about this location.

Table 2.19: Interferer Location 4 Details

Coordinates	43°32'51.47" N, 112°43'18.18" W
Decimal Degrees	43.54763056, -112.72171667
Antenna Height	9.1 m (30 ft)
Radio Type	Interferer

3 Simulation Study for Site Selection

This section describes the simulation study examining the selection of physical sites used for open-range testing. This evaluation primarily considers the line-of-sight between candidate interferer locations and the P2P locations. We select endpoints with the goal of ensuring both an unobstructed P2P link and a diversity of antenna pattern lobes for interference injection.

3.1 Tools Used

This simulation study utilizes the following tools:

- HTZ Warfare software suite¹
 - ITU256 - ITU-R 526 propagation model

The additional contextual considerations for this study include:

- Terrain data from ATDI² is considered.
- The manufacturer provided antenna pattern for the P2P antenna is considered.
- No weather data is considered.
- No external interference sources are considered.

3.2 Methodology

This section outlines the methods used to accomplish this study and the cases considered by this study.

3.2.1 Overall Approach

This study applies the following steps:

1. Identify candidate locations
2. Determine P2P endpoints
3. Determine interferer locations

We discuss the details of each of the above steps in the following sections.

¹<https://atdi.com/products-and-solutions/htz-warfare/>

²<https://atdi.com/map-data-library/>

3.2.2 Identifying Candidate Locations

Locations for testing must exhibit the following qualities:

- Locations must be practically accessible.
- Locations must facilitate operation without interference from existing links.
- Locations for P2P endpoints must facilitate a link range that is typical for operational P2P links in 7-8 GHz.
- Locations for interferers must support interference injection into a variety of lobes.

To determine the range of link ranges that is typical for operational P2P links in 7-8 GHz, we examine all Department of Energy P2P links in the range 7.125 to 8.4 GHz. We focus on this set because the majority of these links support PMA with use cases similar to commercial electric utilities and thus provide a good analog for our target use case. Figure 3.1 displays a histogram of these links. This examination shows that 57% of links are less than or equal to 10 miles in length.

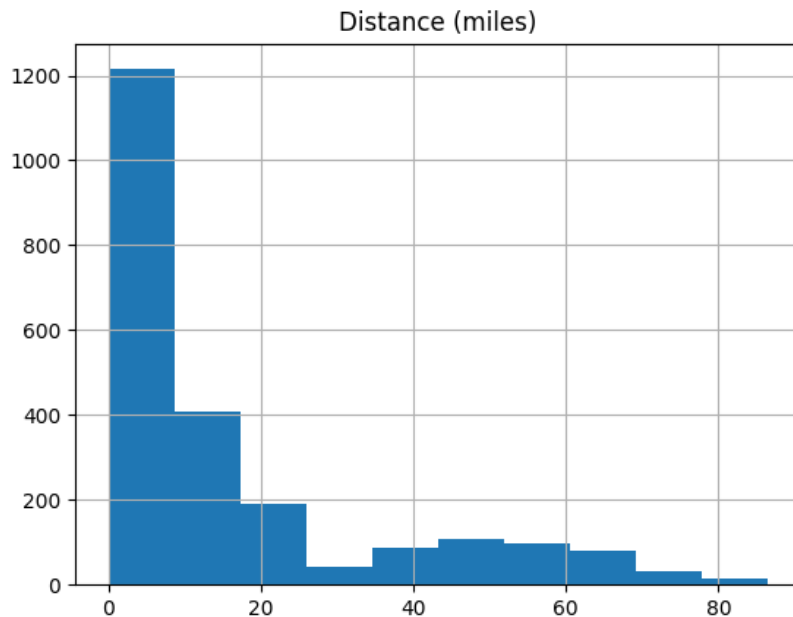


Figure 3.1: Histogram of Department of Energy P2P Links in 7.125-8.4 GHz

3.2.3 Determining P2P Endpoints

Given a set of candidate locations for P2P, we select final P2P locations on the basis of feasibility and realism.

Given that our selection of candidate locations accounts for practical factors (e.g., physical accessibility), our assessment of feasibility here focuses on ensuring that the selected pair of P2P locations can support a P2P link. Therefore, we eliminate unfeasible links from further consideration through the following steps:

1. Simulate the propagation path between pairs of candidate locations
2. Eliminate location pairs without necessary line-of-sight

Once we have selected a feasible set of locations for P2P endpoints, we choose the pair that best represents the situation for rural P2P links employed by electric utilities. Here, we focus on achieving a representative link length, as indicated by Figure 3.1.

3.2.4 Determining Interferer Locations

Given a set of candidate locations for interferers and selected locations for P2P endpoints, we select final interferer locations on the basis of feasibility and diversity.

Here our assessment of feasibility focuses on ensuring that interferer locations support getting interference signals to at least one selected P2P location. Therefore, we eliminate unfeasible links from further consideration through the following steps:

1. Simulate the propagation path from an interferer location to selected P2P endpoints
2. Eliminate locations without necessary line-of-sight

As stated above, our goal is to enable investigation of interference injected into a diversity of antenna pattern links. Thus, we simulate the feasible interferer locations against the P2P antenna pattern to confirm the diversity of antenna lobes available for interference injection.

3.2.5 Simulating Propagation Paths

For the selection of both P2P and interferer locations, we assess feasibility via a simulation of the line-of-sight between locations. We determine the line-of-sight by simulating terrain obstructions between locations using the HTZ Warfare software suite. This simulation generates path profiles as exemplified by Figure 3.2.

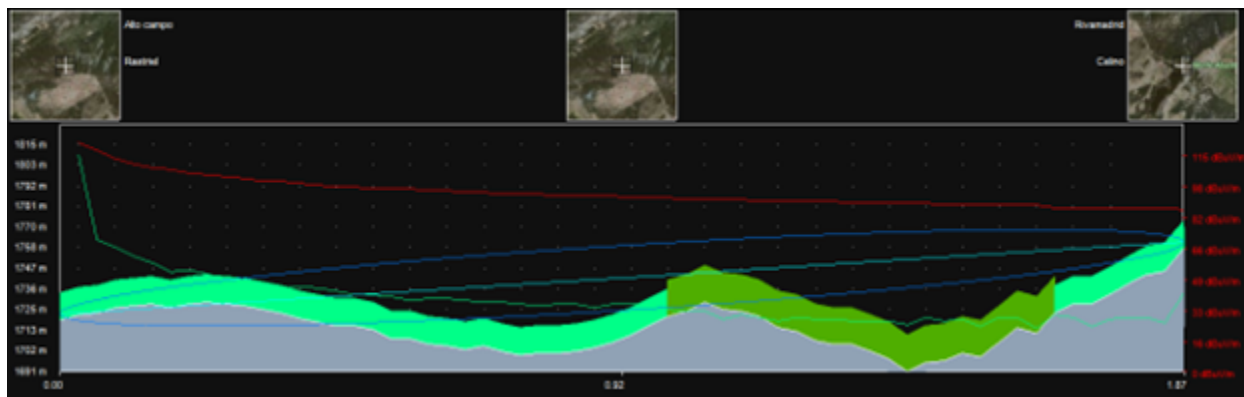


Figure 3.2: Example Path Profile

Path profiles consist of four primary sections: (1) contextual terrain images, (2) the terrain profile, (3) the link diagram, and (4) propagation plots. The latter three of these sections overlap in the central portion of the profile. Each section of the path profile is discussed further below.

The contextual terrain images are positioned at the top of the path profiles. These images provide information about the terrain at critical points along the link path. Three image boxes show these critical points: (1) the terrain at the transmission site (left), (2) the terrain at the link mid-point (middle), and (3) the terrain at the reception site (right).

The terrain profiles are positioned at the bottom of the main section of the path profile. These profiles directly show the ground and clutter levels along the path of the link. The ground level is shown as a solid gray region in the main portion of the plot. Above this the anticipated clutter layer is shown as a solid region of green or blue. This clutter layer is based on the ground-occupancy codes of the terrain and not necessarily reflective of the true physical clutter of the terrain. The scale on the left edge of the main section provides the elevation of the ground or clutter. The scale on the bottom edge of the main section provides the distance along the path from the transmitter to the receiver.

The link diagram is shown as a set of lines in the main section of the path profile. This arrangement directly shows anticipated interaction, or lack thereof, with the ground and clutter displayed in the terrain profiles. The line-of-sight between transmitter and receiver is shown as a green line extending from the transmitter altitude on the left edge of the figure to the receiver altitude on the right edge. Around this line-of-sight, the first Fresnel zone is shown as a purple ellipse. The elevation scale on the left edge applies to

transmitter and receiver positions as well as the line-of-sight and Fresnel zone. The both edge scale regarding the distance from transmitter to receiver also applies to the link diagram.

Finally, the propagation plots are shown as green and red line plots in the main section of the path profile. The signal strength in the case of free space propagation is shown by the red line. The anticipated signal strength given propagation in the modeled environment is shown by the green line. Both of these signal strengths are given in units of dB μ V/m, as reported by the scale on the right side of the main section. The bottom edge scale regarding distance from transmitter to receiver also applies to the propagation plots. For the purposes of our efforts here, the propagation plots are considered secondary to the interaction of the terrain profiles and link diagrams.

Given that our primary interest is determining the feasibility of support clear transmission along the path, we examine one path profile for each pair of locations. That is, we leverage the reciprocity of the propagation path to avoid having to consider each transmission direction between each pair of points. While there will be some pathloss difference related to the two different frequencies employed by the P2P link (i.e., 7390 MHz and 7690 MHz), even these differences are small (i.e., < 0.5 dB) and they do not impact the line-of-sight.

3.3 Results

This section provides the results of the simulation study. Here we discuss three sets of results: (1) candidate locations, (2) P2P locations, and (3) interferer locations. Each of these results sets includes any important intermediary results.

3.3.1 Candidate Locations

This section provides the candidate locations for both the P2P endpoints and the interferer locations. Figure 3.3 shows all the candidate locations considered.



Figure 3.3: Candidate Locations

3.3.1.1 P2P Candidate Locations

We consider four locations for potential P2P endpoints: CFA, Crater, Filmore, and Haul. Each of these are discussed below. The antenna size listed for each location is the maximum feasible antenna for each location.

3.3.1.1.1 CFA Location This location is conveniently located for access at a central point in the INL desert test site. Table 3.1 provides additional details about this location.

3.3.1.1.2 Crater Location This location is positioned on a butte near the INL desert test site. This site provide broad visibility but has limited accessibility. Table 3.2 provides additional details about this location.

Table 3.1: CFA Location Details

Coordinates	43°31'53.48" N, 112°56'41.51" W
Decimal Degrees	43.531522, -112.944864
Antenna Height	9.1 m (30 ft)

Table 3.2: Crater Location Details

Coordinates	43°35'41.40" N, 113°08'59.10" W
Decimal Degrees	43.594844, -113.149736
Antenna Height	4.6 m (15 ft)

3.3.1.1.3 Filmore Location This location is positioned along a road within the INL desert test site. This site is highly accessible. Table 3.3 provides additional details about this location.

Table 3.3: Filmore Location Details

Coordinates	43°31'18.63" N, 112°49'32.12" W
Decimal Degrees	43.521842, -112.825589
Antenna Height	32.3 m (106 ft)

3.3.1.1.4 Haul Location This location is positioned along a road within the INL desert test site. This site is highly accessible. Table 3.4 provides additional details about this location.

Table 3.4: Haul Location Details

Coordinates	43°32'35.49" N, 112°43'38.57" W
Decimal Degrees	43.54319167, -112.72738056
Antenna Height	18.3 m (60 ft)

3.3.1.2 Interferer Candidate Locations

We consider four locations for potential interferer locations, numbered one through four. Each of these are discussed below. The antenna size listed for each location is the maximum feasible antenna for each location.

3.3.1.2.1 Interferer Location 1 This location is positioned along a road within the INL desert test site. This site is highly accessible. Table 3.5 provides additional details about this location.

Table 3.5: Interferer Location 1 Details

Coordinates	43°32'33.52" N, 112°44'7.20" W
Decimal Degrees	43.542644, -112.735333
Antenna Height	9.1 m (30 ft)

3.3.1.2.2 Interferer Location 2 This location is positioned along a road within the INL desert test site. This site is highly accessible. Table 3.6 provides additional details about this location.

3.3.1.2.3 Interferer Location 3 This location is positioned along a road within the INL desert test site. This site is highly accessible. Table 3.7 provides additional details about this location.

Table 3.6: Interferer Location 2 Details

Coordinates	43°32'23.55" N, 112°47'32.73" W
Decimal Degrees	43.539875, -112.792425
Antenna Height	9.1 m (30 ft)

Table 3.7: Interferer Location 3 Details

Coordinates	43°32'8.30" N, 112°49'43.17" W
Decimal Degrees	43.53563889, -112.82865833
Antenna Height	9.1 m (30 ft)

3.3.1.2.4 Interferer Location 4 This location is positioned along a road within the INL desert test site. This site is highly accessible. Table 3.8 provides additional details about this location.

Table 3.8: Interferer Location 4 Details

Coordinates	43°32'51.47" N, 112°43'18.18" W
Decimal Degrees	43.54763056, -112.72171667
Antenna Height	9.1 m (30 ft)

3.3.2 P2P Locations

This section provides results related to the selection of P2P locations. Recall that these locations are selected from the set of candidate locations discussed in Section 3.3.1 on the basis of both feasibility and realism.

3.3.2.1 Feasibility of Locations

Recall that the assessment of feasibility focuses on ensuring that the selected pair of locations can support a P2P through the examination of the path profile between those locations. Here we provide the path profiles for all pairs of candidate P2P locations.

3.3.2.1.1 CFA & Crater Figure 3.4 displays the path profile for this pair of locations.

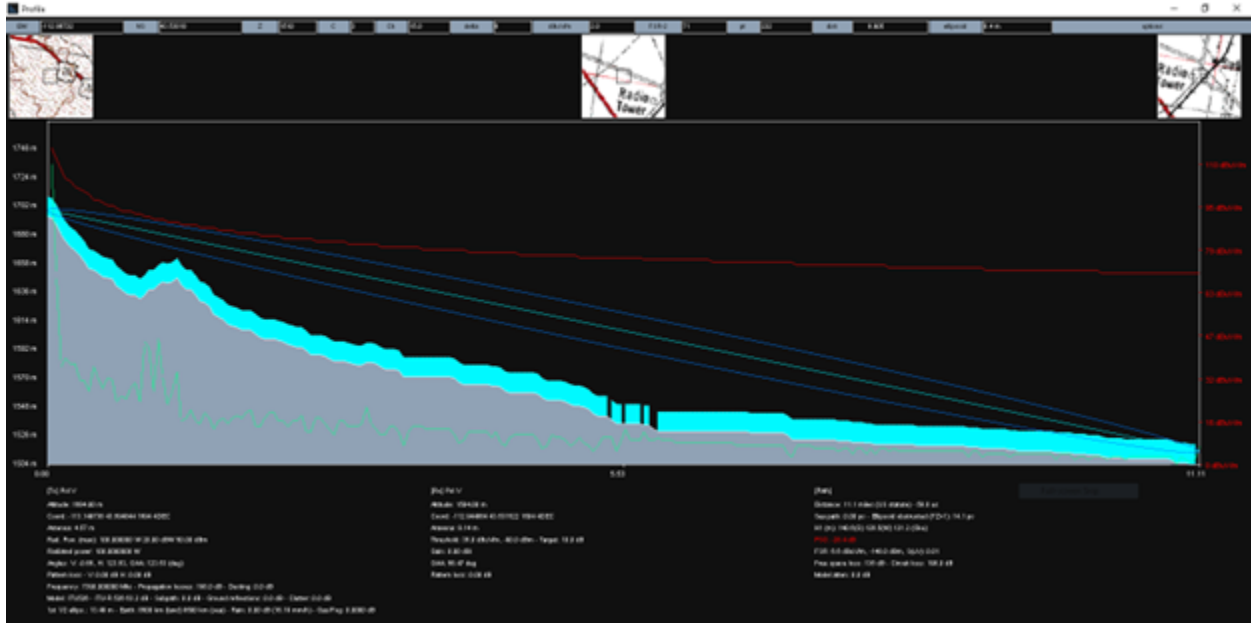


Figure 3.4: Crater to CFA Path Profile

No terrain obstructions exist in this link. Note that the clutter for this region is especially low and lower than the level predicted by the ground-occupancy code.

3.3.2.1.2 CFA & Filmore Figure 3.5 displays the path profile for this pair of locations.

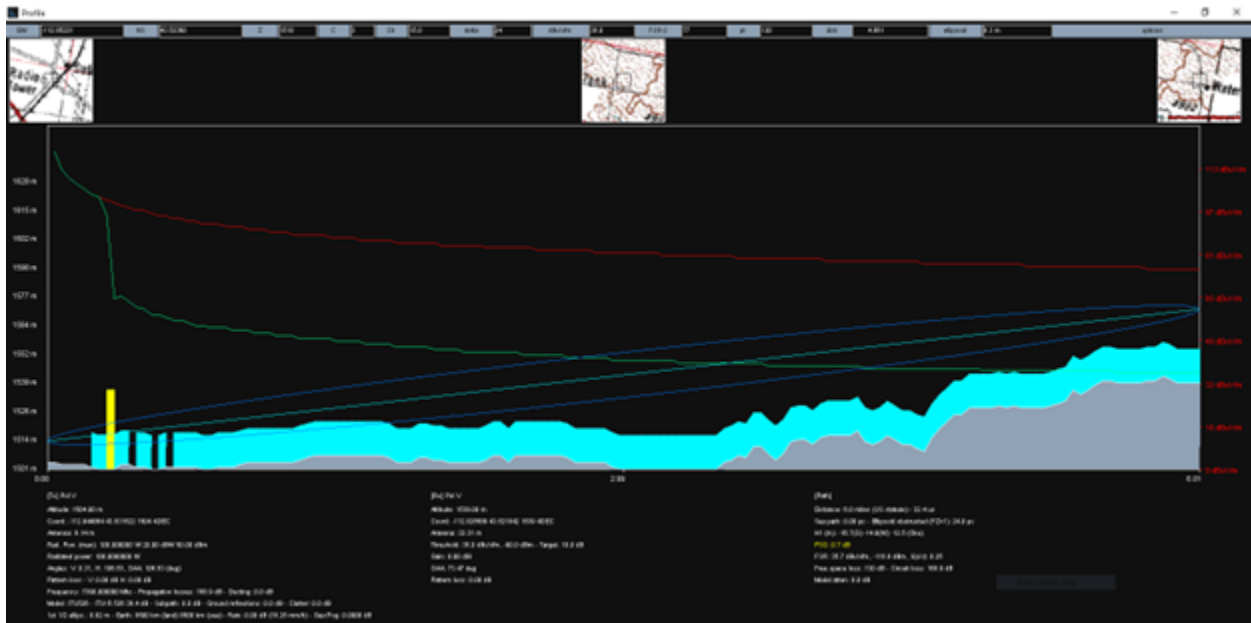


Figure 3.5: CFA to Filmore Path Profile

This path is obstructed by a building and thus this pair is not suitable for a P2P link.

3.3.2.1.3 CFA & Haul Figure 3.6 displays the path profile for this pair of locations.

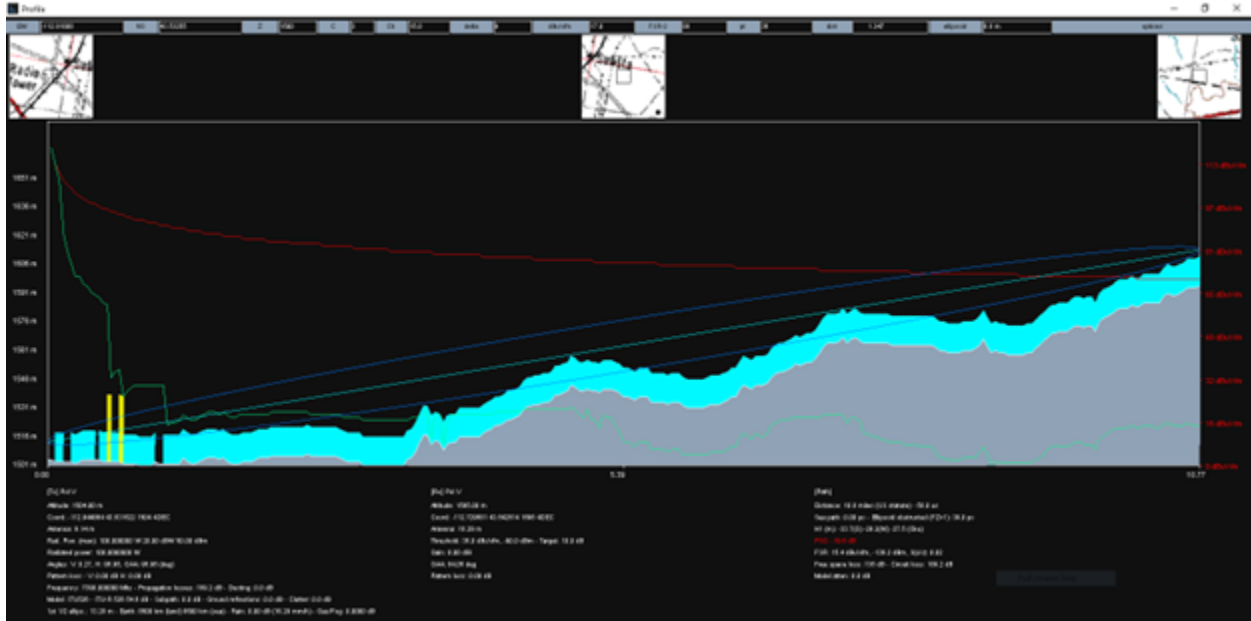


Figure 3.6: CFA to Haul Path Profile

This path is obstructed by a building and thus this pair is not suitable for a P2P link.

3.3.2.1.4 Crater & Filmore Figure 3.7 displays the path profile for this pair of locations.

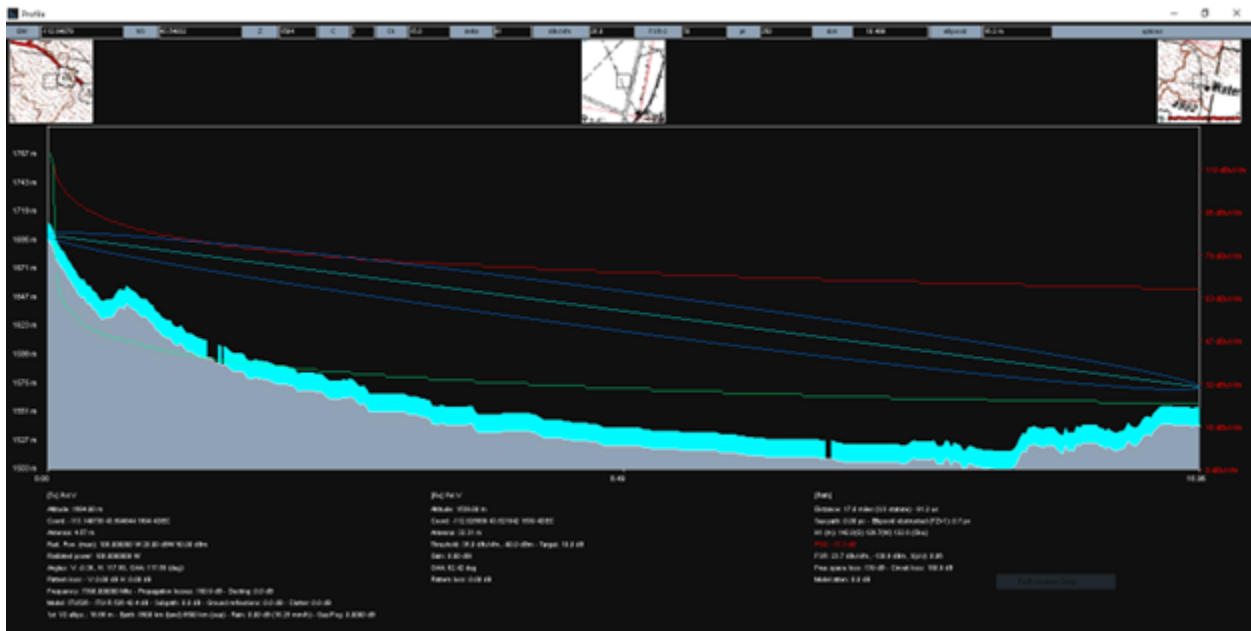


Figure 3.7: Crater to Filmore Path Profile

No terrain obstructions exist in this link. Note that the clutter for this region is especially low and lower than the level predicted by the ground-occupancy code.

3.3.2.1.5 Crater & Haul Figure 3.8 displays the path profile for this pair of locations.

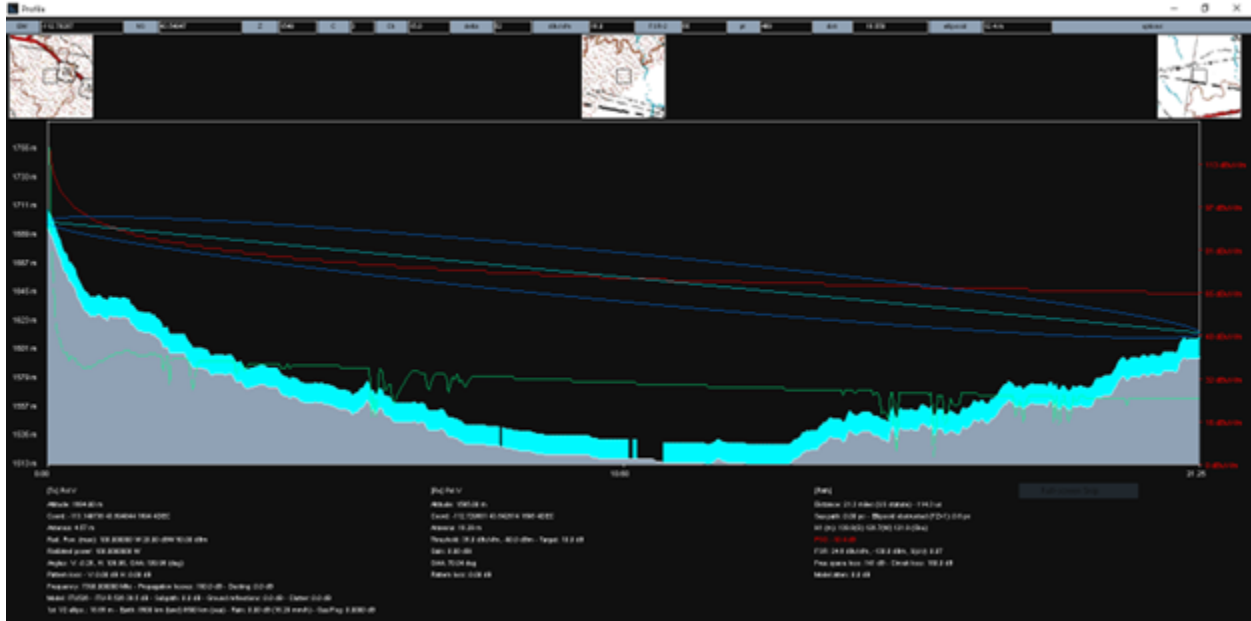


Figure 3.8: Crater to Haul Path Profile

No terrain obstructions exist in this link. Note that the clutter for this region is especially low and lower than the level predicted by the ground-occupancy code.

3.3.2.1.6 Filmore & Haul Figure 3.9 displays the path profile for this pair of locations.



Figure 3.9: Filmore to Haul Path Profile

No terrain obstructions exist in this link. Note that the clutter for this region is especially low and lower than the level predicted by the ground-occupancy code.

3.3.2.2 Final Selection

Table 3.9 provides a summary of all potential pairs of candidate P2P locations.

Table 3.9: Summary of Candidate P2P Location Pairs

Location Pair	Distance (miles)	Comment
CFA & Crater	11.1	No obstructions
CFA & Filmore	6.0	Path obstructed
CFA & Haul	10.9	Path obstructed
Crater & Filmore	17.0	No obstructions
Crater & Haul	21.5	No obstructions
Filmore & Haul	5.2	No obstructions

This analysis shows that both the CFA & Filmore and CFA & Haul pairs lack a clear line of site and thus are excluded from further consideration.

Considering that most real P2P links in the 7 GHz band are 10 miles or less in length (see Figure 3.1), Filmore & Haul present the most realistic option as the only pair less than 10 miles apart. Further considering that both the Filmore and Haul locations are easily accessible, we select these locations as the final P2P location.

3.3.3 Interferer Locations

This section provides results related to the selection of interferer locations. Recall that these locations are selected from the set of candidate locations discussed in Section 3.3.1 on the basis of both feasibility and diversity.

3.3.3.1 Feasibility of Locations

Recall that the assessment of feasibility focuses on ensuring that the selected interferer locations can support getting interference signals to one of the two selected P2P locations. Here we provide the path profiles from each candidate interferer location to both selected P2P locations.

3.3.3.1.1 Interferer Location 1 Figure 3.10 displays the path profile from interferer location 1 to the Filmore location.

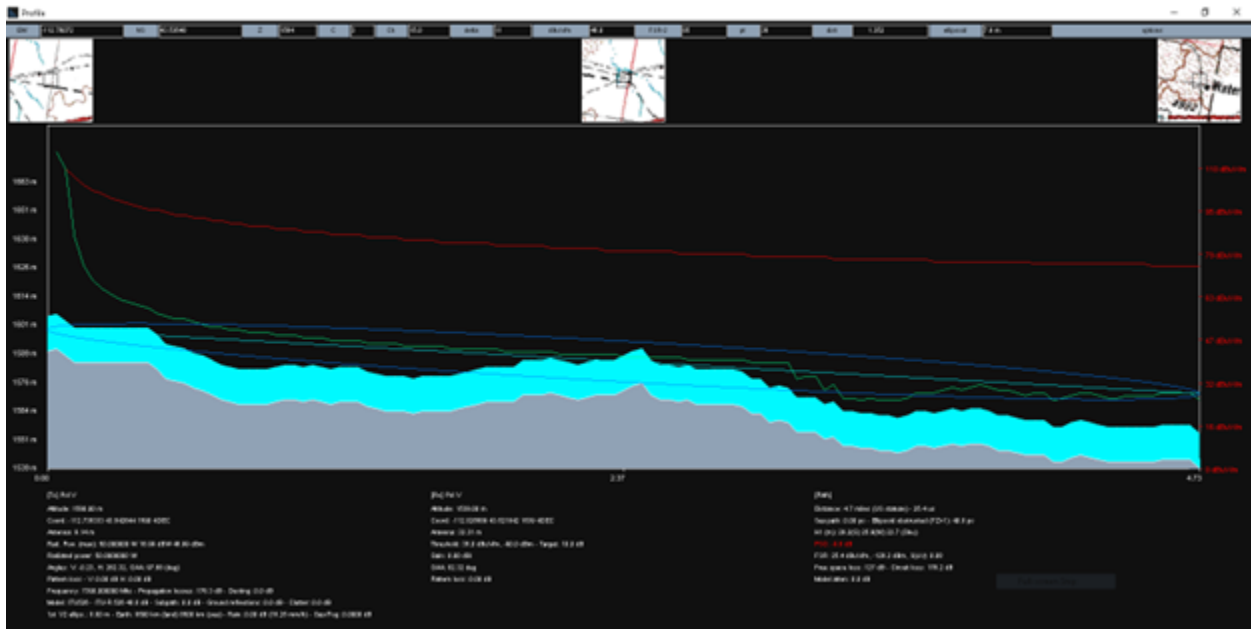


Figure 3.10: Interferer Location 1 to Filmore Path Profile

While this path potentially features a minor terrain obstruction, review of the physical site indicates that this obstruction is unlikely to be problematic for our use.

Figure 3.11 displays the path profile from interferer location 1 to the Haul location.

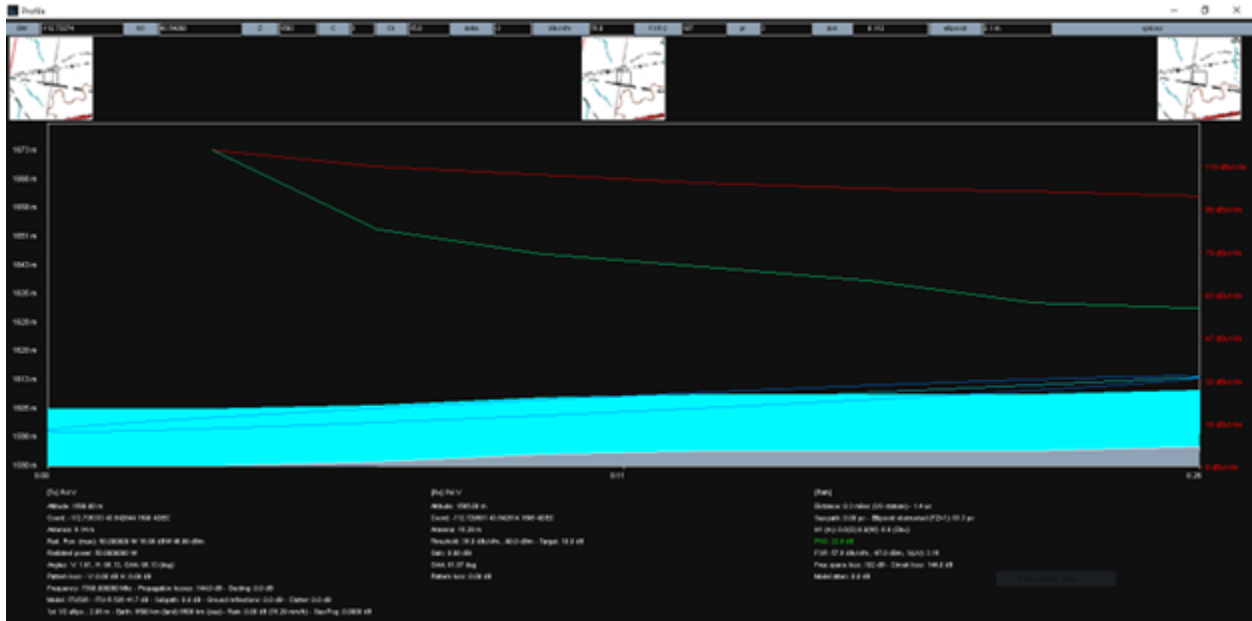


Figure 3.11: Interferer Location 1 to Haul Path Profile

No terrain obstructions exist in this link. Note that the actual clutter is lower than what is indicated by the ground-occupancy code.

3.3.3.1.2 Interferer Location 2 Figure 3.12 displays the path profile from interferer location 2 to the Filmore location.

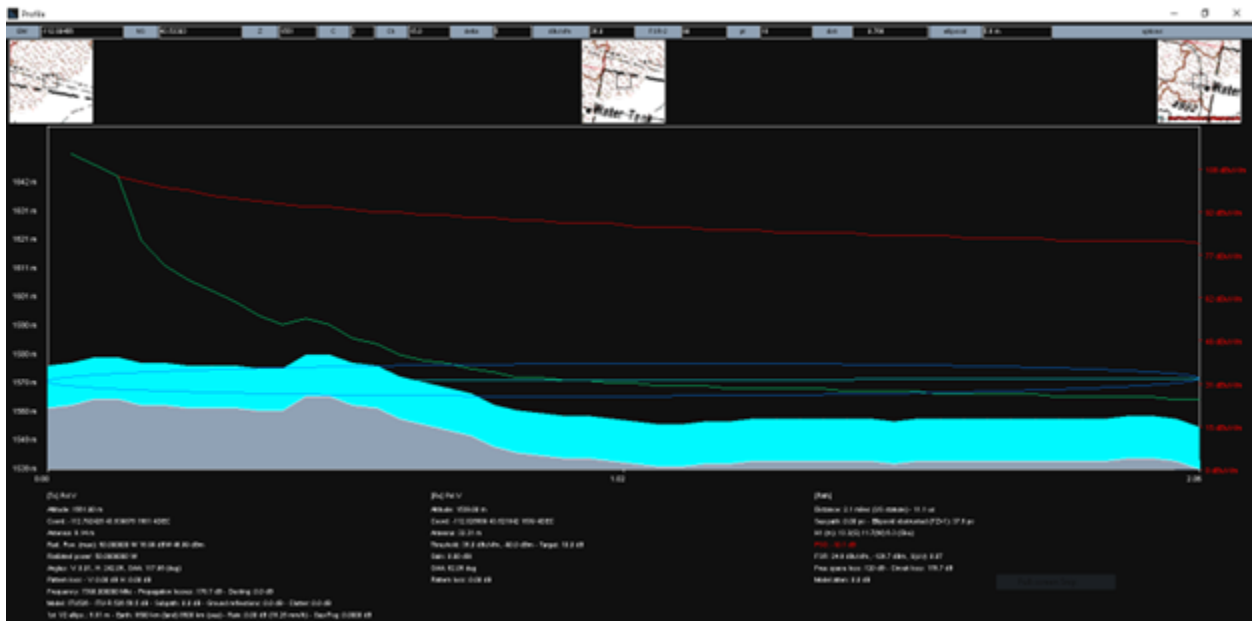


Figure 3.12: Interferer Location 2 to Filmore Path Profile

While this path potentially features a minor terrain obstruction, review of the physical site indicates that this obstruction is unlikely to be problematic for our use.

Figure 3.13 displays the path profile from interferer location 2 to the Haul location.

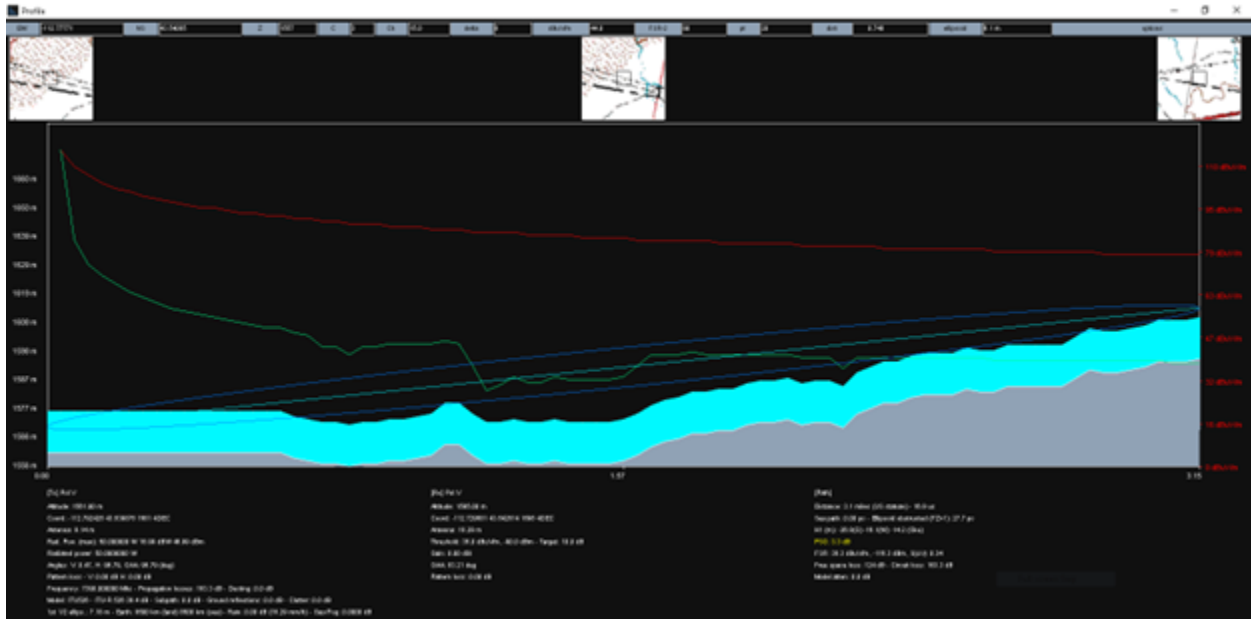


Figure 3.13: Interferer Location 2 to Haul Path Profile

No terrain obstructions exist in this link. Note that the actual clutter is lower than what is indicated by the ground-occupancy code.

3.3.3.1.3 Interferer Location 3 Figure 3.14 displays the path profile from interferer location 3 to the Filmore location.

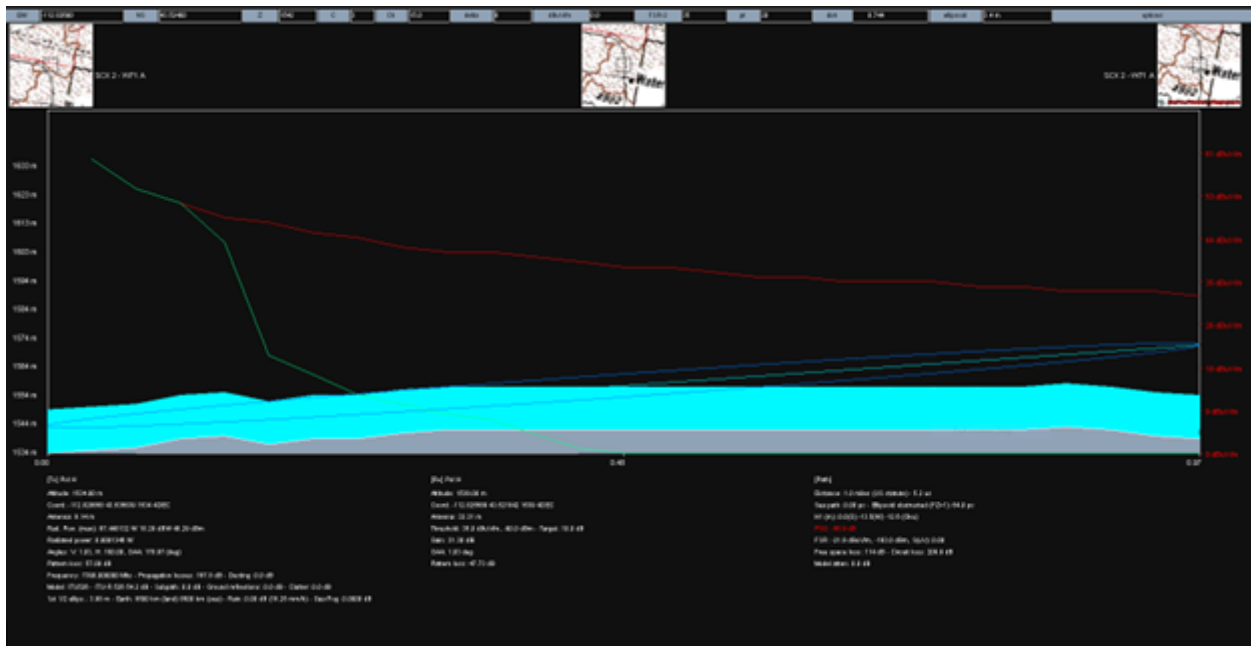


Figure 3.14: Interferer Location 3 to Filmore Path Profile

No terrain obstructions exist in this link. Note that the actual clutter is lower than what is indicated by the ground-occupancy code.

Figure 3.15 displays the path profile from interferer location 3 to the Haul location.

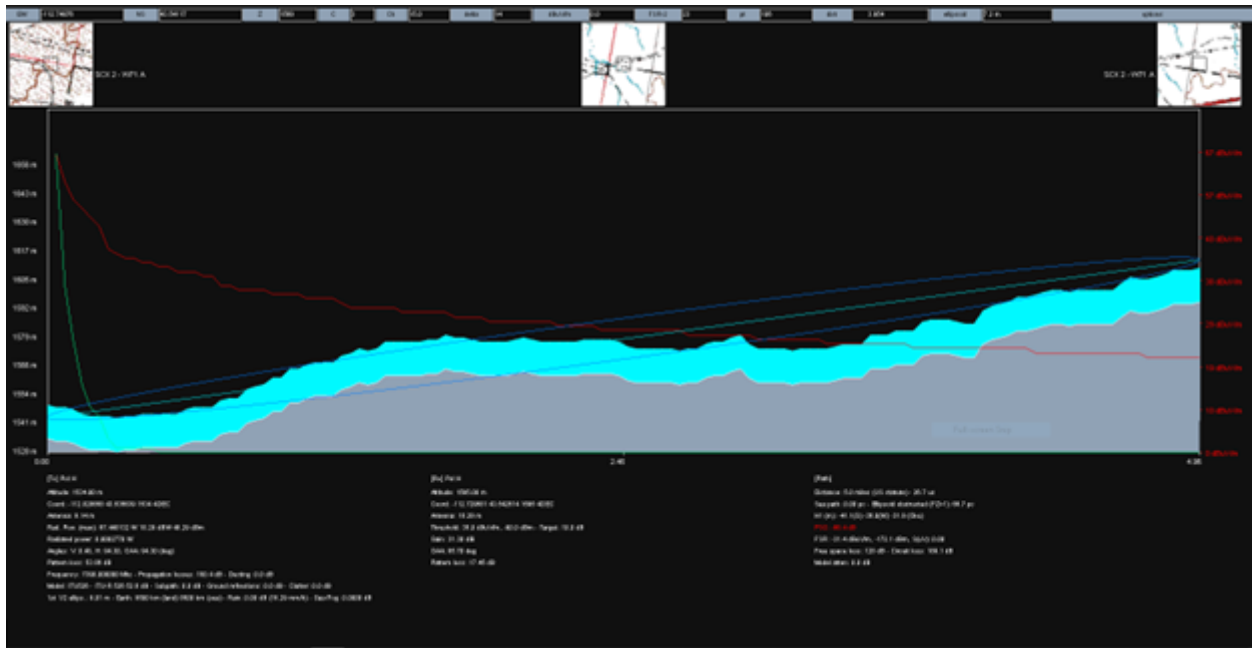


Figure 3.15: Interferer Location 3 to Haul Path Profile

This path is partially obstructed by still provides a pathway for interference that may occur in practical situations.

3.3.3.1.4 Interferer Location 4 Figure 3.16 displays the path profile from interferer location 4 to the Filmore location.

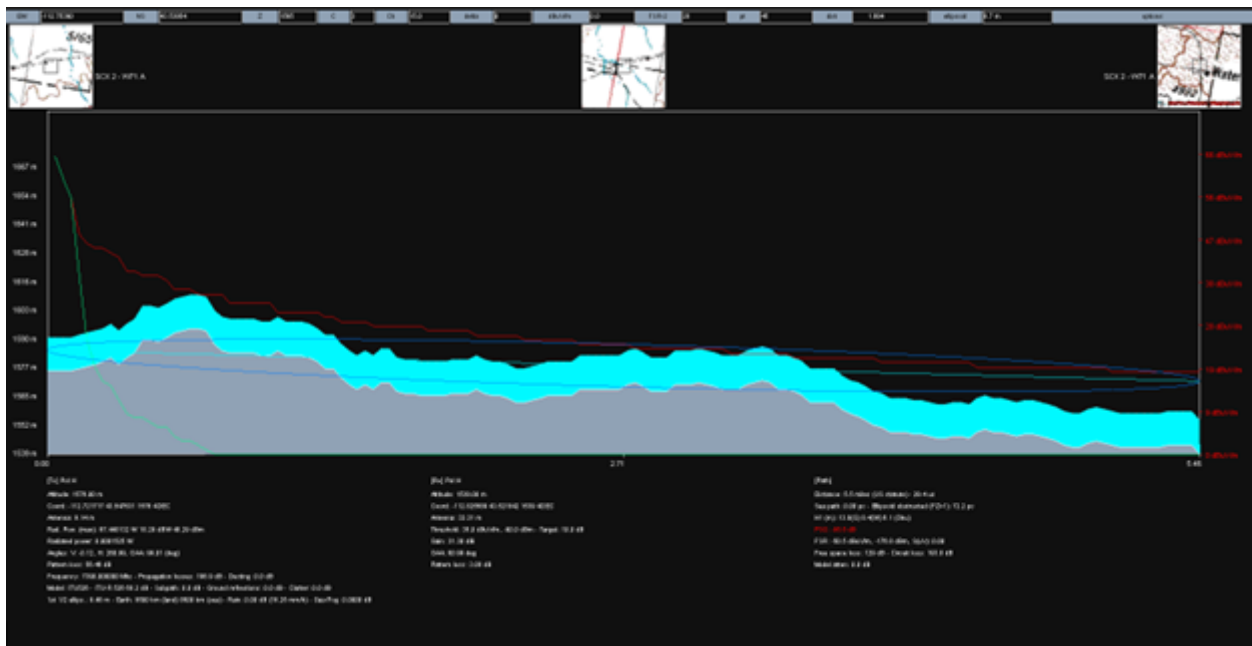


Figure 3.16: Interferer Location 4 to Filmore Path Profile

This path is obstructed by terrain and thus is unlikely to support effective use for interference generation into Filmore.

Figure 3.17 displays the path profile from interferer location 4 to the Haul location.

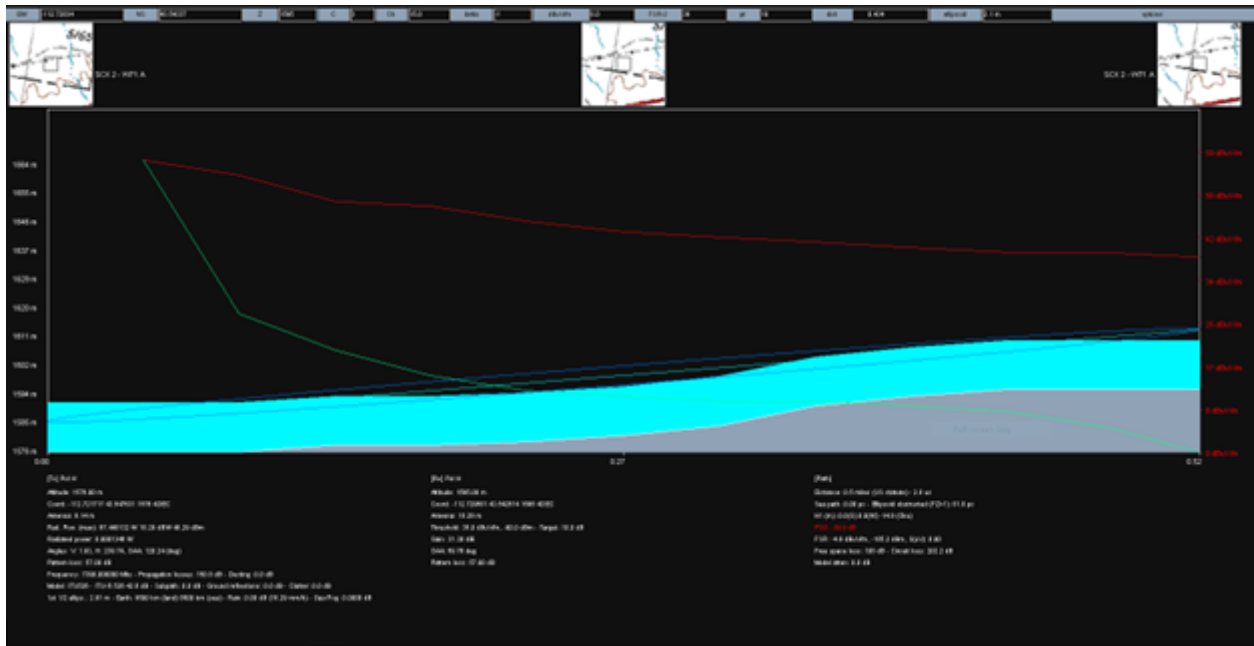


Figure 3.17: Interferer Location 4 to Haul Path Profile

No terrain obstructions exist in this link. Note that the actual clutter is lower than what is indicated by the ground-occupancy code.

3.3.3.2 Diversity of Locations

This section discusses the diversity of interferer locations relative to the P2P antenna patterns. For this analysis we consider the pattern of an Aviat AND-VHLP2-7W-GTU 2 ft antenna, operating with vertical polarization. Figure 3.18 shows the antenna pattern from the perspective of the Filmore P2P location. Figure 3.19 shows the antenna pattern from the perspective of the Haul P2P location. In each of these figures the interferer locations are marked with green squares.

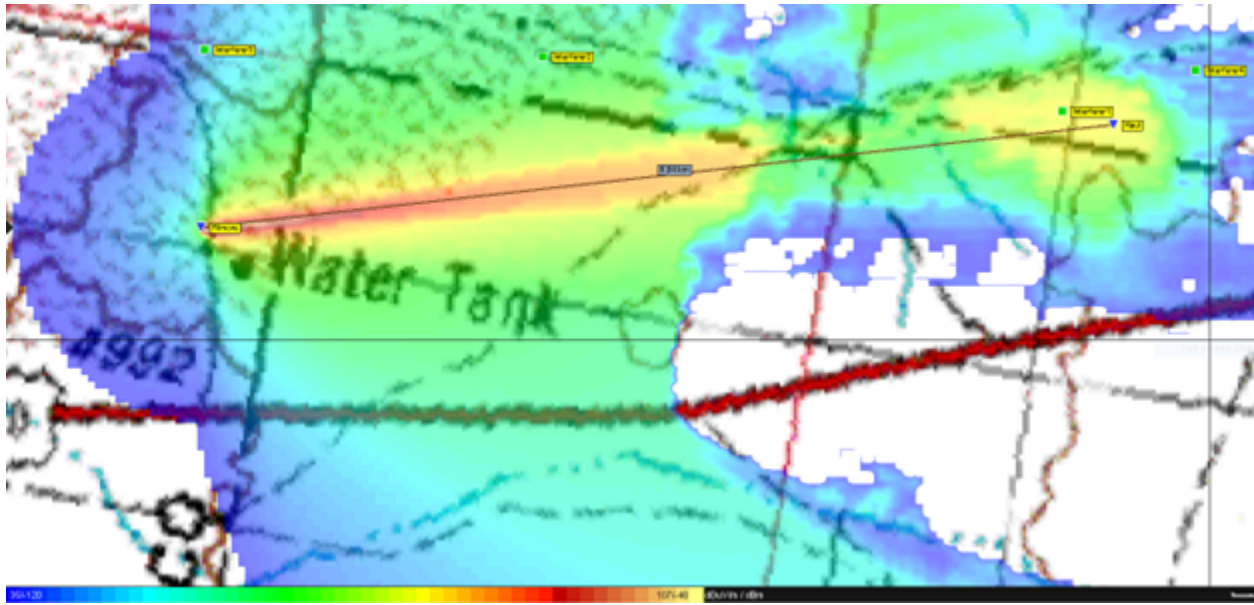


Figure 3.18: Antenna Pattern from Filmore P2P Location

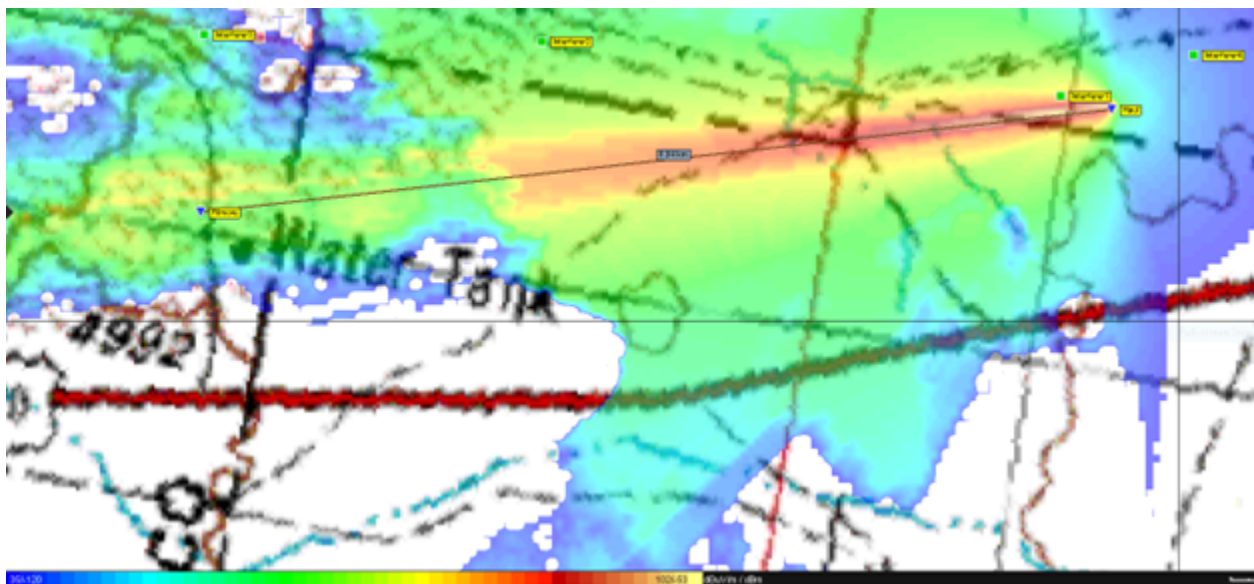


Figure 3.19: Antenna Pattern from Haul P2P Location

Based on the above analysis the antenna patterns, the set of interferer locations provide a variety of options for injecting interference into various P2P antenna lobes.

3.3.3.3 Final Selection

Table 3.10 summarizes both the feasibility and diversity of the candidate interferer locations.

This analysis shows that all candidate interferer locations provide value for investigating different antenna lobes for at least one P2P location. Certainly interferer location 1 provides a primary location for injecting interference on the P2P link but each other location provides additional capability for investigating the impact of the antenna patterns on the vulnerability of the P2P link to interference.

Table 3.10: Summary of Interferer Location Feasibility and Diversity

Interferer Location	Path to Filmore	Path to Haul	Filmore Lobe	Haul Lobe
Interferer 1	Unobstructed	Unobstructed	Main	Main
Interferer 2	Unobstructed	Unobstructed	Primary Side	Primary Side
Interferer 3	Unobstructed	Partially Obstructed	Secondary Side	Beyond Primary Side
Interferer 4	Obstructed	Unobstructed	Beyond Main	Back

3.4 Conclusions

This section provides the conclusions of the site selection simulation study. Here we indicate the locations that we have selected for subsequent testing and the reasoning for these selections.

Based on the examination of candidate locations, we have selected the Filmore and Haul locations as the P2P endpoints. Primarily these two locations have good mutual line-of-sight for establishing the P2P link. The distance between these locations is 8.3 kilometers (5.2 miles), which is typical for P2P links in the 7 GHz band. This distance does not require large antennas that generate excessive wind load. Importantly these locations also provide good line-of-sight to nearly all the candidate interference locations. This enables interference injection across the P2P antenna pattern including the main lobe, side lobes, and a back lobe.

Given the selected P2P endpoint locations, we will leverage all four of the candidate interferer locations. Interferer location 1 provides the opportunity to inject interference into the main lobe of both P2P endpoints at 7.6 kilometers (4.7 miles) from Filmore and 0.6 kilometers (0.4 miles) from Haul. Interferer location 2 allows injecting interference into the secondary lobes of both P2P endpoints at 3.4 kilometers (2.1 miles) from Filmore and 5.3 kilometers (3.3 miles) from Haul. Interferer location 3 allows injecting interference into a tertiary lobe of Filmore at a distance of 1.6 kilometers (1.0 miles) and potentially into the secondary lobe of Haul at a distance of 8.2 kilometers (5.1 miles). Interferer location 4 allows interjecting interference into the back lobe of Haul at a distance of 0.7 kilometers (0.4 miles). This collection of interferer locations allows exploration of a range of interference injection geometries.

4 Simulation Study for Parameter Selection

This section reports on the simulation study examining the parameter ranges for both the P2P link and interferers that should be investigated during open-range testing. This study identifies the expected link margins the P2P link for each operational paradigm. Additionally, this study identifies the range of interference power that is expected to produce observable impacts on the P2P link for each interferer location. Finally, this study identifies the maximum expected impact of interference power on the P2P link for each interferer's location.

4.1 Tools Used

This simulation study utilizes the following tools:

- Link budget spreadsheet
- HTZ Warfare software suite¹
 - ITU256 - ITU-R 526 propagation model

The additional contextual considerations for this study include:

- This study examines the locations discussed in Section 2.4
- Terrain data from ATDI² is considered.
- The manufacturer provided beam pattern for our intended antenna is considered.
- No weather data is considered.
- No external interference sources are considered.

4.2 Methodology

This section outlines the methods used to accomplish this study and the cases considered by this study.

4.2.1 Overall Approach

This study comprises two phases: (1) P2P modeling and (2) interferer modeling.

The P2P modeling phase examines the feasible operating range of the P2P link without interferers. There are two goals for this phase:

1. Estimate the expected loss along the P2P link.
2. Estimate the range of feasible operating margins for each P2P paradigm discussed in Section 2.1.3.

¹<https://atdi.com/products-and-solutions/htz-warfare/>

²<https://atdi.com/map-data-library/>

The interferer modeling phase estimates the impact of the interferer on the P2P link. There are two goals for this phase:

1. Estimate the expected loss from each interferer location to each P2P receiver, including impact of the P2P antenna.
2. Identify the range of interference powers that should be examined during open-range testing.

4.2.2 P2P Modeling

The P2P modeling phase comprises both an analysis of the expected path loss for the link and the feasible operating margins. We discuss our approach to each of these here.

4.2.2.1 P2P Path Loss

Modeling the P2P path loss involves simulating the propagation of a P2P along the path from P2P transmitter to receiver in order to estimate the attenuation experienced by the signal. Here, we assume that the P2P transmitter and receiver antenna are well-pointed such that there is no loss associated with misaligned antennas. Further, we assume that there is no adverse weather that would significantly impact the propagation. Finally, we assume there is an unobstructed path between transmitter and receiver with low clutter. Based on these considerations, we calculate the expected P2P path loss with the HTZ Warfare software. This program uses global positioning system (GPS) locations, terrain data, and the ITU256 - ITU-R 526 channel model to calculate the path loss.

4.2.2.2 P2P Margins

Here, we define the operating margin as the difference between the achieved SNR and the SNR threshold for a given operating paradigm³. There are two conditions that must be met to declare a given margin as feasible: (1) the associated transmission power must be within the limits for the given paradigm and (2) the associated received power must be below the saturation threshold. Recall that Table 2.2 provides the minimum P2P transmission power and Table 2.4 provides the maximum P2P transmission power for each paradigm. Additionally, Table 2.2 provides the P2P saturation threshold.

We employ link budgets to determine the range of feasible P2P operating margins for each operating paradigm discussed in Section 2.1.3. Our approach has three steps: (1) determine the range of feasible received powers, (2) determine the range of feasible achieved SNR, and (3) determine the range of feasible margins. We repeat all three steps for each P2P paradigm.

We use Equation 4.1 to determine the range of feasible received powers:

$$P_{P2P Rx} = P_{P2P Tx} + 2G_{P2P} - L_{P:Filmore,Haul} \quad (4.1)$$

We define each term of Equation 4.1 below:

- $P_{P2P Rx}$ is the achieved receive power for the P2P link in dBm
- $P_{P2P Tx}$ is the selected transmit power for the P2P link in dBm. For our purposes here, we set this value to either the minimum P2P transmission power or the maximum P2P transmission power for a given paradigm.
- $2G_{P2P}$ is the antenna gain for the P2P link in dB. Note that this term includes both the transmitter and receiver antenna gains for the P2P link.
- $L_{P:Filmore,Haul}$ is the path loss between the Filmore and Haul locations in dB.

We use the Equation 4.2 to determine the range of feasible achieved SNR:

$$S_{achieved} = P_{P2P Rx} - N_{P2P} \quad (4.2)$$

We define each term of Equation 4.2 below:

³See Section 2.1.3 for a definition of the SNR Threshold

- $S_{achieved}$ is the achieved SNR for the P2P link in dB.
- $P_{P2P Rx}$ is the achieved receive power calculated with Equation 4.1 in dBm.
- N_{P2P} is the P2P noise floor in dBm. This value is reported in Table 2.2.

We use the Equation 4.3 to determine the range of feasible operating margins:

$$M_{P2P} = S_{achieved} - S_{thres} \quad (4.3)$$

We define each term of Equation 4.3 below:

- M_{P2P} is the operating margin of the P2P link in dB.
- $S_{achieved}$ is the achieved SNR calculated with Equation 4.2 in dB.
- S_{thres} is the SNR threshold for the given paradigm. This value is reported for each paradigm in Table 2.4.

4.2.3 Interferer Modeling

The interferer modeling phase comprises both an analysis of the losses that can be expected from each interferer location to each P2P location and the meaningful range of interference powers. We discuss our approach to each of these here.

4.2.3.1 Interferer Loss

Modeling the losses experienced by interference signals involves simulating the propagation from each interferer location to each P2P location to estimate the attenuation that can be expected. Here, we assume no adverse weather and utilize the HTZ Warfare software, along with the ITU256 - ITU-R 526 channel model, to calculate the path loss between interferer and P2P locations. Beyond this we also consider the impact of the P2P antennas.

All transmitters and receivers use directional antennas, so gain is expected from both the transmitting and receiving antennas. Further our approach to testing involves aiming each transmitter directly at its intended receiver, so no loss is expected related to misalignment of the transmitting antenna. However, since both P2P antennas are pointed at each other, interference signals experience some loss associated with the use of antenna sidelobes at the receiver. Determining the amount of this loss involves first determining the angle at which interference signals will hit the P2P receiver and then assessing the reduction in antenna gain associated with this angle. These steps are discussed in detail below.

The interference reception angles are calculated by using the "Orient Antennas" feature in the HTZ Warfare suite which points the antennas in the direction of selected locations. After pointing the antennas at the relevant locations, the antenna angle orientation is recorded. This is done for all relevant antenna locations to get the sidelobe angles for each interferer locations relative to both P2P locations.

Sidelobe attenuation is calculated using the antenna model provided by the antenna manufacturer. This antenna model file contains radiation pattern envelope (RPE) data which outlines the radiation pattern envelope of the antenna. The radiation pattern shows how much a signal is attenuated based on the receive angle.

4.2.3.2 Interferer Powers

Here we determine the range of interference powers that could feasibly impact the P2P link during open-range testing by applying link budgets. For this analysis, we consider the P2P link to be impacted when the received interference power is sufficient to push the BER above the 1×10^{-6} threshold. We determine the level of interference power required for this impact across all feasible operating margins for each P2P paradigm. Given the interference generation method discussed in Section 2.2.3, we declare an interference power to be feasible if the required input to the interferer antenna is less than or equal to the 1 dB compression of either interference amplifier, as reported in Table 2.10.

Our interferer analysis has three steps: (1) determine the amount of interference power that must be received at the P2P receiver to impact the P2P link, (2) determine the amount of interference power that must be transmitted from each location to achieve the received interference power, and (3) assess the feasibility of the transmitted interference power level. We work through these steps for each P2P paradigm.

We use the Equation 4.4 to determine the amount of interference power that must be received at the P2P receiver to impact the P2P link:

$$P_{Int Rx thres} = M_{P2P} + N_{P2P} \quad (4.4)$$

We define each term of Equation 4.4 below:

- $P_{Int Rx thres}$ is the interference power that must be received at the P2P receiver to impact the P2P link in dBm.
- M_{P2P} is the operating margin of the P2P link targeted by the interference in dB.
- N_{P2P} is the noise floor of the P2P link in dBm.

Note that this analysis considers the P2P operating margin as the input and is not impacted by the location of the interferer. Further, this approach allows us to consider the same approach across all P2P paradigms by focusing on the operating margin rather than specific thresholds. Below we show how we arrive at Equation 4.4:

- Recall that $S_{achieved} = P_{P2P Rx} - N_{P2P}$ (see Equation 4.2)
- Additionally recall that $M_{P2P} = S_{achieved} - S_{thres}$ (see Equation 4.3)
- We define $P_{Int Rx thres} = P_{P2P Rx} - S_{thres}$.
 - That is the interference power that must be received at the P2P receiver to impact the P2P link is the difference between the P2P signal power and the minimum P2P SNR required to achieve a BER of 1×10^{-6} or better.
 - This is true because the interference signal effectively increases the amount of noise at the P2P receiver.
 - Thus, the amount of interference power necessary to push the P2P BER to 1×10^{-6} matches the P2P received signal power less the required distance from the noise floor.
- Combining the first lines and reorganizing gives us $S_{thres} = P_{P2P Rx} - N_{P2P} - M_{P2P}$
- Applying the prior result to our definition gives us $P_{Int Rx thres} = P_{P2P Rx} - (P_{P2P Rx} - N_{P2P} - M_{P2P})$
- Simplifying yields Equation 4.4

We use the Equation 4.5 to determine the amount of interference power that must be transmitted from a given location to impact the P2P link:

$$P_{Int Tx thres;i,j} = P_{Int Rx thres} + L_{P:i,j} + L_{S:i,j} - G_{P2P} - G_{Int} \quad (4.5)$$

We define each term of Equation 4.5 below:

- $P_{Int Tx thres;i,j}$ is the interference power that must be transmitted from location i toward the P2P receiver at location j to impact the P2P link in dBm.
- $P_{Int Rx thres}$ is the interference power that must be received at a P2P receiver to impact the P2P link, calculated by Equation 4.4, in dBm.
- $L_{P:i,j}$ is the path loss from location i to location j in dB.
- $L_{S:i,j}$ is the sidelobe attenuation from location i to location j in dB.

- G_{P2P} is the gain of the P2P antenna in dB. This value is reported in Table 2.2.
- G_{Int} is the gain of the interferer antenna in dB. This value is reported in Table 2.10.

Note that we also report the EIRP that corresponds to $P_{IntTx\,thres;i,j}$. Equation 4.6 shows how this EIRP is calculated.

$$P_{Int\,EIRP\,thres;i,j} = P_{IntTx\,thres;i,j} + G_{Int} \quad (4.6)$$

Once we have determined the amount of interference power that must be transmitted, we can determine whether this power is feasible to generate. Specifically, we define transmission power levels at or below the 1 dB compression point of either interference amplifier (see Table 2.10) as being feasible to generate. Note that this is a maximal condition across all interference signals; some interference signals will not be able to reach this power level in practice. For example, 5G signals generally have a peak to average power ratio (PAPR) of 15 dB and thus typically operate with an average power 15 dB below the compression point to avoid undue distortion. We seek to avoid distortion to ensure that our interference signals maintain their distinctive structure.

4.3 Results

This section provides the results of the simulation study. Here we discuss the results for both the P2P modeling and interferer modeling phases.

4.3.1 P2P Results

This section discusses the results of the P2P modeling phase. We first discuss the results of P2P path loss modeling and then we cover the P2P operating margin analysis.

4.3.1.1 P2P Path Loss

Table 4.1 provides the path loss results for the P2P link. Note that this loss is dominated by the free-space loss due to the largely clutter free nature of the environment of testing.

Table 4.1: P2P Path Loss

Transmit Location	Receive Location	Frequency	Path Loss
Filmore	Haul	7390 MHz	128.3 dB
Haul	Filmore	7690 MHz	128.6 dB

Given the similarity of the path loss in each direction, subsequent analysis will utilize a symmetric loss of 128.5 dB for the P2P link.

4.3.1.2 P2P Margins

Here we discuss the results of the P2P operating margin analysis. To determine the range of feasible operating margins we applied the link budget analysis described in Section 4.2.2.2 to the minimum, mid-point, and maximum P2P transmission powers for each P2P operating paradigm. Table 4.2 provides the results for the low-rate paradigm. Table 4.3 provides the results for the mid-rate paradigm. Table 4.4 provides the results from the high-rate paradigm. Below we describe each column for these tables:

- Tx Pwr (dBm) is the transmit power of the P2P link. The values in this column are in dBm.
- Tx Pwr (Watts) is the transmit power of the P2P link. The values in this column are in Watts. These values are provided for convenience.
- EIRP (dBm) is the EIRP of the P2P link. The values in this column are in dBm.

- EIRP (Watts) is the EIRP of the P2P link. The values in this column are in Watts. These values are provided for convenience.
- Rx Pwr (dBm) is the P2P signal power at the P2P receiver. The values in this column are in dBm.
- Rx Pwr (Watts) is the P2P signal power at the P2P receiver. The values in this column are in Watts. These values are provided for convenience.
- SNR (dB) is the achieved P2P SNR. The values in this column are in dB.
- Margin (dB) is the achieved operating margin for the P2P link. The values in this column are in dB.

Table 4.2: Low-Rate Paradigm Operating Margins

Tx Pwr (dBm)	Tx Pwr (Watts)	EIRP (dBm)	EIRP (Watts)	Rx Pwr (dBm)	Rx Pwr (Watts)	SNR (dB)	Margin (dB)
11.5	1.4×10^{-2}	42.6	1.8×10^{-6}	-54.8	3.3×10^{-9}	36.2	34.7
21.0	0.13	52.1	1.6×10^2	-45.3	3.0×10^{-8}	45.7	44.2
30.5	1.1	61.6	1.5×10^3	-35.8	2.6×10^{-7}	55.2	53.7

Table 4.3: Mid-Rate Paradigm Operating Margins

Tx Pwr (dBm)	Tx Pwr (Watts)	EIRP (dBm)	EIRP (Watts)	Rx Pwr (dBm)	Rx Pwr (Watts)	SNR (dB)	Margin (dB)
11.5	1.4×10^{-2}	42.6	1.8×10^{-6}	-54.8	3.3×10^{-9}	36.2	20.7
20.0	0.10	51.1	1.3×10^2	-46.3	2.3×10^{-8}	44.7	29.2
28.5	0.71	59.6	9.1×10^2	-37.8	1.7×10^{-7}	53.2	37.7

Table 4.4: High-Rate Paradigm Operating Margins

Tx Pwr (dBm)	Tx Pwr (Watts)	EIRP (dBm)	EIRP (Watts)	Rx Pwr (dBm)	Rx Pwr (Watts)	SNR (dB)	Margin (dB)
11.5	1.4×10^{-2}	42.6	1.8×10^{-6}	-54.8	3.3×10^{-9}	36.2	1.2 ⁴
18.5	7.1×10^{-2}	49.6	9.1×10^1	-47.8	1.7×10^{-8}	43.2	8.2
25.5	0.36	56.6	4.6×10^2	-40.8	8.3×10^{-8}	50.2	15.2

4.3.2 Interferer Results

This section discusses the results of the interferer modeling phase. We first discuss the results of propagation losses for interference signals. Then we discuss the range of interference powers that we anticipate will impact the P2P link.

4.3.2.1 Interferer Loss

Table 4.5 provides the propagation loss results from each interferer location to each P2P location. Similarly to the P2P case, the path loss here is dominated by the free-space loss due to the largely clutter free nature of the environment of testing.

Note that the losses from interferer location four to Filmore are not include because this path is significantly obstructed by terrain.

⁴We note that this margin is likely below what would be typically used in practice. We consider this value primarily as a limiting value.

Table 4.5: Interferer Propagation Loss

Transmit Location	Receive Location	Frequency	Path Loss	Sidelobe Angle	Sidelobe Loss
Interferer 1	Filmore	7690 MHz	127.0 dB	0.8°	0.4 dB
Interferer 1	Haul	7390 MHz	102.0 dB	15.0°	23.0 dB
Interferer 2	Filmore	7690 MHz	120.0 dB	21.1°	26.0 dB
Interferer 2	Haul	7390 MHz	124.0 dB	13.7°	20.0 dB
Interferer 3	Filmore	7690 MHz	114.0 dB	83.1°	47.0 dB
Interferer 3	Haul	7390 MHz	128.0 dB	11.2°	17.0 dB
Interferer 4	Haul	7390 MHz	108.0 dB	156.6°	57.0 dB

4.3.2.2 Interferer Powers

Here we discuss the range of interference powers that could feasibly impact the P2P link during open-range testing. Recall from Section 4.2.3.2 that this analysis has three steps: (1) determining the amount of interference power necessary at the P2P receiver, (2) determining the amount of transmit power that should be transmitted from each interferer location, and (3) assessing the feasibility of impacting P2P margins based on the required transmit power. We discuss the results of each step here.

Table 4.6 provides the interference power required at the P2P receiver to impact the P2P link for each operating margin shown in Section 4.3.1.2. This set of margins covers the full set of feasible P2P margins across all paradigms.

Table 4.6: Required Interference Power at the P2P Receiver

P2P Margin (dB)	Power at P2P Receiver (dBm)	Power at P2P Receiver (Watts)
1.2	-89.8	1.1×10^{12}
8.2	-82.8	5.3×10^{-12}
15.2	-75.8	2.6×10^{-11}
20.7	-70.3	9.4×10^{-11}
29.2	-61.8	6.6×10^{-10}
34.7	-56.3	2.4×10^{-9}
37.7	-53.3	4.7×10^{-9}
44.2	-46.8	2.1×10^{-8}
53.7	-37.3	1.9×10^{-7}

The next set of tables provides the transmitted interference power and EIRP from each interferer location necessary to impact the P2P receiver at each P2P location. These tables show these figures for each of the P2P margins discussed above. Table 4.7 shows the results for interferer location 1. Table 4.8 shows the results for interferer location 2. Table 4.9 shows the results for interferer location 3. Table 4.10 shows the results for interferer location 4.

Table 4.11 shows the maximum P2P margins that can feasibly be impacted for each pair of interferer transmit location and P2P receive locations. Note that we do not include transmission from interferer location four to Filmore because this path is significantly obscured by terrain. This table shows the maximum that can be impacted for each of our two potential interference amplifiers (see Section 2.2.2).

Examining Table 4.11 indicates which P2P paradigms can be impacted from which interferer locations. As expected, interferer location one is our primary location for impacting the P2P link and should be able to impact all paradigms at either P2P receive location. Interferer location two is only slightly more limited in that this location is likely to not impact the low-rate paradigm, outside of the lower end of margins for this paradigm, and requires the higher power amplifier to impact the highest margins for the mid-rate paradigm. Interferer location three seems to be limited to impacting only the high-rate paradigm at Filmore and up to the mid-rate paradigm at Haul. Interferer location four is the most limited location in that it is likely to only impact the high-rate paradigm with the P2P receiver at Haul.

Table 4.7: Required Interference Power Transmitted from Interferer Location 1

P2P Margin (dB)	To Filmore				To Haul			
	Tx Pwr (dBm)	Tx Pwr (Watts)	EIRP (dBm)	EIRP (Watts)	Tx Pwr (dBm)	Tx Pwr (Watts)	EIRP (dBm)	EIRP (Watts)
1.2	-13.5	4.5×10^{-5}	6.5	4.5×10^{-3}	-15.9	2.6×10^{-5}	4.1	2.6×10^{-3}
8.2	-6.5	2.2×10^{-4}	13.5	2.2×10^{-2}	-8.9	1.3×10^{-4}	11.1	1.3×10^{-2}
15.2	0.5	1.1×10^{-3}	20.5	0.11	-1.9	6.5×10^{-4}	18.1	6.5×10^{-2}
20.7	6.0	4.0×10^{-3}	26.0	0.40	3.6	2.3×10^{-3}	23.6	0.23
29.2	14.5	2.8×10^{-2}	34.5	2.8	12.1	1.6×10^{-2}	32.1	1.6
34.7	20.0	0.10	40.0	1.0×10	17.6	5.8×10^{-2}	37.6	5.8
37.7	23.0	0.20	43.0	2.0×10	20.6	0.12	40.6	1.2×10
44.2	29.5	0.90	49.5	9.0×10	27.1	0.52	47.1	5.2×10
53.7	39.0	8.0	59.0	8.0×10^2	36.6	4.6	56.6	4.6×10^2
47.2	32.5	1.8	52.5	1.8×10^2	35.6	3.6	55.6	3.6×10^2

Table 4.8: Required Interference Power Transmitted from Interferer Location 2

P2P Margin (dB)	To Filmore				To Haul			
	Tx Pwr (dBm)	Tx Pwr (Watts)	EIRP (dBm)	EIRP (Watts)	Tx Pwr (dBm)	Tx Pwr (Watts)	EIRP (dBm)	EIRP (Watts)
1.2	5.1	3.2×10^{-3}	25.1	0.33	3.1	2.1×10^{-3}	23.1	0.20
8.2	12.1	1.6×10^{-2}	32.1	1.6	10.1	1.0×10^{-2}	30.1	1.0
15.2	19.1	8.2×10^{-2}	39.1	8.2	17.1	5.1×10^{-2}	37.1	5.2
20.7	24.6	0.29	44.6	2.9×10	22.6	0.18	42.6	1.8×10
29.2	33.1	2.0	53.1	2.0×10^2	31.1	1.3	51.1	1.3×10^2
34.7	38.6	7.3	58.6	7.3×10^2	36.6	4.6	56.6	4.6×10^2
37.7	41.6	1.4×10	61.6	1.4×10^3	39.6	9.2	59.6	9.2×10^2
44.2	48.1	6.5×10	68.1	6.5×10^3	46.1	4.1×10	66.1	4.1×10^3
53.7	57.6	5.8×10^2	77.6	5.8×10^4	55.6	3.6×10^2	75.6	3.6×10^4
52.7	56.6	4.6×10^2	76.6	4.6×10^4	54.6	2.9×10^2	74.6	2.9×10^4

Table 4.9: Required Interference Power Transmitted from Interferer Location 3

P2P Margin (dB)	To Filmore				To Haul			
	Tx Pwr (dBm)	Tx Pwr (Watts)	EIRP (dBm)	EIRP (Watts)	Tx Pwr (dBm)	Tx Pwr (Watts)	EIRP (dBm)	EIRP (Watts)
1.2	20.1	0.10	40.1	1.0×10	4.1	2.6×10^{-3}	24.1	0.26
8.2	27.1	0.52	47.1	5.2×10	11.1	1.3×10^{-2}	31.1	1.3
15.2	34.1	2.6	54.1	2.6×10^2	18.1	6.5×10^{-2}	38.1	6.5
20.7	39.6	9.2	59.6	9.2×10^2	23.6	0.23	43.6	2.3×10
29.2	48.1	6.5×10	68.1	6.5×10^3	32.1	1.6	52.1	1.6×10^2
34.7	53.6	2.3×10^2	73.6	2.3×10^4	37.6	5.8	57.6	5.8×10^2
37.7	56.6	4.6×10^2	76.6	4.6×10^4	40.6	1.2×10	60.6	1.2×10^3
44.2	63.1	2.0×10^3	83.1	2.0×10^5	47.1	5.2×10	67.1	5.2×10^3
53.7	72.6	1.8×10^4	92.6	1.8×10^6	56.6	4.6×10^2	76.6	4.6×10^4
52.7	71.6	1.4×10^4	91.6	1.4×10^6	55.6	3.6×10^2	75.6	3.6×10^4

Table 4.10: Required Interference Power Transmitted from Interferer Location 4

P2P Margin (dB)	To Haul			
	Tx Pwr (dBm)	Tx Pwr (Watts)	EIRP (dBm)	EIRP (Watts)
1.2	24.1	0.26	44.1	2.6×10
8.2	31.1	1.3	51.1	1.3×10^2
15.2	38.1	6.5	58.1	6.5×10^2
20.7	43.6	2.3×10	63.6	2.3×10^3
29.2	52.1	1.6×10^2	72.1	1.6×10^4
34.7	57.6	5.8×10^2	77.6	5.8×10^4
37.7	60.6	1.2×10^3	80.6	1.2×10^5
44.2	67.1	5.2×10^3	87.1	5.2×10^5
53.7	76.6	4.6×10^4	96.6	4.6×10^6
52.7	75.6	3.6×10^4	95.6	3.6×10^6

Table 4.11: Feasible Range of Impacted Margins from Interferer Locations

Interferer Location	Receiver Location	Maximum Margin Amplifier 1	Maximum Margin Amplifier 2
Interferer 1	Filmore	48.7 dB	56.7 dB
Interferer 1	Haul	51.1 dB	59.1 dB
Interferer 2	Filmore	30.1 dB	38.1 dB
Interferer 2	Haul	32.1 dB	40.1 dB
Interferer 3	Filmore	15.1 dB	23.1 dB
Interferer 3	Haul	31.1 dB	39.1 dB
Interferer 4	Haul	11.1 dB	19.1 dB

Table 4.12: Maximum Feasible P2P Margins

Operational Paradigm	Maximum Feasible Margin
Low-Rate	53.7 dB
Mid-Rate	37.7 dB
High-Rate	15.2 dB

Table 4.13: Critical Ratio of Interference Power to Signal Power at the P2P Receiver

Operational Paradigm	Critical Ratio
Low-Rate	-1.5 dB
Mid-Rate	-15.5 dB
High-Rate	-35.0 dB

4.4 Conclusions

This simulation study examines the parameter ranges for the P2P link and interferers to support open-range testing. In particular, this study identifies: (1) the feasible range of P2P operating margins for all operational paradigms and (2) the feasible range of interference powers that can impact the P2P link from each interferer location. In support of this, this study also characterizes the expected losses on the P2P link and from each interferer location to both P2P locations.

Table 4.12 shows the maximum feasible margin for each P2P operational paradigm.

Our interference impact analysis shows that P2P links can be impacted from all interferer locations for at least one operational paradigm. The antenna pattern of the P2P receiver certainly impacts the potential margins that could be impacted. Ultimately the impact of the interference depends on the ratio of the interference power at the P2P receiver to the P2P signal power at the P2P receiver. Table 4.13 shows the critical values of this ratio for each P2P paradigm where we expect the interference to begin impacting the P2P link. Note that this ratio corresponds to the minimum SNR necessary to achieve a BER of 1×10^{-6} for each paradigm (see Table 2.4). The impact of the interference is to effectively raise the noise experienced by the P2P receiver. Thus raising the noise in a proportion to the minimum SNR effectively means that the P2P link is never able to reach a point where it can effectively decode the transmitted signal. Of course, this characterization ignores factors such as the distribution of interference power in time and frequency, but it does provide a starting point for selecting parameters for open-range testing.

5 Initial Testing of Components

This section describes the initial open-range testing of our P2P link. The goals for this test are as follows:

1. Establish the operation of the P2P link.
2. Validate the data collection approach.
3. Examine the behavior of the P2P link the presence of interference.

5.1 Tools Used

This testing utilizes the following components:

- Our representative P2P link (see Section 2.1)
- The AWGN interferer (see Section 2.2.1.3)
- Spectrum monitoring (see Section 2.3)

5.2 Locations

The locations used for initial testing are different those described in Section 2.4 to facilitate more rapid iteration in testing. Figure 5.1 summarizes the locations used for the initial testing and the subsequent material in this section provides further details.



Figure 5.1: Locations for Initial Testing

5.2.1 Transmit

This location provides the transmission position for both the P2P link and the interferer used in this testing. A P2P antenna and an interferer antenna are both mount on a 2.4 m (8 ft) mast at this location. Spectrum monitoring will be conducted approximately 2 m (6.6 ft) above the ground at this location. Table 5.1 provides additional details about this location.

This location hosts one P2P endpoint (see Section 2.1.1).

Table 5.1: Transmit Location Details

Coordinates	43°31'48.38" N, 112°49'44.81" W
Decimal Degrees	43.5301055556, -112.8291138889
Antenna Height	2.4 m (8 ft)
Transmit Frequency	7390 MHz
Receive Frequency	7690 MHz

5.2.2 Receive

This locations provides the receive position for the P2P link. A P2P antenna and a monitoring antenna are mounted on a 2.4 m (8 ft) mast as this location. Table 5.2 provides additional details about this location.

This location hosts one P2P endpoint (see Section 2.1.1) and spectrum monitoring equipment (see Section 2.3.1).

Table 5.2: Receive Location Details

Coordinates	43°31'28.46" N, 112°49'34.72" W
Decimal Degrees	43.5245722222, -112.8263111111
Antenna Height	2.4 m (8 ft)
Transmit Frequency	7690 MHz
Receive Frequency	7390 MHz

5.2.3 Path Parameters

The distance between the two locations is approximately 650 m (2133 ft). At 7390 MHz, this distance indicates a free space path loss of 106.1 dB. Given that this path is free of terrain obstructions or clutter we will utilize the free space path loss for subsequent analysis.

5.3 Supporting Analysis

This section describes the analysis for determining the parameters to be used in initial testing.

5.3.1 Defining P2P Power Levels

This section describes the P2P power level and paradigms examined during testing. We consider power levels for two P2P link conditions: (1) main lobe P2P transmission and (2) sidelobe P2P transmission. These two conditions allow examining different ranges of P2P transmission power within the space available for testing. WE determine the power levels for both link conditions through a link budget analysis.

We use Equation 5.1 to determine the expected received powers for both link conditions:

$$P_{P2P Rx} = P_{P2P Tx} + 2G_{P2P} - L_{P:Transmit,Receive} - L_{S:i} \quad (5.1)$$

We define each term of Equation 5.1 below:

- $P_{P2P Rx}$ is the achieved receive power for the P2P link in dBm
- $P_{P2P Tx}$ is the selected transmit power for the P2P link in dBm.
- $2G_{P2P}$ is the antenna gain for the P2P link in dB. Note that this term includes both the transmitter and receiver antenna gains for the P2P link.
- $L_{P:Transmit,Receive}$ is the path loss between the Transmit and Receive locations in dB. (See Section 5.2.3)

- $L_{S:i}$ is the sidelobe attenuation associated with link condition i in dB.

To facilitate determination of the maximum allowable P2P transmission power, we solve Equation 5.1 for the transmission power. This yields Equation 5.2.

$$P_{P2P Tx} = P_{P2P Rx} - 2G_{P2P} + L_{P:Transmit,Receive} + L_{S:i} \quad (5.2)$$

We employ these two equations to determine the range of powers for which we can operate the P2P link without saturating the receiver. We examine both link conditions below.

5.3.1.1 Main Lobe P2P Transmission

For this link condition, the P2P transmit antenna is oriented to align with the P2P receive antenna main lobe. This orientation results in no attenuation of the P2P transmit antenna gain.

Table 5.3 lists the limiting power values for this link condition.

Table 5.3: Limiting Power Values for Main Lobe Transmission

Power Type	Minimum (dBm)	Minimum (Watts)	Maximum (dBm)	Maximum (Watts)
Power at Receiver	-32.4	5.8×10^{-7}	-20.0	1.0×10^{-5}
Power at Rx Antenna	-63.5	4.5×10^{-10}	-51.1	7.8×10^{-9}
Transmitted	11.5	1.4×10^{-2}	23.9	0.25

Below we describe each column for Table 5.3 below:

- Power Type is the type of power limits reported in each row, here we explore three types:
 - Power at Receiver is the power at the P2P receiver.
 - Power at the Rx Antenna is the power that can be measured at the P2P receive antenna
 - Transmitted is the power output by the P2P transmitter, into the P2P transmit antenna
- Minimum (dBm) is the minimum power for the type indicated by the row. The values in this column are in dBm. These values correspond to utilizing the minimum P2P transmit power shown in Table 2.2.
- Minimum (Watts) is the minimum power for the type indicated by the row. The values in this column are in Watts. These values are provided for convenience.
- Maximum (dBm) is the maximum power for the type indicated by the row. The values in this column are in dBm. These values correspond to achieving the receiver saturation power shown in Table 2.2 at the P2P receiver.
- Minimum (Watts) is the maximum power for the type indicated by the row. The values in this column are in Watts. These values are provided for convenience.

The values shown in Table 5.3 are the outside limits of feasible powers under this link condition. Within this range, we select the specific power levels shown in Table 5.4 for initial testing.

Table 5.4: Main Lobe Condition Selected Power Settings

Tx Power (dBm)	Tx Power (Watts)	Pwr at Rx Ant (dBm)	Pwr at Rx Ant (Watts)	Rx Power (dBm)	Rx Power (Watts)
11.5	1.4×10^{-2}	-63.5	4.5×10^{-10}	-32.4	5.8×10^{-7}
17.0	5.0×10^{-2}	-58.0	1.6×10^{-9}	-26.9	2.0×10^{-6}

Below we describe each column for Table 5.4 below:

- Tx Power (dBm) is the selected transmit power setting for the P2P link. The values in this column are in dBm.
- Tx Power (Watts) is the selected transmit power setting for the P2P link. The values in this column are in Watts. These values are provided for convenience.
- Pwr at Rx Ant (dBm) is the power at the P2P receive antenna expected for the selected transmit power. The values in this column are in dBm.
- Pwr at Rx Ant (Watts) is the power at the P2P receive antenna expected for the selected transmit power. The values in this column are in Watts. These values are provided for convenience.
- Rx Power (dBm) is the power at the P2P receiver expected for the selected transmit power. The values in this column are in dBm.
- Rx Power (Watts) is the power at the P2P receiver expected for the selected transmit power. The values in this column are in Watts. These values are provided for convenience.

Table 5.5 shows the margins that can be achieved for each P2P paradigm for the selected powers shown in Table 5.4. The margins shown here demonstrate that the selected powers allow for confirming the operation of each P2P paradigm while avoiding saturation of the P2P receiver.

Table 5.5: Main Lobe Condition Expected Margins

Tx Power	Low-Rate Margin	Mid-Rate Margin	High-Rate Margin
11.5 dBm	57.1 dB	43.1 dB	23.6 dB
17.0 dBm	62.6 dB	48.6 dB	29.1 dB

5.3.1.2 Sidelobe P2P Transmission

For this link condition, the P2P transmit antenna is intentionally skewed relative to the P2P receive antenna main lobe. This intentional mis-alignment of the transmit antenna yields an effective attenuation that results from using the sidelobe rather than the main lobe. The magnitude of this sidelobe attenuation is calculated using the radiation pattern envelope data provided by the antenna manufacturer.

For this link condition, we skew the transmit antenna by 20 degrees which yields a sidelobe attenuation of 26.0 dB.

Table 5.6 lists the limiting power value for this link condition.

Table 5.6: Limiting Power Values for Sidelobe Transmission

Power Type	Minimum (dBm)	Minimum (Watts)	Maximum (dBm)	Maximum (Watts)
Power at Receiver	-58.4	1.5×10^{-9}	-38.4	1.5×10^{-7}
Power at Rx Antenna	-89.5	1.1×10^{-12}	-69.5	1.1×10^{-10}
Transmitted	11.5	1.4×10^{-2}	31.5	1.4

The columns of Table 5.6 follow the same format as those of Table 5.3. Here, the maximum values correspond to utilizing the maximum transmit power for the low-rate P2P paradigm shown in Table 2.4. The transmit power necessary to achieve the saturation level of the P2P receiver for this link condition is 49.9 dBm (9.77×10^1 Watts), which is above the achievable transmit power for any paradigm.

Table 5.7 shows the powers levels we select for testing this condition.

Table 5.8 shows the margins that can be achieved for each P2P paradigm for the selected powers shown in Table 5.7. The margins shown here are intentionally reduced relative to main lobe link condition to support investigation of P2P behavior in the presence of interference.

Table 5.7: Sidelobe Condition Selected Power Settings

Tx Power (dBm)	Tx Power (Watts)	Pwr at Rx Ant (dBm)	Pwr at Rx Ant (Watts)	Rx Power (dBm)	Rx Power (Watts)
11.5	1.4×10^{-2}	-89.5	1.1×10^{-12}	-58.4	1.5×10^{-9}
18.0	6.3×10^{-2}	-83.0	5.0×10^{-12}	-51.9	6.5×10^{-9}

Table 5.8: Sidelobe Condition Expected Margins

Tx Power	Low-Rate Margin	Mid-Rate Margin	High-Rate Margin
11.5 dBm	31.1 dB	17.1 dB	-2.4 dB
18.0 dBm	37.6 dB	23.6 dB	4.1 dB

5.3.2 Defining Interferer Power Levels

This section describes the interferer power level and associated expected impact on the P2P link. Here, we follow the approach for determining feasibly interferer powers that could impact the P2P described in Section 4.2.3.2. Recall that for this initial testing, we employ one interferer location which is directly in the main lobe of the P2P receiver thus this analysis utilizes the path loss provided in Section 5.2.3 and no attenuation associated with sidelobe usage.

Table 5.9 provides the interference power required at the P2P receiver to impact the P2P for each operating margin across both link conditions.

Table 5.9: Required Interference Power at the P2P Receiver

P2P Margin (dB)	Power at P2P Receiver (dBm)	Power at P2P Receiver (Watts)
4.1	-85.4	2.9×10^{-12}
17.1	-72.4	5.8×10^{-11}
23.6	-65.9	2.6×10^{-10}
29.1	-60.4	9.1×10^{-10}
31.1	-58.4	1.5×10^{-9}
37.6	-51.9	6.5×10^{-9}
43.1	-46.4	2.3×10^{-8}
48.6	-40.9	8.2×10^{-8}
57.1	-32.4	5.8×10^{-7}
62.6	-26.9	2.0×10^{-6}

Table 5.10 provides the transmitted interference power and EIRP necessary to impact P2P link for each operating margin covered in Table 5.9.

Considering the compression margins for both interferer amplifiers, shown in Table 2.10, allows us to determine the feasible range of operating margin that can be impacted during initial testing. The maximum margin that is feasibly impacted using amplifier 1 is 48.5 dB. Using amplifier 2 increases this margin to 56.5 dB. Therefore, we expect that most P2P margins used in this initial testing should be impacted even with the lower power interferer amplifier 1.

Table 5.11 shows the interference power settings selected for initial testing.

5.4 Methodology

This section outlines the method used in this initial testing. These methods are intended to facilitate developing experience with the equipment and ensure data collection in larger scale testing.

Table 5.10: Required Transmitted Interference Power

Margin (dB)	Tx Pwr (dBm)	Tx Pwr (Watts)	EIRP (dBm)	EIRP (Watts)
4.1	-30.4	9.1×10^{-7}	-10.4	9.1×10^{-5}
17.1	-17.4	1.8×10^{-5}	2.6	1.8×10^{-3}
23.6	-10.9	8.1×10^{-5}	9.1	8.1×10^{-3}
29.1	-5.4	2.9×10^{-4}	14.6	2.9×10^{-2}
31.1	-3.4	4.6×10^{-4}	16.6	4.6×10^{-2}
37.6	3.1	2.0×10^{-3}	23.1	0.2
43.1	8.6	7.2×10^{-3}	28.6	0.72
48.6	14.1	2.6×10^{-2}	34.1	2.6
57.1	22.6	0.18	42.6	1.8×10^1
62.6	28.1	0.65	48.1	6.5×10^1

Table 5.11: Interference Power Levels Selected for Initial Testing

Tx Power (dBm)	Tx Power (Watts)	Pwr at Rx Ant (dBm)	Pwr at Rx Ant (Watts)	Rx Power (dBm)	Rx Power (Watts)
-25.0	3.2×10^{-6}	-111.1	7.8×10^{-15}	-80.0	1.0×10^{-11}
7.6	5.8×10^{-3}	-78.5	1.4×10^{-11}	-47.4	1.8×10^{-8}
12.0	1.6×10^{-2}	-74.1	3.9×10^{-11}	-43.0	4.0×10^{-8}

5.4.1 Overall Approach

This testing is organized into three phases:

1. Confirmation of expected power levels.
2. Characterization of P2P link.
3. Examination of interference impact.

5.4.2 Data Examined

This section lists the data examined during this testing. The discussion here is organized according to the source of data.

5.4.2.1 Terminal Data

The data described here is collected from the P2P terminal internal link monitoring capability. This data can be harvested via an SSH connection to the terminal.

SNR This is the signal-to-noise ratio for the P2P link.

Link Margin This is the margin of the P2P link above the received power required to achieve the various achievable rates.

BER This is the BER of the P2P link.

Transmit Power This is the transmit power of the P2P link.

5.4.2.2 iPerf Data

The data described here is collected from the iPerf tool running over the P2P link. This data can be harvested as output of the iPerf tool.

Data Rate This is the data rate achieved over the IP connection supported by the P2P link.

Lost Packet Percent This is the percentage of packets that have been lost over the iPerf link.

Jitter This is the measured variance in the timing of the packets sent through a UDP between two laptops.

5.4.2.3 Spectrum Monitoring Data

The data described here is collected from independent spectrum monitoring equipment.

Received Power Level This is the power level of the signal incident to the P2P receive antenna.

5.4.3 Phase 1: Examination of Received Power Level

This section describes the approach to the first phase of testing. The goal of this test phase is to ensure that the power levels at the P2P antennas are within the expected range. This test phase examines both the main lobe P2P transmission and sidelobe P2P transmission link conditions. This phase of testing examines one P2P terminal operating at a time rather than examining the complete P2P link. Table 5.4 lists the power levels that will be used for the main lobe link condition. Table 5.7 lists the power levels that will be used for the sidelobe link condition. This test phase will drive decisions that impact subsequent testing.

5.4.3.1 Test Sequence

1. Aim the P2P transmit antenna (at the Transmit location) directly at the Receive location. Aim the P2P receive antenna (at the Receive location) directly at the Transmit location.
2. Deactivate the P2P endpoint at the Receive location; activate the P2P endpoint at the Transmit location.
3. Position the spectrum monitoring equipment at the Receive location.
4. Transmit at each main lobe transmission power (see Table 5.4) from the Transmit location; record the power level at the Receive location for each transmission level.
5. Aim the P2P antenna at Transmit location 20 degrees away from the Receive location.
6. Transmit at each sidelobe transmission power (see Table 5.7) from the Transmit location; record the power level at the Receive location for each transmission level.

5.4.3.2 Decision Points

- If any power received from an antenna without a 20 degree offset is at or above -51.1 dBm (7.76×10^{-9} Watts) (i.e., the P2P saturation level minus the P2P antenna gain), the corresponding transmit power level will not be utilized for further testing.
- If any power received from an antenna with a 20 degree offset is at or above -25.1 dBm (3.09×10^{-6} Watts) (i.e., the P2P saturation level minus the P2P antenna gain plus the sidelobe attenuation), the corresponding transmit power level will not be utilized for further testing.
- If the minimum difference power received with and without a 20 degree offset for a transmission power of 11.5 dBm (1.41×10^{-2} Watts) is less than 26.0 dB, then all sidelobe P2P power levels will be lowered according to the observed difference.

5.4.4 Phase 2: Evaluation of P2P Link

This section describes the approach to the second phase of testing. The goals of this test phase are to (1) establish the full operational link and (2) evaluate the data collection approach. This test phase examines only the main lobe P2P transmission condition.

This test phase will examine two data profiles: (1) iPerf and (2) video. Under the iPerf data profile the link will be loaded by the iPerf tool. Under the video data profile the link will be loaded with a streaming video.

This test phase builds experience to inform later test events.

5.4.4.1 Test Sequence

1. Aim the P2P transmit antenna (at the Transmit location) directly at the Receive location. Aim the P2P receive antenna (at the Receive location) directly at the Transmit location.
2. Activate both P2P endpoints.
3. For each main lobe transmission power level (see Table 5.4), do the following:
 - (a) For each P2P operating paradigm (see Section 2.1.3), do the following:
 - i. Establish a P2P link utilizing the power level and link rate combination.
 - ii. Load the link utilizing the iPerf data profile with data flowing from the Transmit location to the Receive location.
 - iii. Examine the data reported by the terminal (see Section 5.4.2.1)
 - iv. Examine the data reported by the iPerf tool (see Section 5.4.2.2)
4. For each main lobe transmission power level (see Table 5.4), do the following:
 - (a) For each P2P operating paradigm (see Section 2.1.3), do the following:
 - i. Establish a P2P link utilizing the power level and link rate combination.
 - ii. Load the link utilizing the video data profile with data flowing from the Transmit location to the Receive location.
 - iii. Examine the data reported by the terminal (see Section 5.4.2.1)

5.4.5 Phase 3: Exploration of Interference

This section describes the approach to the third phase of testing. The goal of this test phase is to examine the impact of interference on the P2P link. This test phase examines only the sidelobe P2P transmission condition.

This test phase will examine both data profiles examined in the prior test phase (see Section 5.4.4).

This test phase builds experience to inform later test events.

5.4.5.1 Test Sequence

1. Aim the P2P transmit antenna (at the Transmit location) 20 degrees away from the Receive location. Aim the P2P receive antenna (at the Receive location) directly at the Transmit location.
2. Activate both P2P endpoints.
3. For each sidelobe transmission power level (see Table 5.7), do the following:
 - (a) For each P2P operating paradigm (see Section 2.1.3), do the following:
 - i. Establish a P2P link utilizing the power level and link rate combination.
 - ii. Load the link utilizing the iPerf data profile with data flowing from the Transmit location to the Receive location.
 - iii. Examine the data reported by the terminal (see Section 5.4.2.1)

- iv. Examine the data reported by the iPerf tool (see Section 5.4.2.2)
 - v. For each interference power (see Table 5.11), do the following:
 - A. Activate the interferer with the selected power level.
 - B. Examine the data reported by the terminal (see Section 5.4.2.1)
 - C. Examine the data reported by the iPerf tool (see Section 5.4.2.2)
4. For each sidelobe transmission power level (see Table 5.7), do the following:
- (a) For each P2P operating paradigm (see Section 2.1.3), do the following:
 - i. Establish a P2P link utilizing the power level and link rate combination.
 - ii. Load the link utilizing the video data profile with data flowing from the Transmit location to the Receive location.
 - iii. Examine the data reported by the terminal (see Section 5.4.2.1)
 - iv. For each interference power (see Table 5.11), do the following:
 - A. Activate the interferer with the selected power level.
 - B. Examine the data reported by the terminal (see Section 5.4.2.1)

5.5 Results

This section provides the results of the initial testing. Here we discuss the results the for each phase of the testing. Given that the primary goal of this testing is proving out our approach to testing, much these results are simply validations of expectations.

5.5.1 Phase 1: Examination of Received Power Level

Phase 1 testing showed that all P2P transmitted power levels are within ± 0.1 dBm of the intended setting and within ± 1 dBm of the expected power level at the location of the receiver. Further this test confirmed that mis-aligning the transmit antenna did indeed introduction an attenuation of at least 26 dB. As such, no power levels were eliminated from additional consideration and no additional modification is necessary for the sidelobe link condition.

5.5.2 Phase 2: Evaluation of P2P Link

Phase 2 testing showed that a P2P link can be effectively established and carry both iPerf traffic and video streaming across a range of settings to model different P2P paradigms. Importantly, we validated that terminal data described in Section 5.4.2.1 and the iPerf data described in Section 5.4.2.2 can be collected.

5.5.3 Phase 3: Exploration of Interference

Phase 3 testing showed that our approach to generating interference does indeed impact the P2P link. Here we examined three interference powers. As expected the lowest interference power was only able to impact the lowest margin link and showed no effect on other P2P settings. Each subsequent increase of interference power expands the range of P2P settings that can be impacted as predicted by the analysis in Section 5.3.2. In this testing we found that the P2P exhibited a binary reaction to interference in that interference generated no impact or totally prevented link operation. For example, observation of the streaming video either showed no evidence of interference or was rendered inoperable by interference.

5.6 Conclusions

The initial testing described here is a small-scale version of the overall P2P testing of this project. This initial testing progresses from analysis and simulation to over-the-testing. As such this initial testing proves out the feasibility of the overall method and sets the stage for larger scale data collection.

6 Open-Range Testing

This section describes the open-range testing to collect data on the impact of interference on P2P links. This open-range testing is the central source of data for this overall project. The goals for this test are as follows:

1. Characterize the impact of interference on P2P links
2. Generate empirical data.
3. Evaluate the real-world attenuation associated with side or back lobe interference injection.

6.1 Tools Used

This testing utilizes the following components:

- Our representative P2P link (see Section 2.1)
- Our set of representative interferer (see Section 2.2)
- Spectrum monitoring (see Section 2.3)

This open-range testing employs the locations described in Section 2.4.

6.2 Methodology

This section outlines the method used in open-range testing.

6.2.1 Overall Approach

This testing focuses on collecting empirical, over-the-air data on the impact of interference on P2P links in a variety of situations. The general approach to this testing is as follows:

1. Operate the P2P link without interference as a baseline.
2. Operate the P2P in the presence of interference.

We describe the approach to each of these steps in the subsequent sub-sections here.

6.2.2 Data Examined

This section lists the data examined during this testing. The discussion here is organized according to the source of data. The data described here is collect across all sequences for open-range testing.

6.2.2.1 Terminal Data

The data described here is collected from the P2P terminal internal link monitoring capability. We collect this data via an SSH connection to the terminal and each terminal is queried independently. Below is a list of the full set of data provided for each query:

Bandwidth This is the bandwidth utilized by the link. This metric is primarily used to ensure the link is configured as intended.

Transmit Frequency This is the transmit frequency of the queried terminal. This metric is primarily used to ensure that the link is configured as intended.

Receive Frequency This is the receive frequency of the queried terminal. This metric is primarily used to ensure that the link is configured as intended.

Transmit Modulation This is the transmit modulation of the queried terminal. This metric is primarily used to ensure that the link is configured as intended.

Receive Modulation This is the receive modulation of the queried terminal. This metric is primarily used to ensure that the link is configured as intended.

Transmit Power This is the transmit power of the queried terminal. This metric is primarily used to ensure that the link is configured as intended.

SNR This is the estimated SNR at the queried terminal. This metric provides an indicator of the performance of the link.

Remote SNR This is the estimated SNR at the non-queried terminal. This metric provides an indicator of the performance of the link. The availability of this metric depends on the operation of the link.

Received signal level (RSL) This is the RSL at the queried terminal. This metric provides an indicator of the performance of the link.

Remote RSL This is the RSL at the non-queried terminal. This metric provides an indicator of the performance of the link. The availability of this metric depends on the operation of the link.

Fade Margin This is the margin of the P2P link above the received power required to achieve the various achievable rates at the queried terminal. This metric provides an indicator of the performance of the link.

Remote Fade Margin This is the margin of the P2P link above the received power required to achieved the various achievable rates at the non-queried terminal. This metric provides an indicator of the performance of the link. The availability of this metric depends on the operation of the link.

BER This is the BER of the P2P link. This metric provides an indicator of the performance of the link.

During the course of testing we discovered that the BER reported by the terminal depends on the data flowing through the link, which has some important results that we'll discuss below.

6.2.2.2 iPerf Data

The data described here is collected from the iPerf tool running over the P2P link. We collect this data by the running the iPerf tool with flow going from the transmit terminal to receive terminal. Below is a list of the full set of data provided from each iPerf test instance.

Seconds This is the duration of the iPerf test in seconds.

Bytes This is the total number of bytes sent during the iPerf test.

Bits per Second This is the data rate achieved over the IP connection supported by the P2P link.

Jitter This is the measured variance in the timing of the packets sent through a UDP between two laptops.

Lost Packets This is the number of packets that have been lost over the iPerf link.

Packets This is the total number of packets transmitted during the iPerf setting.

Lost Packet Percent This is the percentage of packets that have been lost over the iPerf link.

6.2.2.3 Spectrum Monitoring Data

The data described here is collected from independent spectrum monitoring equipment.

6.2.3 Test Sequence

The sequence for open-range testing is a composition of an overarching test sequence, a sequence for selecting interferer power, and a sequence for an individual test instance. We describe each of these sequences here. Each test instance collects the data described in Section 6.2.2 for one test case. The full set of test cases examined is described in Section 6.2.5.

6.2.3.1 Overarching Test Sequence

The overarching test sequence follows:

1. Aim the P2P antenna at Filmore directly at the P2P antenna at Haul.
2. Activate both P2P endpoints.
3. For each P2P paradigm and P2P transmission power, do the following:
 - (a) Configure the P2P link according to the selected settings.
 - (b) Collect baseline metrics by examining a test instance (see Section 6.2.3.3).
 - (c) For each interferer location and interferer type, do the following:
 - i. Configure the interferer according to the selected settings.
 - ii. For each considered P2P receiver, do the following:
 - A. Aim the interferer antenna at the selected P2P receiver.
 - B. Vary interference power (see Section 6.2.3.2).
 - C. Activate the interferer with the selected power.
 - D. Collect metrics by running a test sequence (see Section 6.2.3.3).

6.2.3.2 Interference Power Selection

The interference power selection sequence follows:

1. Check impact on the P2P of last interferer power for the current parameter set. The parameter set here is composed of P2P paradigm, P2P transmission, interferer location, and interferer type. P2P link.
 - If setting power for the first test instance of this parameter set, then select the maximum available interference power.
 - If the last instance of this parameter set rendered the P2P inoperable, then reduce the interferer power by 20 dB.
 - If the last instance of this parameter set resulted in some packet lost (as reported by iPerf), then reduce the interferer power by 10 dB.
 - If the last instance of this parameter set resulted in no packet lost (as reported by iPerf), then increase interference power by 5 dB.

Table 6.1: iPerf Data Rates

P2P Paradigm	Data Rate
Low-Rate	52 Mbps
Mid-Rate	179 Mbps
High-Rate	368 Mbps

2. Compare the selected interference power to prior interference powers for this parameter set.
 - If setting power for the first test instance of this parameter set, then use the selected power.
 - If the selected power is more than 5 dB less than the lowest power shown to render the P2P link inoperable for the current parameter set, then use the selected power.
 - If the selected power is within 5 dB of the lowest power shown to render the P2P link inoperable for the current parameter set, then stop testing the current parameter set and move on to other sets.

This approach is intended to quickly outline the impact of interferers on the P2P link quickly and then fill in details about the transition period between an inoperable P2P link and an unaffected P2P link. Note that we decreased the granularity of power selection for interferer locations two through four because the parameter selection study indicated less potential for impact from these locations (see Section 4). In these cases, we increased the interference power by 10 dB if the prior instance showed no impact.

6.2.3.3 Individual Test Instance

The individual test instance to collect metrics follows:

1. Select a iPerf rate based on the P2P paradigm (see Table 6.1).
2. Do the following ten times:
 - (a) Setup iPerf to run for 10 seconds using UDP and the selected data rate
 - (b) Run iPerf and collect data (see Section 6.2.2.2)
 - (c) Query the transmit terminal for data (see Section 6.2.2.1)

6.2.4 Test Sets

We execute the open-range testing in three sets of test cases. The first set of cases was conducted over the course of a week. The second and third sets were on single days each. The third set of cases specifically focused on examining 5G interference with the use of the higher power interference amplifier (i.e., interference amplifier 2).

During test set one we observed two errors:

1. We had configured the iPerf data rate for the Low-Rate P2P paradigm to be 54 Mbps instead of the intended 52 Mbps.
2. We discovered that the BER reported by the terminal depends on the amount of data flowing over the P2P link. Given that the test instance sequence queried the transmit terminal after the conclusion of the iPerf session, no data was flowing during the time of the query.

The impact of these errors are discussed in Section 6.3.

We corrected these errors for subsequent test sets with the following:

- We corrected the iPerf data rate for the Low-Rate P2P paradigm to the intended 52 Mbps.
- We shifted our approach to collecting terminal data to querying the receiving P2P terminal every seven seconds for the duration of the test set. The data elements collected from the terminal remained as discussed in Section 6.2.2.1.

Table 6.2: P2P Baseline Test Cases

P2P Paradigm	P2P Modulation	P2P Transmit Location	P2P Tx Power (dBm)	Testing Set
Low-Rate	QPSK	Filmore	11.5	1, 2
Low-Rate	QPSK	Filmore	30.5	1
Low-Rate	QPSK	Haul	11.5	1, 2, 3
Low-Rate	QPSK	Haul	30.5	1
Mid-Rate	64 QAM	Filmore	11.5	1
Mid-Rate	64 QAM	Filmore	28.5	1
Mid-Rate	64 QAM	Haul	11.5	1, 3
Mid-Rate	64 QAM	Haul	28.5	1
Not used	256 QAM	Filmore	11.5	1
Not used	256 QAM	Filmore	28.5	1
Not used	256 QAM	Haul	11.5	1
Not used	256 QAM	Haul	28.5	1
Not used	512 QAM	Filmore	11.5	1
Not used	512 QAM	Filmore	28.0	1
High-Rate	4096 QAM	Filmore	11.5	1
High-Rate	4096 QAM	Filmore	25.5	1
High-Rate	4096 QAM	Haul	11.5	1, 3
High-Rate	4096 QAM	Haul	25.5	1

6.2.5 Test Cases

Table 6.2 lists the baseline test cases that established the operation of the P2P link without interference. These baseline cases span all the P2P paradigms discussed in Section 2.1.3 as well as spot checks for 256 QAM and 512 QAM.

Table 6.3 shows the test cases that examine interference generated from Interferer Location 1 (see Section 2.4.3). This location is the primary location for interference generation, which is reflected by the large number of test cases conducted here.

Table 6.4 shows the test cases that examine interference generated from Interferer Location 2 (see Section 2.4.4). This location is largely supplementary to Interferer Location 1, which is reflected by the comparatively low number of test cases that utilize this location.

Table 6.5 shows the test cases that examine interference generated from Interferer Location 3 (see Section 2.4.5). This location is primarily focused on investigating the injection of interference into the sidelobe of the P2P receiver at the Filmore location. The test cases utilizing this location focus on this purpose.

Table 6.6 shows the test cases that examine interference generated from Interferer Location 4 (see Section 2.4.6). This location is heavily disadvantaged relative to both P2P locations and thus not significantly utilized. Rather this we employ this location to evaluate the terrain impacts and investigate any potential refraction interference into the Filmore location.

6.2.6 Power Ratio Analysis

To facilitate examining the impact of interference on the P2P across the range of test cases that we examine, we present our results here in terms of the ratio of interference power to P2P power. We refer to this as the interference to signal ratio (ISR). We discuss different variations of this ratio below.

6.2.6.1 Transmitted Interference to Signal Ratio

Here, we discuss the ratio of the interference EIRP at the interference antenna to the P2P EIRP at the transmitting P2P antenna. We refer to this as the Transmit ISR. We use Equation 6.1 to calculate this ratio.

$$I_{Tx} = P_{Int\ EIRP} - P_{P2P\ EIRP} \quad (6.1)$$

Table 6.3: Interference Test Case for Location 1

P2P Paradigm	P2P Modulation	P2P Transmit Location	P2P Tx Power (dBm)	Testing Set	Interferer Type
Low-Rate	QPSK	Filmore	11.5	1, 2	5G, AWGN, CW, Wi-Fi
Low-Rate	QPSK	Filmore	30.5	1	5G, AWGN, Wi-Fi
Low-Rate	QPSK	Haul	11.5	1, 2, 3	5G, AWGN, CW, Wi-Fi
Low-Rate	QPSK	Haul	30.5	1	5G, AWGN, CW, Wi-Fi
Mid-Rate	64 QAM	Filmore	11.5	1, 2	5G, AWGN, CW, Wi-Fi
Mid-Rate	64 QAM	Filmore	28.5	1	5G, AWGN, Wi-Fi
Mid-Rate	64 QAM	Haul	11.5	1, 2, 3	5G, AWGN, CW, Wi-Fi
Mid-Rate	64 QAM	Haul	28.5	1	5G, AWGN, CW, Wi-Fi
Not Used	256 QAM	Filmore	11.5	1	5G
High-Rate	4096 QAM	Filmore	11.5	1, 2	5G, AWGN, CW, Wi-Fi
High-Rate	4096 QAM	Filmore	25.5	1	5G, AWGN, Wi-Fi
High-Rate	4096 QAM	Haul	11.5	1, 2, 3	5G, AWGN, CW, Wi-Fi
High-Rate	4096 QAM	Haul	25.5	1	5G, AWGN, CW, Wi-Fi

Table 6.4: Interference Test Case for Location 2

P2P Paradigm	P2P Modulation	P2P Transmit Location	P2P Tx Power (dBm)	Testing Set	Interferer Type
Low-Rate	QPSK	Haul	11.5	1	5G, AWGN, Wi-Fi
Low-Rate	QPSK	Haul	30.5	1	5G, AWGN, Wi-Fi
Mid-Rate	64 QAM	Haul	11.5	1	5G, AWGN, Wi-Fi
Mid-Rate	64 QAM	Haul	28.5	1	5G, AWGN, Wi-Fi
High-Rate	4096 QAM	Haul	11.5	1	5G, AWGN, Wi-Fi
High-Rate	4096 QAM	Haul	25.5	1	5G, AWGN, Wi-Fi

Table 6.5: Interference Test Case for Location 3

P2P Paradigm	P2P Modulation	P2P Transmit Location	P2P Tx Power (dBm)	Testing Set	Interferer Type
Low-Rate	QPSK	Haul	11.5	1	5G, AWGN, Wi-Fi
Low-Rate	QPSK	Haul	30.5	1	5G, AWGN, Wi-Fi
Mid-Rate	64 QAM	Haul	11.5	1	5G, AWGN, CW, Wi-Fi
High-Rate	4096 QAM	Haul	11.5	1	5G, AWGN, CW, Wi-Fi

Table 6.6: Interference Test Case for Location 4

P2P Paradigm	P2P Modulation	P2P Transmit Location	P2P Tx Power (dBm)	Testing Set	Interferer Type
Low-Rate	QPSK	Filmore	11.5	1	5G, AWGN, CW, Wi-Fi
Low-Rate	QPSK	Haul	11.5	1	5G, AWGN, CW, Wi-Fi
Mid-Rate	64 QAM	Filmore	11.5	1	5G, AWGN, CW, Wi-Fi
Mid-Rate	64 QAM	Haul	11.5	1	5G, AWGN, CW, Wi-Fi
High-Rate	4096 QAM	Filmore	11.5	1	5G, AWGN, CW, Wi-Fi
High-Rate	4096 QAM	Haul	11.5	1	5G, AWGN, CW, Wi-Fi

We define each term of Equation 6.1 below:

- I_{Tx} is the ratio of interference EIRP to the P2P EIRP in dB.
- $P_{Int\ EIRP}$ is the interference EIRP in dBm. Calculated as the transmitted interference power plus the gain of the interference antenna ($P_{Int\ Tx} + G_{Int}$).
- $P_{P2P\ EIRP}$ is the P2P EIRP in dBm.

Recall that we set the interferer transmit power by varying a programmable attenuator and utilizing a fixed gain attenuator (see Section 2.2.5).

Note that the Transmit ISR allows for comparison among interference transmitted from a single interferer location, but does not capture the impact of the differing attenuations associated with each pair of interferer and P2P receive locations.

6.2.6.2 Received Interference to Signal Ratio

Here, we discuss the ratio of the interference power at the P2P receiver to the P2P power at the P2P receiver. We refer to this as the Receive ISR. To determine this ratio we first calculate the interference power at the P2P receiver using Equation 6.2.

$$P_{Int\ Rx:i,j} = P_{Int\ EIRP} + G_{P2P} - L_{P:i,j} - L_{S:i,j} \quad (6.2)$$

We define each term of Equation 6.2 below:

- $P_{Int\ Rx:i,j}$ is the interference power from location i at the P2P receiver at location j . This value is in dBm.
- $P_{Int\ EIRP}$ is the interference EIRP in dBm.
- G_{P2P} is the gain of the P2P receiving antenna in dB.
- $L_{P:i,j}$ is the path loss between location i and location j in dB. This value is from the simulated loss discussed in Section 4.3.2.1.
- $L_{S:i,j}$ is the sidelobe loss between location i and location j in dB. This value is from the simulated loss discussed in Section 4.3.2.1.

We then calculate the P2P power at the P2P receiver using Equation 6.3.

$$P_{P2P\ Rx} = P_{P2P\ EIRP} + G_{P2P} - L_{P:Filmore,Haul} \quad (6.3)$$

We define each term of Equation 6.3 below:

- $P_{P2P\ Rx}$ is the P2P signal power at the P2P receiver in dBm.
- $P_{P2P\ EIRP}$ is the P2P EIRP in dBm.
- $L_{P:Filmore,Haul}$ is the path loss between the Filmore and Haul P2P location. This value is from the simulated loss discussed in Section 4.3.1.1.

We can then calculate the Receive ISR using Equation 6.4.

$$I_{Rx} = P_{Int\ Rx:i,j} - P_{P2P\ Rx} \quad (6.4)$$

Note that the Receive ISR allows for comparison among interference transmitted across all the interferer locations. This comparability results from factoring the variation of losses between locations into the ratio. Although this is based on the simulated loss.

Table 6.7: Approximate RSL for Transmit Power Settings

P2P Tx Power Setting	Approximate RSL
11.5 dBm	-54 dBm
25.5 dBm	-40 dBm
28.0 dBm	-36.5 dBm
28.5 dBm	-37 dBm
30.5 dBm	-35 dBm

6.3 Results

This section discusses the results of the open-range testing. Here we highlight a subset of the total results that expose particular trends. The complete set of plots is provided in Section 3 of the plot supplement document.

Here we present results as box plots and scatter plots.

The box plots here show boxes for each power level or ratio considered. Each box includes an orange center line that provides the average. The size of the box corresponds to one standard deviation away from the average, capped by the theoretical maximum and minimum for the value observed (i.e., BER spans from 0 to 0.5). The whiskers show the maximum and minimum observed values.

The scatter plots here show observations of a given value for each power level or ratio considered. The marker shape indicates the type of interferer associated with the observation, where applicable.

6.3.1 Baseline Results

This section provides the results of the P2P baseline cases listed in Table 6.2. As discussed in Section 6.2.4 we observed some errors during the execution of test set one which changed our approach to testing for test sets two and three. We present these results separately where these differences are impactful.

Plots in this section show the average RSL in dBm for a given test instance on the horizontal axis. The averaging here considers all the terminal data collected during a given test instance. Table 6.7 lists the approximate RSL observed for each transmit power setting used in baseline test cases (see Table 6.2).

Figure 6.1 shows the distribution of lost packet percentage during test set one for the low-rate paradigm. Figure 6.2 shows the distribution of lost packet percentage during test sets two and three. Note that one of the test cases show in Figure 6.1 has an average RSL that doesn't correspond to any transmit power setting used for baselining the low-rate paradigm. In this test case the transmit power was changed from 11.5 dBm to 30.5 dBm one-third of the duration into the test. These plots highlight the error related to overloading the low-rate P2P link with the iPerf traffic, discussed in Section 6.2.4. The plots as demonstrate the effectiveness of our solution to this error.

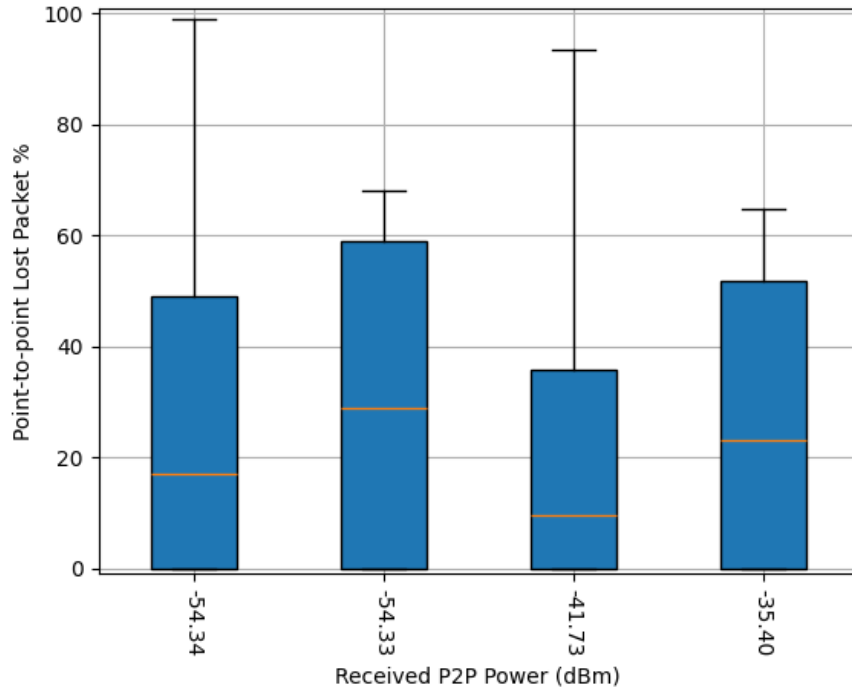


Figure 6.1: Distribution of Lost Packet % for Low-Rate Baseline during Test Set 1

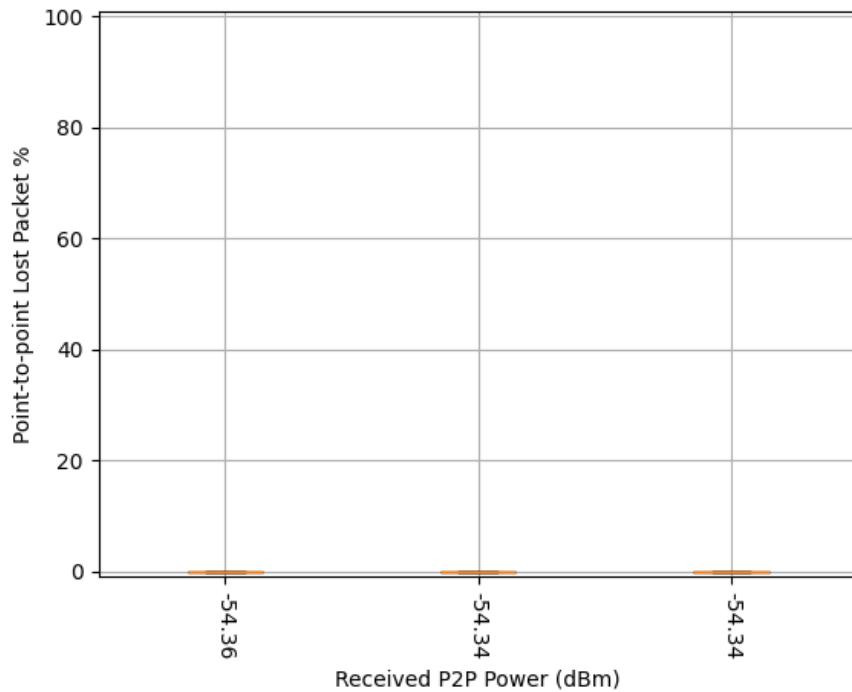


Figure 6.2: Distribution of Lost Packet % for Low-Rate Baseline during Test Sets 2 & 3

Figure 6.3 shows the distribution of lost packet percentage across all test sets for the mid-rate paradigm. Figure 6.4 shows the distribution of lost packet percentage across all test sets for the high-rate paradigm. In both of these case, there are not significant loses, which demonstrates that the P2P link is operating as intended.

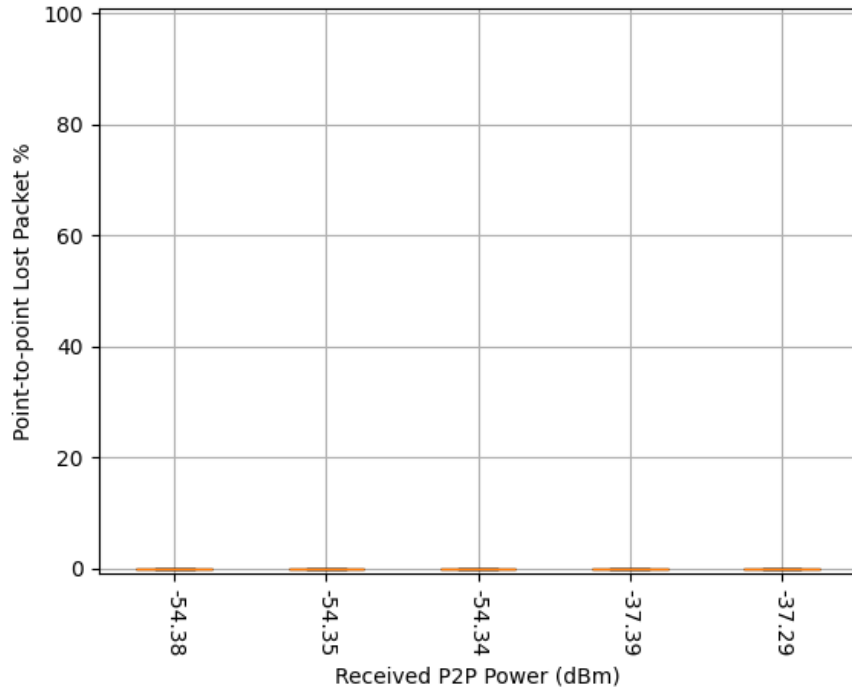


Figure 6.3: Distribution of Lost Packet % for Mid-Rate Baseline during all Test Sets

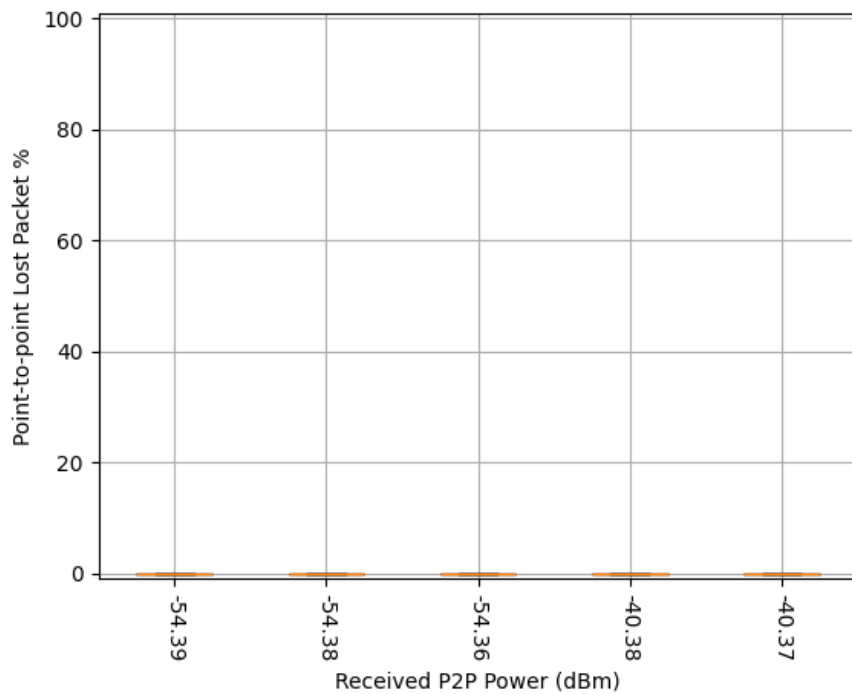


Figure 6.4: Distribution of Lost Packet % for High-Rate Baseline during all Test Sets

Overall the above plots demonstrate that the P2P links are able to carry data with no loss across all the paradigms. Of course, this has some dependence on the applications utilizing the P2P being aware of the capacity of the link.

Examining the jitter of the links provides information about the baseline variation in timing achieved by the links. Figure 6.5 shows the distribution of jitter across test sets two and three for the low-rate paradigm.

Figure 6.6 shows the distribution of jitter across all test sets for the mid-rate paradigm. Figure 6.7 shows the distribution of jitter across all test sets for the high-rate paradigm. Note that we excluded test set one results for the low-rate paradigm to avoid the impact of the iPerf overloading on the jitter results (see Section 3.1.1.1.1 of the plot supplement document for these results). In the cases shown here the link displays a small timing variability.

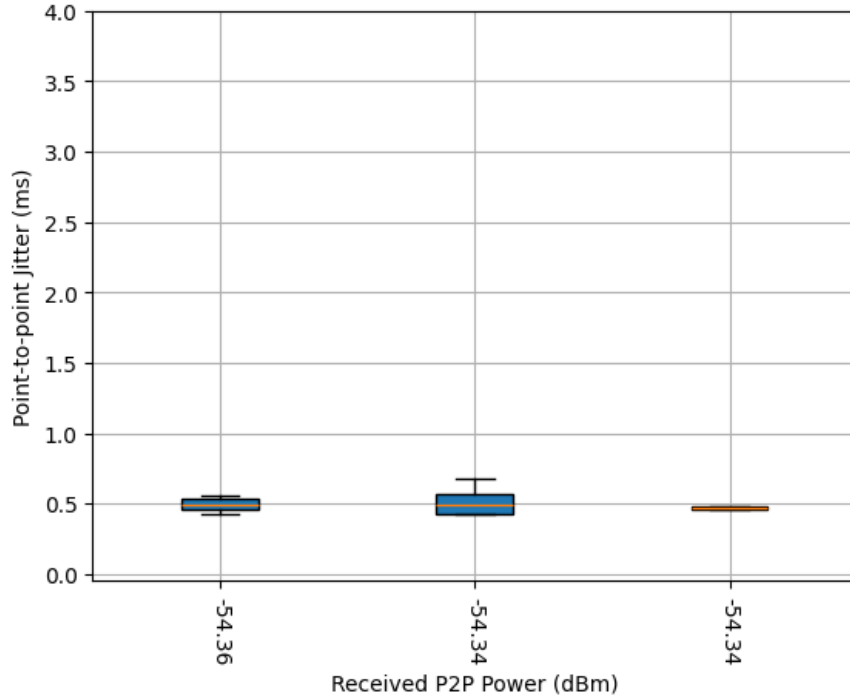


Figure 6.5: Distribution of Jitter for Low-Rate Baseline during Test Sets 2 & 3

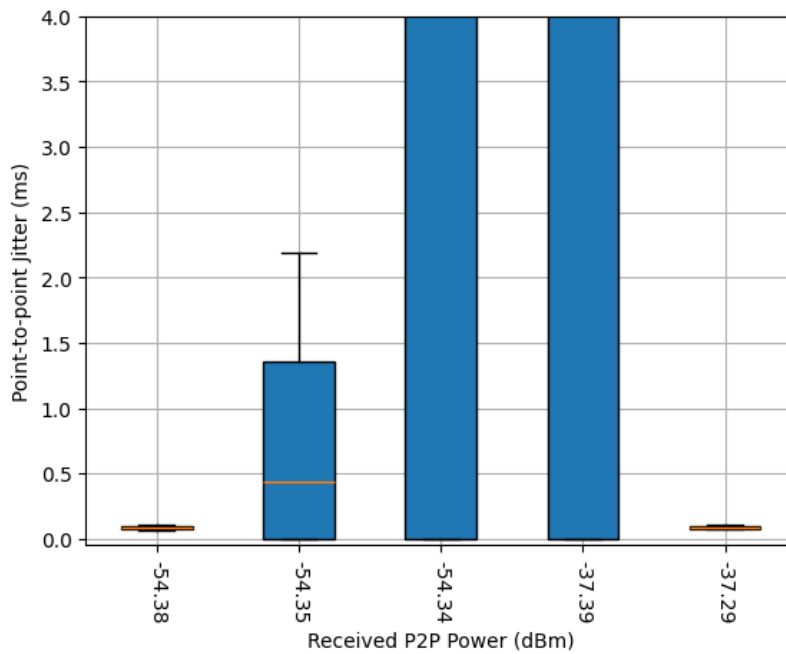


Figure 6.6: Distribution of Jitter for Mid-Rate Baseline during all Test Sets

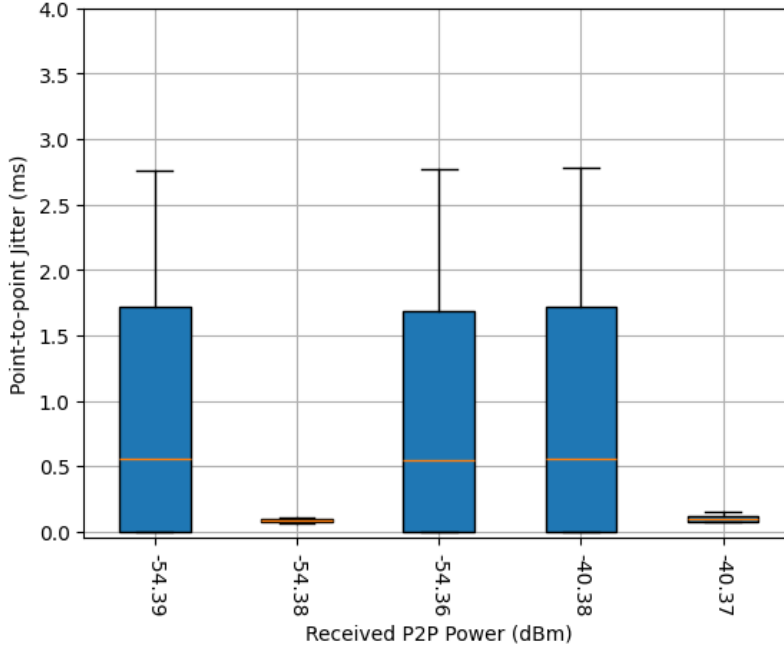


Figure 6.7: Distribution of Jitter for High-Rate Baseline during all Test Sets

6.3.2 Interference Thresholds

This section summarizes the Receive ISR¹ at which each interferer type reliably impacts the P2P link. Here, a reliable impact means that all collected iPerf session data shows non-zero packet loss. These results highlight the differing impact of each type of interferer on each P2P paradigm. Table 6.8 shows the threshold Receive ISR values.

Table 6.8: Threshold Received ISR for each Interferer Type

P2P Paradigm	P2P Link Modulation	Interferer Type	Threshold Rx ISR
Low-Rate	QPSK	5G	-2.5 dB
Mid-Rate	64 QAM	5G	-8.0 dB
Mid-Rate	64 QAM	AWGN	-16.8 dB
Mid-Rate	64 QAM	CW	-14.8 dB
Mid-Rate	64 QAM	Wi-Fi	-15.9 dB
High-Rate	4096 QAM	5G	-25.5 dB
High-Rate	4096 QAM	AWGN	-36.8 dB
High-Rate	4096 QAM	CW	-44.8 dB
High-Rate	4096 QAM	Wi-Fi	-33.3 dB

Note that test set one data was not considered for these thresholds. While the iPerf overload error contributes to this, the larger factor in this case is simply the fact that the interference power required to impact the low-rate paradigm necessitated the use of interference amplifier 2.

Considering the Mid-Rate paradigm, we see that 5G requires a notably higher Receive ISR than the other other interferer types. This is likely a result of the comparatively low duty cycle of 5G (see Section 2.2.1).

Considering the High-Rate paradigm, we see that a significantly higher sensitivity to the CW interferer relative to other types. We conjecture that this may be related to the CW signal degrading the detection or synchronization of the high-rate signal. Importantly, this sensitivity goes beyond simple duty cycle because both the CW and the AWGN interferers employ 100% duty cycle.

¹We use Receive ISR here to enable comparison of results across interference sites. See Section 6.2.6.2 for a discussion of how this value is calculated

Figure 6.8 displays the average lost packet percentage that results from each interferer type on a low-rate P2P link for test sets two and three. Figure 6.9 displays the average lost packet percentage that results from each interferer type on a mid-rate P2P link across all test sets. Figure 6.10 displays the average lost packet percentage that results from each interferer type on a high-rate P2P link across all test sets.

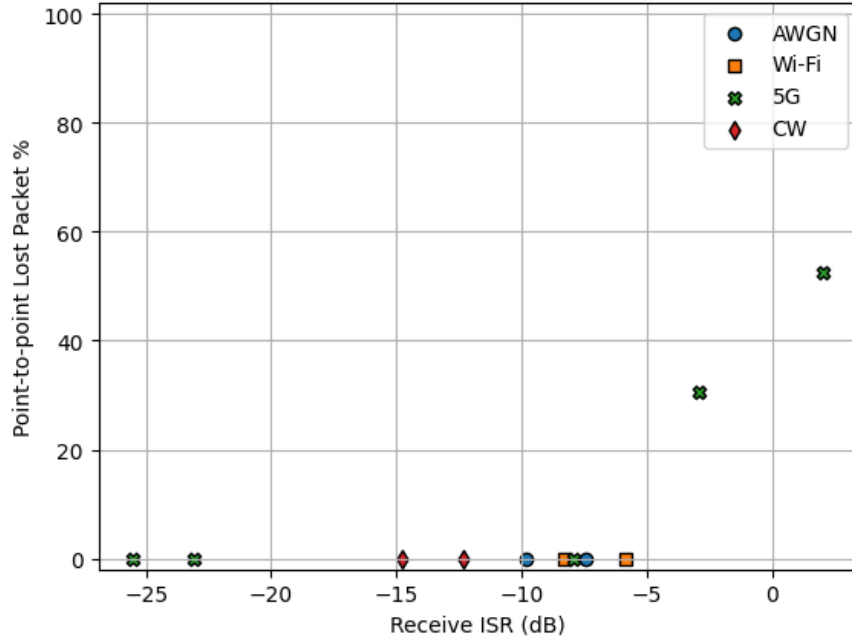


Figure 6.8: Average Lost Packet Percentages in Low-Rate Link for Test Sets 2 & 3

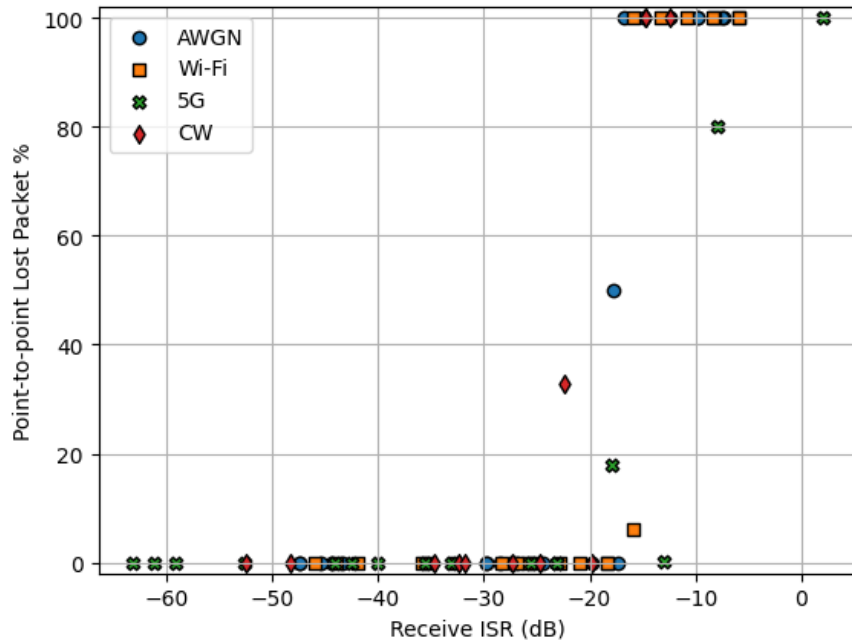


Figure 6.9: Average Lost Packet Percentages in Mid-Rate Link for all Test Sets

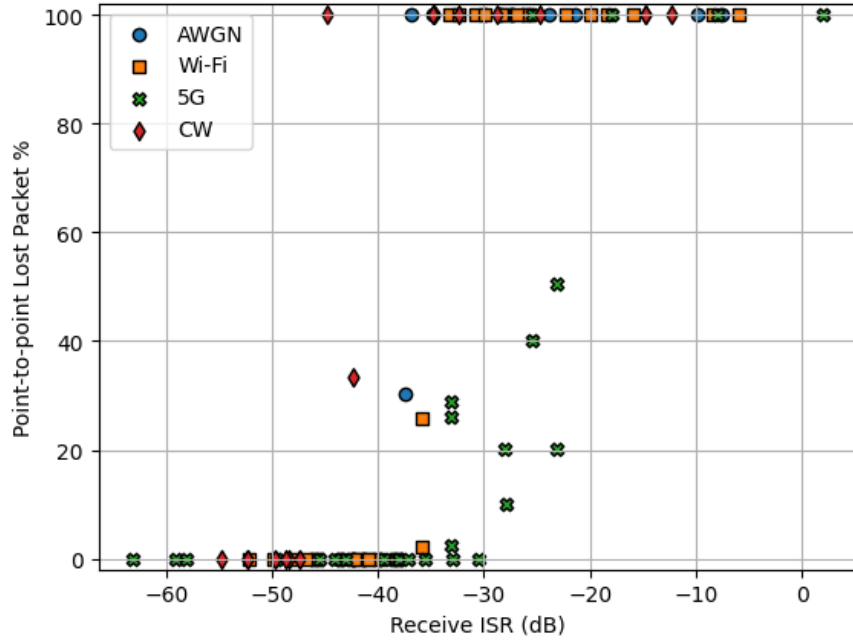


Figure 6.10: Average Lost Packet Percentages in High-Rate Link for all Test Sets

Figure 6.11 displays the average jitter that results from each interferer type on a low-rate P2P link for test sets two and three. Figure 6.12 displays the average jitter that results from each interferer type on a mid-rate P2P link across all test sets. Figure 6.13 displays the average jitter that results from each interferer type on a high-rate P2P link across all test sets.

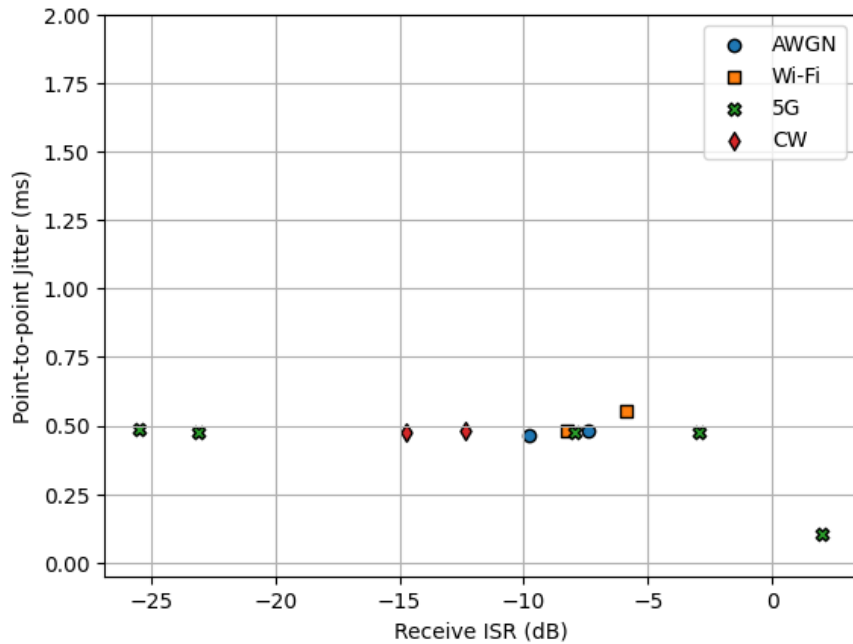


Figure 6.11: Average Jitter in Low-Rate Link for Test Sets 2 & 3

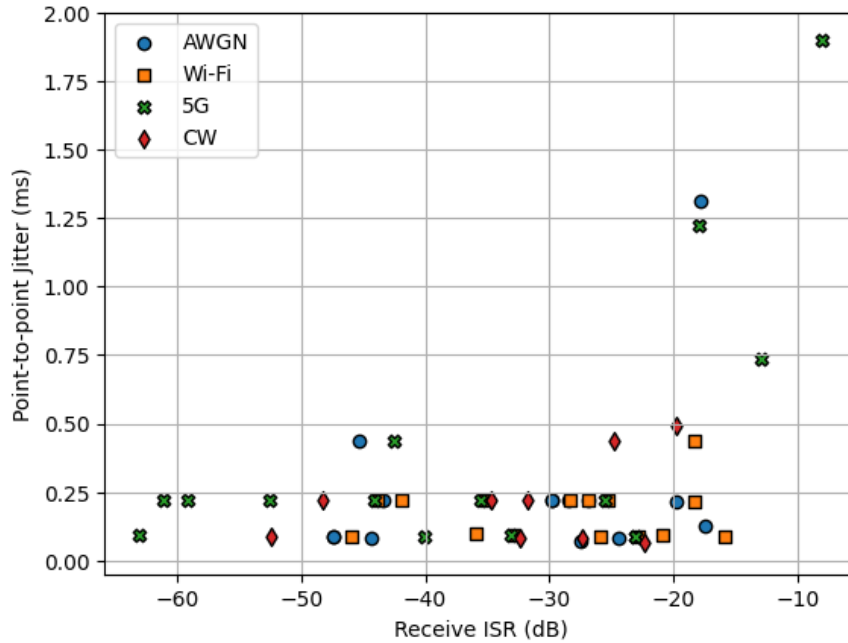


Figure 6.12: Average Jitter in Mid-Rate Link for all Test Sets

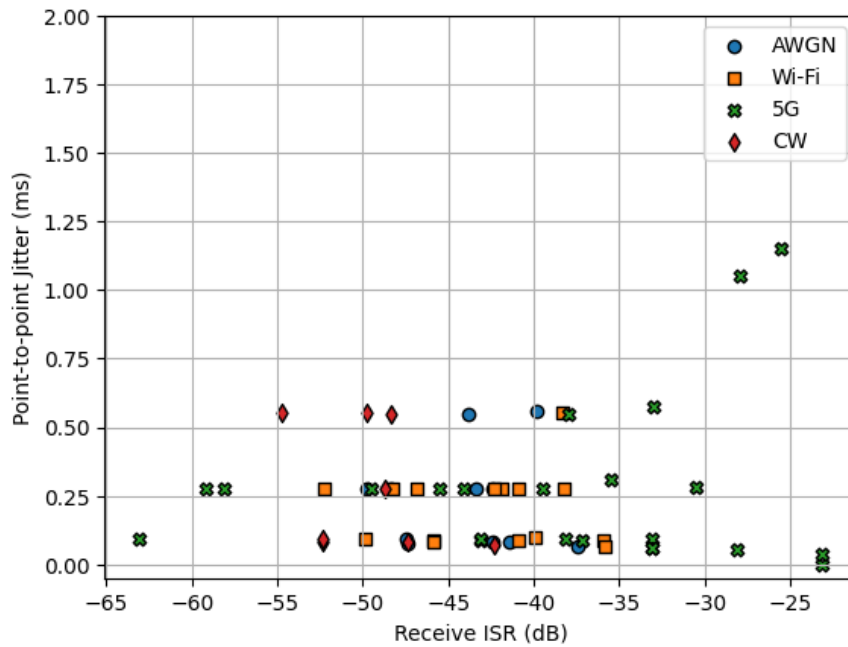


Figure 6.13: Average Jitter in High-Rate Link for all Test Sets

6.3.3 Interferer Locations

This section presents the results of interference from each interferer location. The results in this section are presented in terms of the Transmit ISR to avoid including the simulated path losses involved in calculating the Receive ISR. As such specific values should only be compared within a given interferer location and not across locations. See Section 6.2.6.1 for additional information about the Transmit ISR.

6.3.3.1 Interferer Location 1

Figure 6.14 displays the average lost packet percentage from an interferer at location 1 on a low-rate P2P link with a receiver at Haul for test sets two and three. Figure 6.16 displays the average lost packet percentage from an interferer at location 1 on a mid-rate P2P link with a receiver at Haul for all test sets. Figure 6.18 displays the average lost packet percentage from an interferer at location 1 on a high-rate P2P link with a receiver at Haul for all test sets. Figure 6.15 displays the average lost packet percentage from an interferer at location 1 on a low-rate P2P link with a receiver at Filmore for test sets two and three. Figure 6.17 displays the average lost packet percentage from an interferer at location 1 on a mid-rate P2P link with a receiver at Filmore for all test sets. Figure 6.19 displays the average lost packet percentage from an interferer at location 1 on a high-rate P2P link with a receiver at Filmore for all test sets.

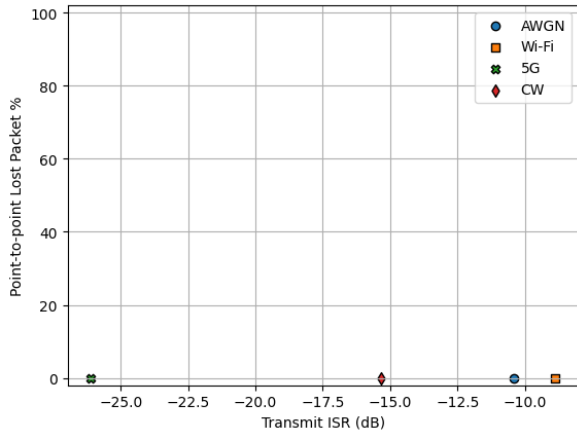


Figure 6.14: Average Lost Packet % for Interferer 1 to Haul Low-Rate for Test Set 2 & 3

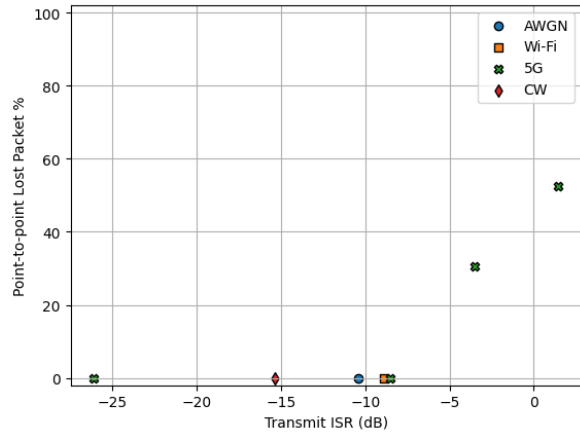


Figure 6.15: Average Lost Packet % for Interferer 1 to Filmore Low-Rate for Test Sets 2 & 3

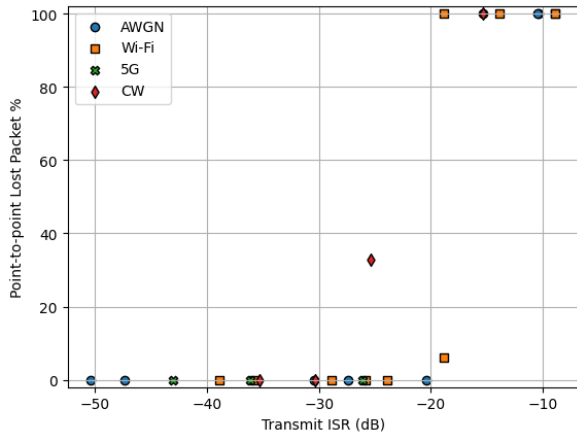


Figure 6.16: Average Lost Packet % for Interferer 1 to Haul Mid-Rate for all Test Sets

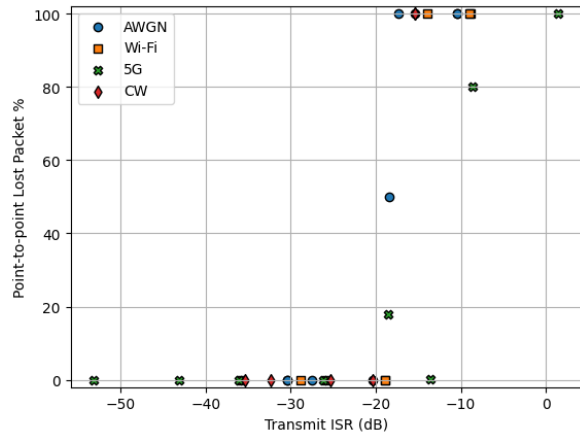


Figure 6.17: Average Lost Packet % for Interferer 1 to Filmore Mid-Rate for all Test Sets

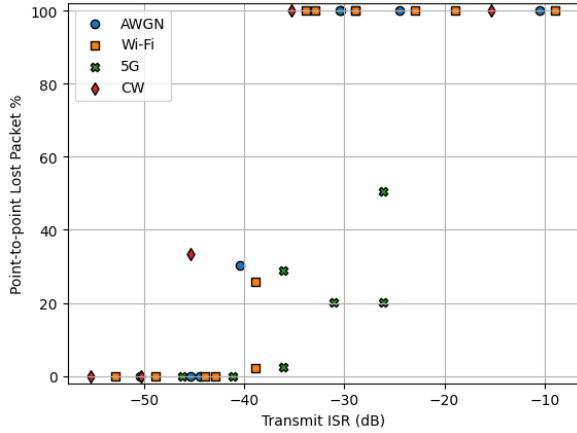


Figure 6.18: Average Lost Packet % for Interferer 1 to Haul High-Rate for all Test Sets

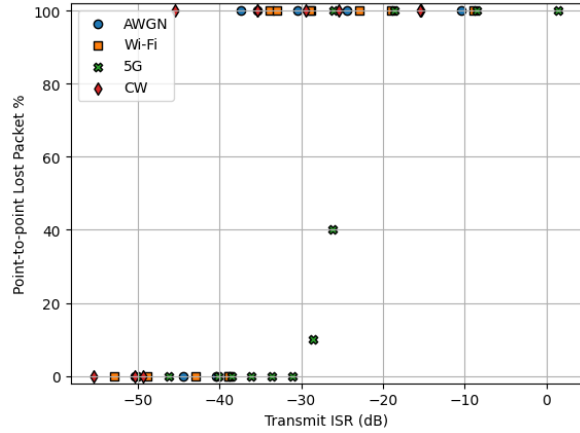


Figure 6.19: Average Lost Packet % for Interferer 1 to Filmore High-Rate for all Test Sets

6.3.3.2 Interferer Location 2

Filmore for test sets two and three. Figure 6.20 displays the average lost packet percentage from an interferer at location 2 on a mid-rate P2P link with a receiver at Filmore for all test sets. Figure 6.21 displays the average lost packet percentage from an interferer at location 2 on a high-rate P2P link with a receiver at Filmore for all test sets.

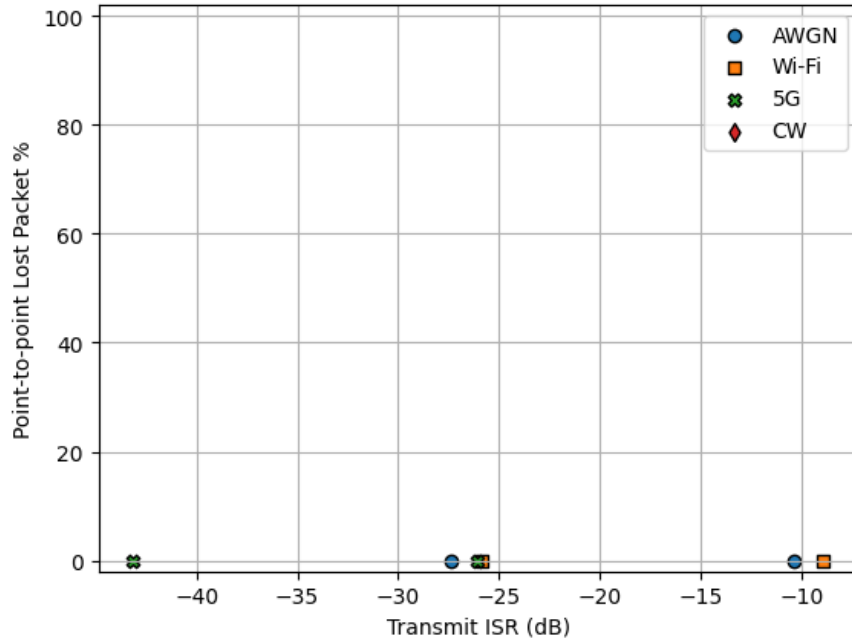


Figure 6.20: Average Lost Packet % for Interferer 2 to Filmore Mid-Rate for all Test Sets

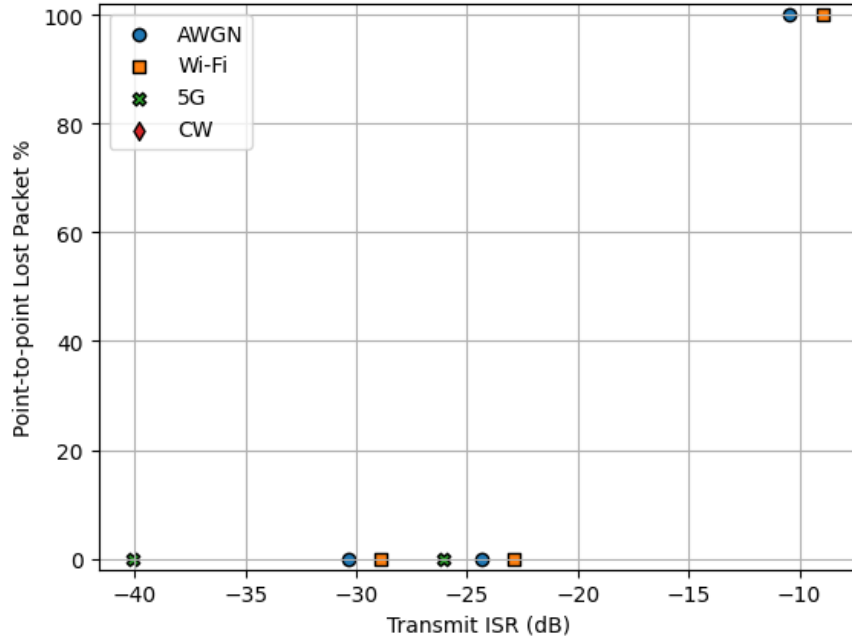


Figure 6.21: Average Lost Packet % for Interferer 2 to Filmore High-Rate for all Test Sets

6.3.3.3 Interferer Location 3

Filmore for test sets two and three. Figure 6.22 displays the average lost packet percentage from an interferer at location 3 on a mid-rate P2P link with a receiver at Filmore for all test sets. Figure 6.23 displays the average lost packet percentage from an interferer at location 3 on a high-rate P2P link with a receiver at Filmore for all test sets.

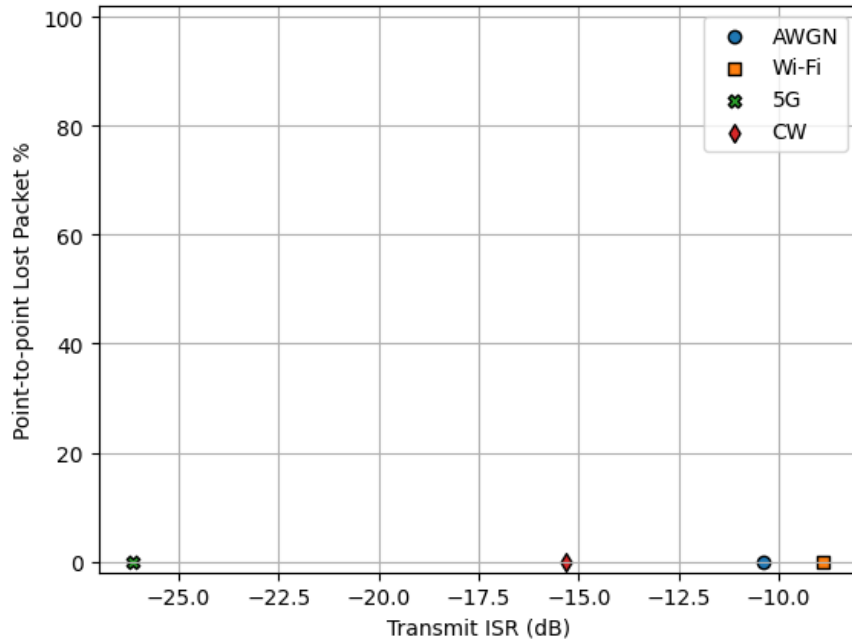


Figure 6.22: Average Lost Packet % for Interferer 3 to Filmore Mid-Rate for all Test Sets

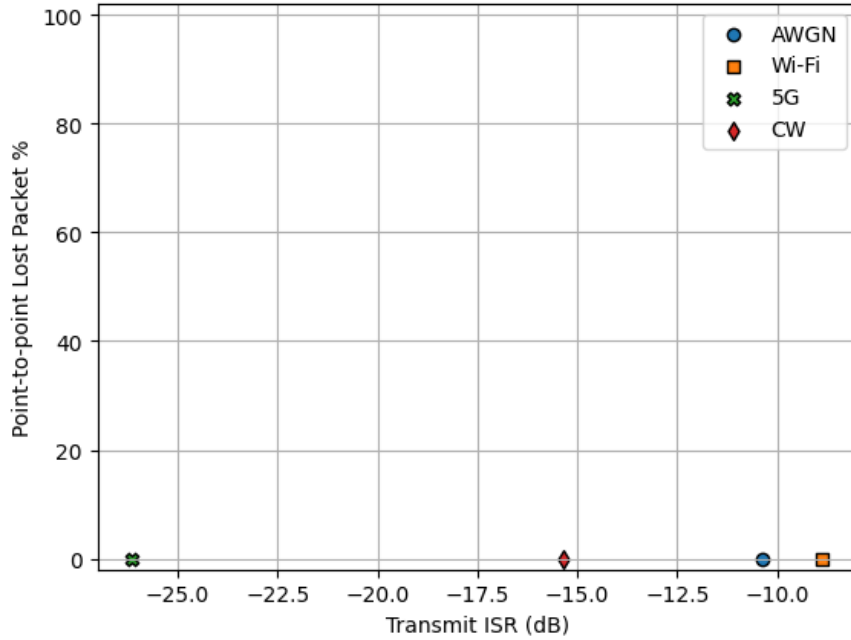


Figure 6.23: Average Lost Packet % for Interferer 3 to Filmore High-Rate for all Test Sets

6.3.3.4 Interferer Location 4

Figure 6.24 displays the average lost packet percentage from an interferer at location 4 on a mid-rate P2P link with a receiver at Haul for all test sets. Figure 6.26 displays the average lost packet percentage from an interferer at location 4 on a high-rate P2P link with a receiver at Haul for all test sets. Figure 6.25 displays the average lost packet percentage from an interferer at location 4 on a mid-rate P2P link with a receiver at Filmore for all test sets. Figure 6.27 displays the average lost packet percentage from an interferer at location 4 on a high-rate P2P link with a receiver at Filmore for all test sets.

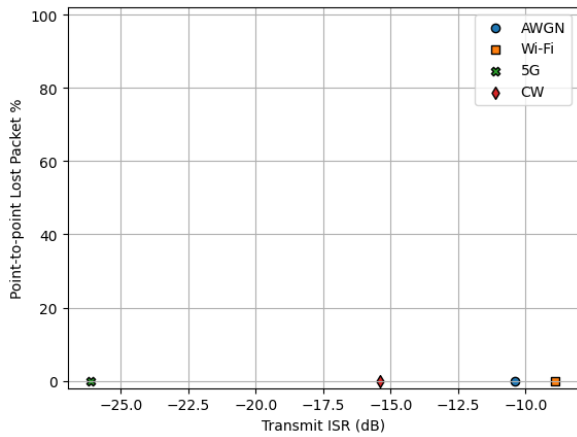


Figure 6.24: Average Lost Packet % for Interferer 4 to Haul Mid-Rate for all Test Sets

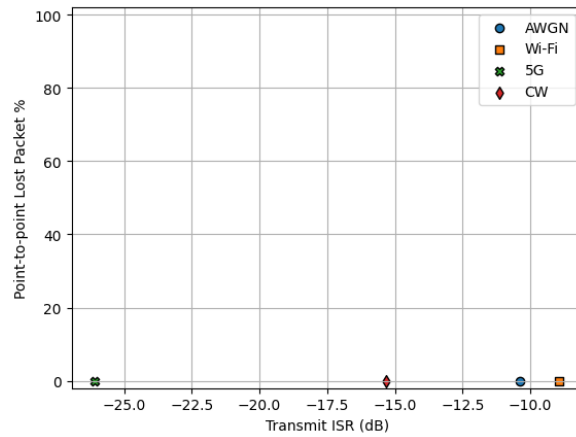


Figure 6.25: Average Lost Packet % for Interferer 4 to Filmore Mid-Rate for all Test Sets

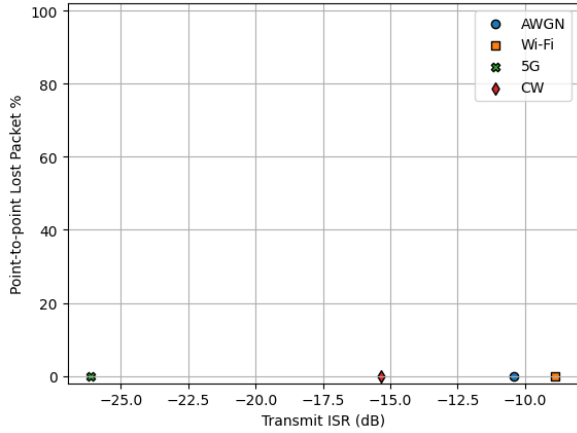


Figure 6.26: Average Lost Packet % for Interferer 4 to Haul High-Rate for all Test Sets

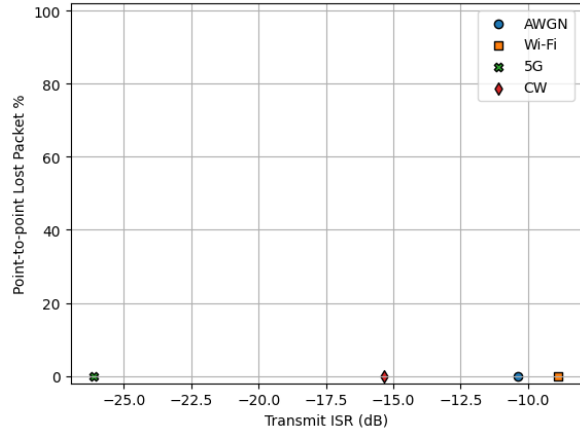


Figure 6.27: Average Lost Packet % for Interferer 4 to Filmore High-Rate for all Test Sets

6.3.4 Unexpected Results

This section highlights some unexpected results with important implications.

6.3.4.1 BER Behavior

The BER reported by the terminals returns to zero when the P2P link is rendered inoperable.

Figure 6.28 shows the average BER value that results from interference at interferer location 1 onto a P2P receiver at Haul for the mid-rate paradigm during test sets two and three. Figure 6.29 shows the average packet lost percentage that results from interference at interferer location 1 onto a P2P receiver at Haul for the mid-rate paradigm during test sets two and three. Figure 6.30 shows the average BER value that results from interference at interferer location 1 onto a P2P receiver at Filmore for the high-rate paradigm during tests two and three. Figure 6.31 shows the average packet lost percentage that results from interference at interferer location 1 onto a P2P receiver at Filmore for the high-rate paradigm during test sets two and three.

In the test cases depicted here, the lost packets clearly indicate that the interference has rendered the P2P link inoperable as the interference power increases. Simultaneously the metric reported by the terminal indicates increasing impact followed by a return to no impact.

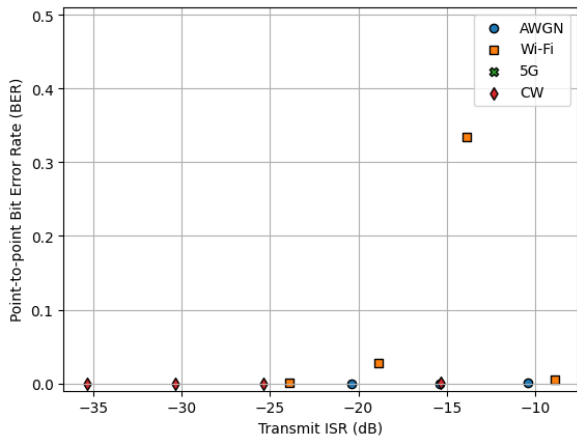


Figure 6.28: Average BER for Interferer 1 to Haul Mid-Rate for Sets 2 & 3

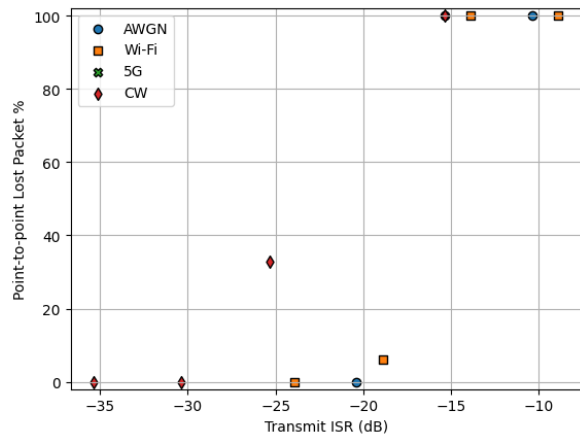


Figure 6.29: Average Packet Loss % for Interferer 1 to Haul Mid-Rate for Sets 2 & 3

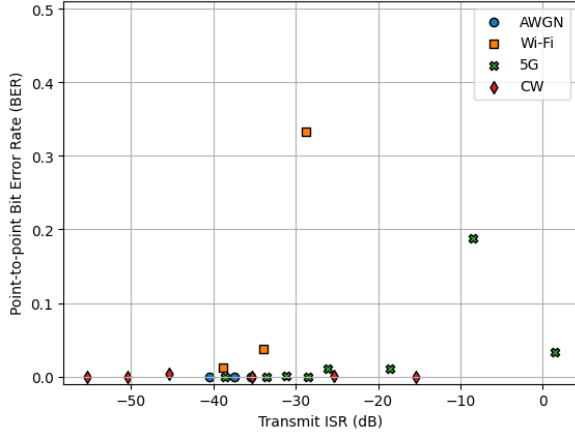


Figure 6.30: BER for Interferer 1 to Filmore High-Rate for Sets 2 & 3

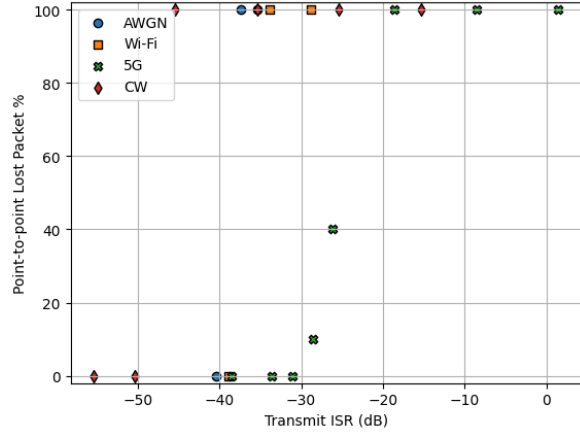


Figure 6.31: Average Packet Lost % for Interferer 1 to Filmore High-Rate for Sets 2 & 3

6.3.4.2 Stratified Jitter

The jitter become stratified for high rate paradigms.

Figure 6.32 shows the jitter for the mid-rate paradigm across all interferer sites and test sets. Figure 6.33 shows the packet lost percentage for the mid-rate paradigm across all interferer sites and test sets. Figure 6.34 shows the jitter for the high-rate paradigm across all interferer sites and test sets. Figure 6.35 shows the packet lost percentage for the high-rate paradigm across all interferer sites and test sets.

In the test cases depicted here, the jitter shows clear stratification even at interference levels well below those that impact the P2P link. We speculate that this stratification may be related to packet size sent across the link.

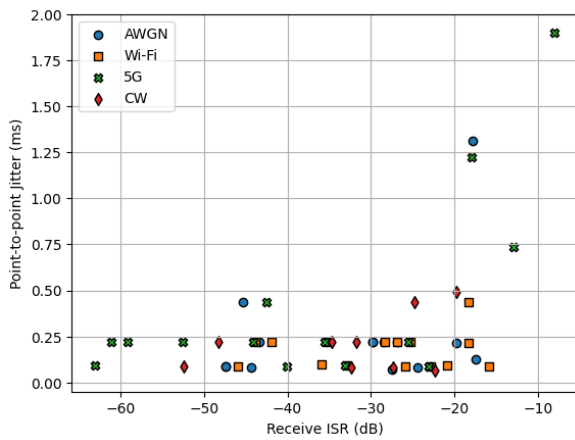


Figure 6.32: Average Jitter of Mid-Rate P2P

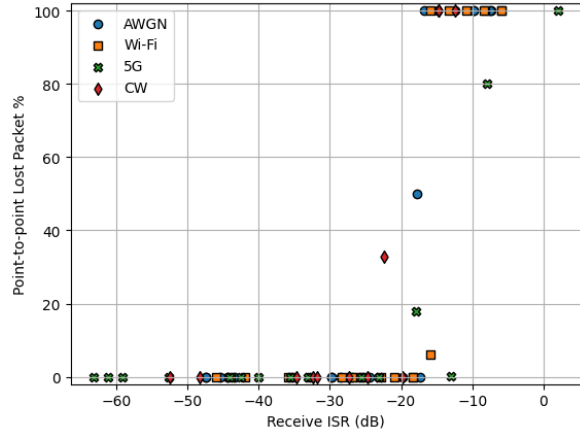


Figure 6.33: Average Packet Loss % of Mid-Rate P2P

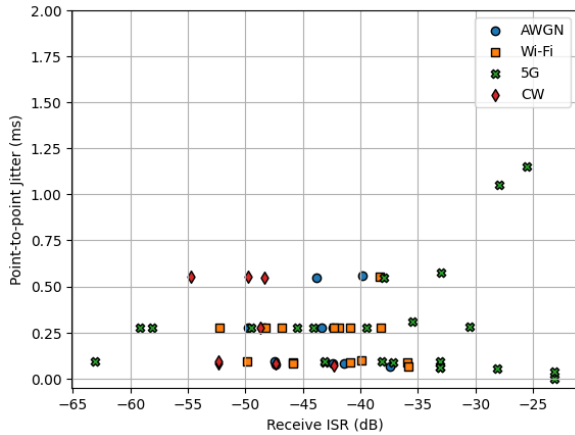


Figure 6.34: Average Jitter of High-Rate P2P

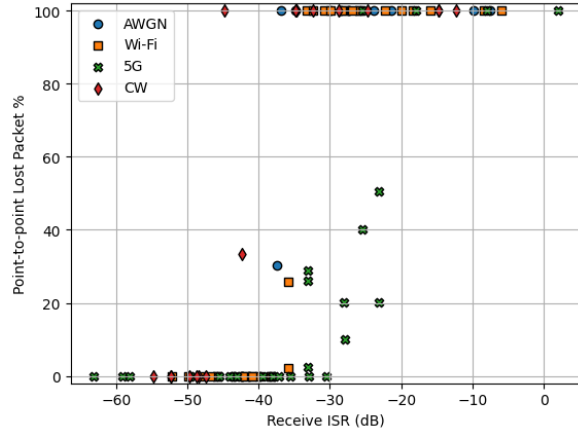


Figure 6.35: Average Packet Loss % of High-Rate P2P

6.4 Conclusions

The open range testing discussed here outlines the impacts of interference on P2P and raises several important considerations.

First and foremost this work highlights the importance of testing to augment simulations. We see this most clearly by comparing the predicted threshold Received ISR shown in Table 4.13 to the measured threshold Received ISR shown in Table 6.8. Examining the low-rate paradigm, we see that the lowest measured ISR is 1 dB lower than the predicted ISR threshold. The mid-rate paradigm shows less deviation with only a 0.7 dB difference between the lowest measured ISR threshold and the predicted ISR threshold. The high-rate paradigm shows a significant difference, with the lowest measured ISR threshold 9.8 dB lower than the predicted ISR threshold. The significant gap between the predicted and measured threshold for the high-rate case is related to the additional sensitivity of the high-rate P2P link to the CW interferer type, which is a factor not captured by the simulation effort. Further it is notable that even in cases without such a specific sensitivity, the lowest measured ISR threshold is universally lower than the predicted ISR threshold, which runs counter to the standard intuition. Simultaneously, both the mid-rate and high-rate paradigms exhibit one measured ISR threshold that is higher than the predicted ISR threshold. For both of these paradigms, the 5G interferer was much less impactful than the others, with a measured ISR 7.5 dB higher than predicted for the mid-rate paradigm and 9.5 dB higher for the high-rate paradigm. This is especially notable when considering that the low-rate paradigm is seemingly more sensitive to 5G relative to the predicted ISR threshold. Therefore, while the lower duty cycle of the 5G interferer is certainly a factor, particular sensitivities of the P2P are also at play. These results clearly demonstrate the importance of confirming simulation with over-the-air testing.

Second the results shown here demonstrate that the modem itself does not always provide a clear picture of the P2P link. In particular, the BER reported by the terminal exhibits a return to near-zero behavior after a critical threshold of link impact (see Section 6.3.4.1).

Finally the results collected here demonstrate some of the behaviors of P2P links themselves. For example, Section 6.3.4.2 shows that there is some relationship to the rate of data being sent on the link that is independent of the interference experienced by the link. Additionally, we note in Section 6.2.4 that communication errors can arise as a result of application configurations that do not match the link configuration. Together these elements demonstrate that P2P links are part of a broader, complex communication system whose performance depends on the interaction of several components.

7 Simulation to Interpolate Results

This section describes the simulation used to expand beyond what can practically be accomplished in open range testing alone. Specifically, this simulation study uses the results from open-range testing to predict the geographic regions where interferers are likely to meet or exceed the threshold of received power necessary to impact the P2P link. We refer to these regions as impact regions.

7.1 Tools Used

This simulation study uses the Improved Many-on-Many (IMOM) simulation engine to facilitate examination of the impact regions. IMOM is a multi-dimensional, graphically oriented, Windows desktop application. It contains a suite of RF modeling tools that can be used to analyze the capabilities of a variety of communications and jamming systems. The core IMOM application includes a map that allows multiple overlays to be visualized along with analysis results and a scenario editor that allows control over asset location, orientation, and parameters. RF models in IMOM range from simple line-of-sight models to complex parabolic equations that take atmospheric, dielectric, and ionospheric considerations into account.

7.2 Methodology

This section describes the method used to determine impact regions for each interferer type.

7.2.1 Modeling Impactful Locations

This study employs the Moving Transmitter IMOM analysis. This analysis considers a receiver at a fixed location with mobile transmitter to produce a coverage polygon around the receiver that shows where a transmitter could be placed to meet the receiver sensitivity. Here, the orientation of the receive antenna is fixed but the transmit antenna adapts such that it is always aimed directly at the receive antenna. The RF model chosen considers a medium level of granularity over terrain, basic atmospheric, and basic dielectrics conditions.

Our study adapts the IMOM Moving Transmitter analysis, to determine the impact regions for combinations of interferer types and P2P paradigms. To accomplish this, we model P2P receiver as the fixed receiver and the interferer as the mobile transmitter. Here, we consider receivers at both P2P locations (see Section 2.4). The receiver model includes the P2P antenna pattern, antenna heights, polarization, and frequencies. We aim each P2P antenna directly at the opposite P2P location. We set the receiver sensitivity according to the level of received interference power shown to impact the P2P link during open-range testing. The mobile transmitter model of an interferer includes the interferer antenna pattern, polarization, and frequencies. We orient the interferer antenna to always directly at the P2P receiver. We consider three different interferer antenna heights above the terrain: (1) 3 ft (0.91 m), (2) 15 ft (4.6 m), (3) 30 ft (9.1 m). These heights capture the interferer height examined during testing (i.e., 30 ft), a height more typical of ground based interferer (i.e., 3 ft), and a mid-point between these two (i.e., 15 ft). We examined each combination of interferer type and P2P paradigm where the P2P link was impacted during open-range testing. We examined several interferer heights to span a range of potential interferer scenarios.

This simulation produces maps of the impact region for each considered pair of interferer and P2P paradigm. The regions shown on these maps are colored according to the level of impacted expected from interferers within the region. The largest region, colored lavender, indicates areas where an interferer induces

Table 7.1: Received Interference Power Thresholds

P2P Paradigm	Interferer Type	Rx Location	Rx Interferer Thres. (dBm)	Rx Interferer Thres. (Watts)
Low	5G	Filmore	-57.3	1.9×10^{-9}
Mid-Rate	5G	Filmore	-62.3	5.9×10^{-10}
		AWGN	Filmore	-71.2
	Haul		-66.8	2.1×10^{-10}
	CW	Filmore	-69.1	1.2×10^{-10}
		Haul	-66.7	2.1×10^{-10}
	Wi-Fi	Filmore	-67.6	1.7×10^{-10}
Haul		-70.2	9.5×10^{-11}	
High-Rate	5G	Filmore	-77.9	1.9×10^{-11}
		AWGN	Filmore	-91.2
	Haul		-81.4	6.7×10^{-12}
	CW	Filmore	-99.1	1.2×10^{-13}
		Haul	-87.6	1.7×10^{-12}
	Wi-Fi	Filmore	-87.6	1.7×10^{-12}
		Haul	-85.2	3.0×10^{-12}

a received interference power under the impact threshold, but within 6 dB of it. The mid-sized region, colored cyan, indicates areas where an interferer induces a received power above the threshold but within 6 dB of it. The smallest region, colored pink, indicates areas where an interferer induces a received power that is more than 6 dB above the threshold. Each analysis displays the impact of the terrain and antenna pattern of the degree to which interferers impact the P2P link.

7.2.2 Selecting Received Interference Thresholds

We determined the threshold received interference power level for each interferer type to impact each P2P paradigm by examining the results of open-range testing. In particular, we found the minimum received interference power necessary to impact the P2P link for each interferer type. As discussed in Section 7.2.1, these thresholds are used to determine the impact regions for interferer type and P2P paradigm combination. Table 7.1 shows the thresholds for each combination of interferer type and P2P paradigm where an impact was observed during open-range testing.

7.3 Results

This section discusses the results of this simulation study. Here we highlight a subset of the results that expose particular trends. The complete set of plots is provided in Section 3.5 of the plots supplement document.

7.3.1 Low-Rate Paradigm

This section discusses the impact regions associated with the low-rate P2P paradigm. Impact to the low-rate paradigm was only observed in open-range testing with the P2P receiver at Filmore and a 5G interferer. Figure 7.1 displays the impact region for a 5G interferer at 30 ft. Figure 7.2 displays the impact region for a 5G interferer at 15 ft. Figure 7.3 displays the impact region for a 5G interferer at 3 ft. In each of these cases, the impact region is relatively narrow which is indicative of the robustness of the low-rate P2P paradigm. That is, interferers must be positioned close to the main beam of the P2P link to impact the low rate paradigm. Further, these results demonstrate the reduction of impact region with reduction in the height of the interferer.

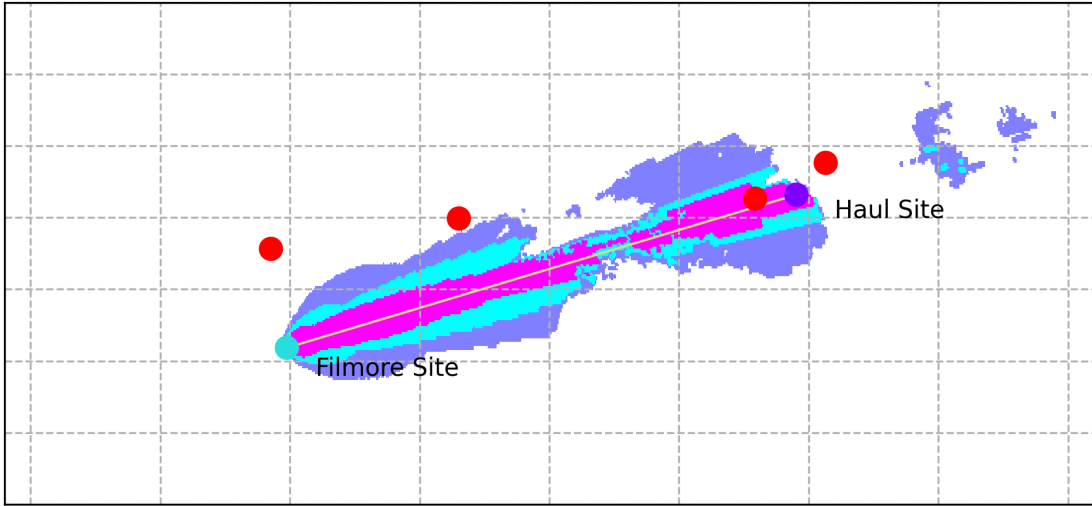


Figure 7.1: Sensitivity of Low-Rate Link Received at Filmore to 5G at 30 ft

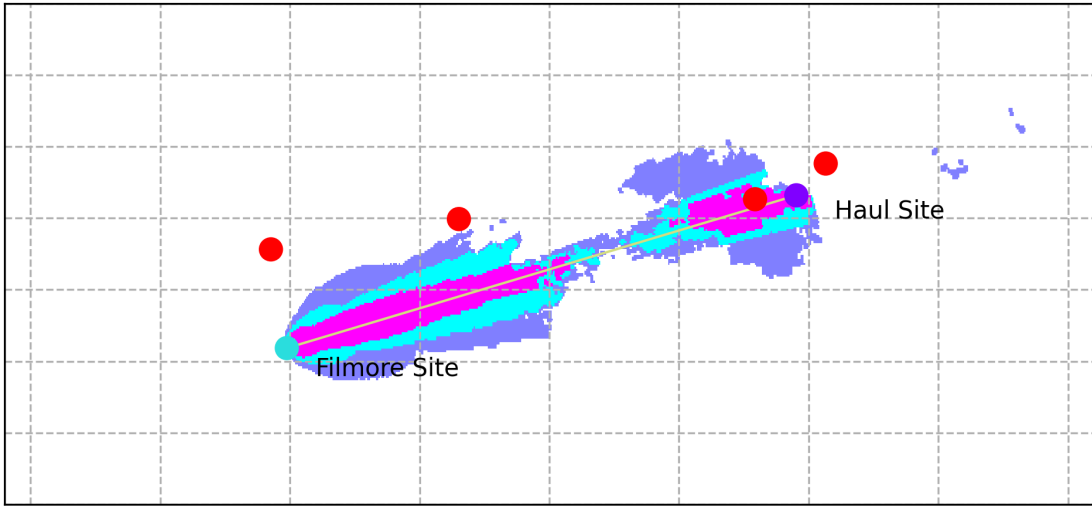


Figure 7.2: Sensitivity of Low-Rate Link Received at Filmore to 5G at 15 ft

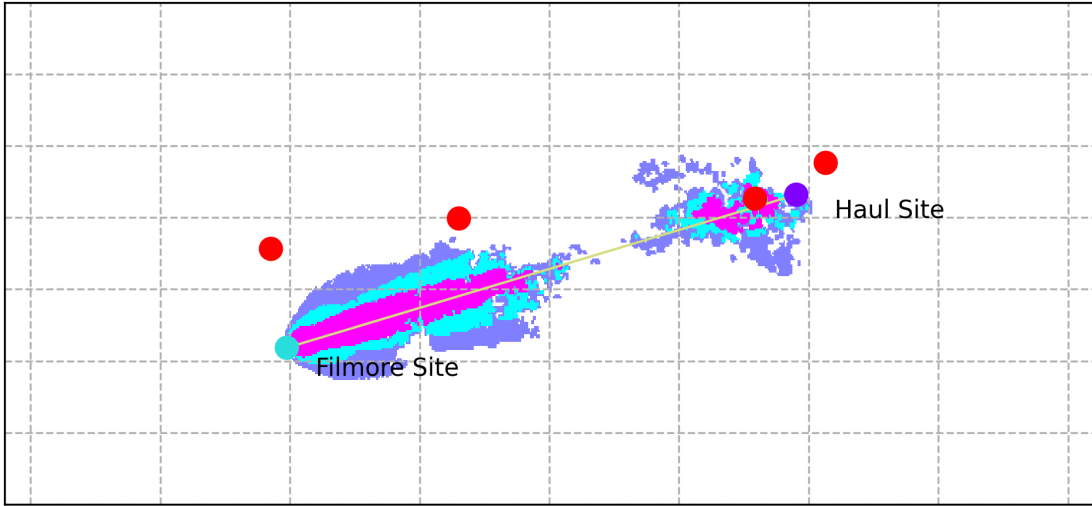


Figure 7.3: Sensitivity of Low-Rate Link Received at Filmore to 5G at 3 ft

7.3.2 Mid-Rate Paradigm

This section discusses the impact regions associated with the mid-rate P2P paradigm. Here, we focus on the impact regions for interferers at 30 ft to facilitate comparisons among the various interferer types.

Figure 7.4 displays the impact region for a 5G interferer with the P2P receiver at Filmore. Figure 7.5 displays the impact region for a AWGN interferer with the P2P receiver at Filmore. Figure 7.6 displays the impact region for a CW interferer with the P2P receiver at Filmore. Figure 7.7 displays the impact region for a Wi-Fi interferer with the P2P receiver at Filmore. Comparing these plots highlights the variable potential of interferers to impact the P2P link. Here we see that the 5G interferer must be placed more precisely than other interferer types to impact the mid-rate P2P link.

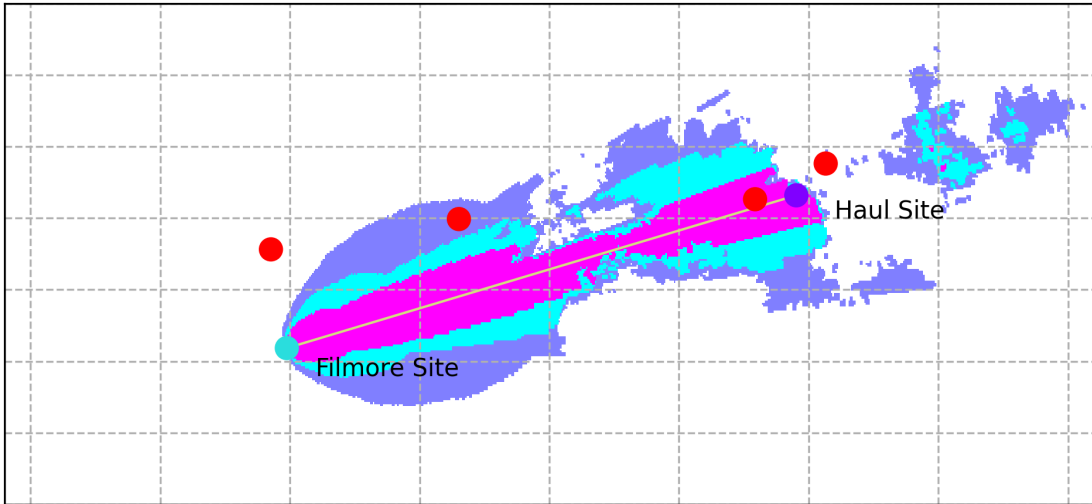


Figure 7.4: Sensitivity of Mid-Rate Link Received at Filmore to 5G at 30 ft

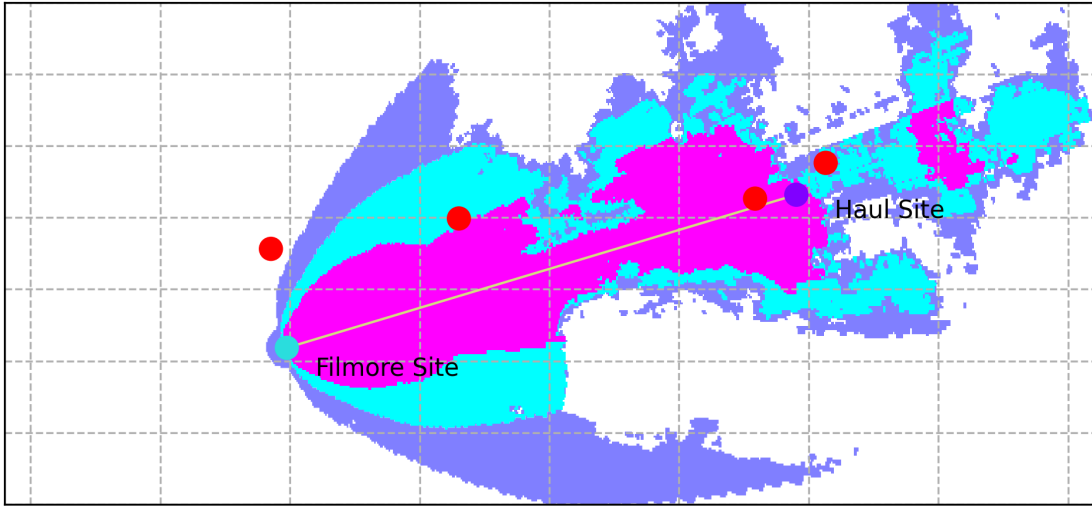


Figure 7.5: Sensitivity of Mid-Rate Link Received at Filmore to AWGN at 30 ft

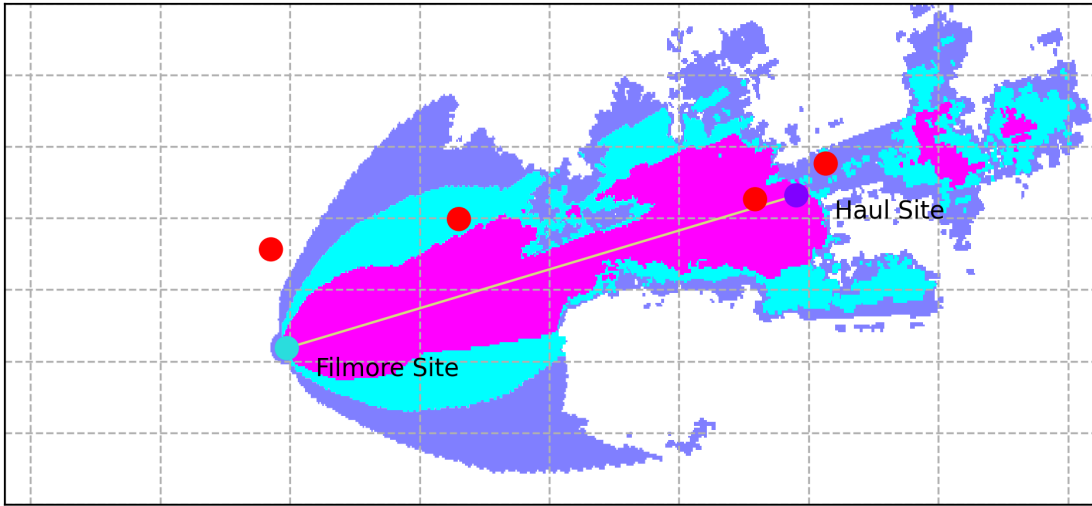


Figure 7.6: Sensitivity of Mid-Rate Link Received at Filmore to CW at 30 ft

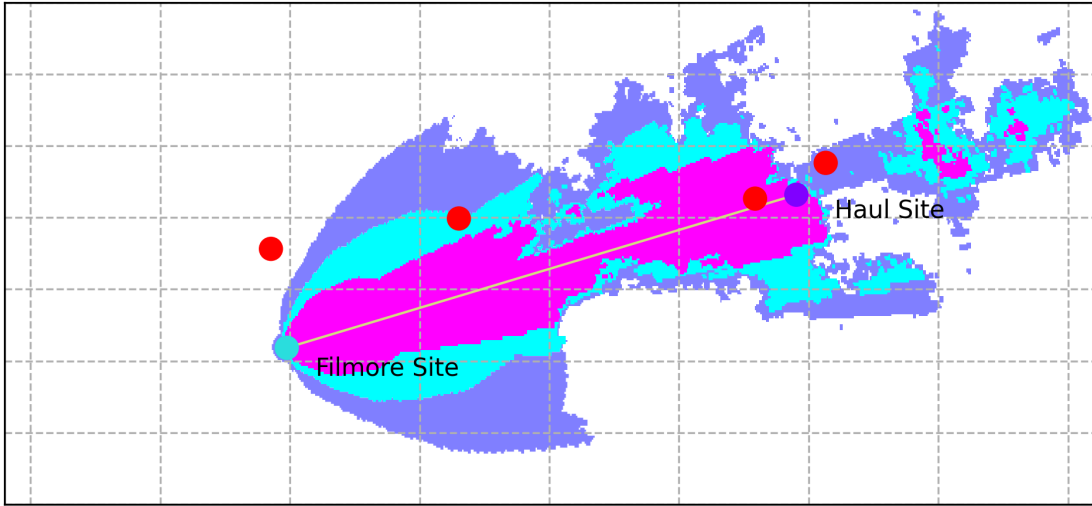


Figure 7.7: Sensitivity of Mid-Rate Link Received at Filmore to Wi-Fi at 30 ft

Figure 7.8 displays the impact region for an AWGN interferer with the P2P receiver at Haul. Figure 7.9 displays the impact region for a Wi-Fi interferer with the P2P receiver at Haul. These figures demonstrate that while the terrain varies between the P2P receive locations the overall trends remain intact.

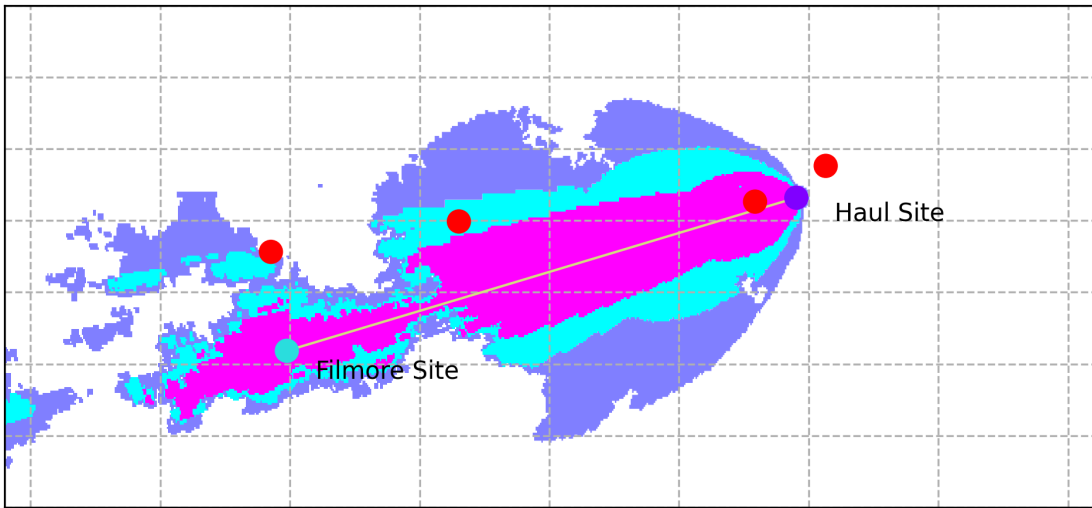


Figure 7.8: Sensitivity of Mid-Rate Link Received at Haul to AWGN at 30 ft

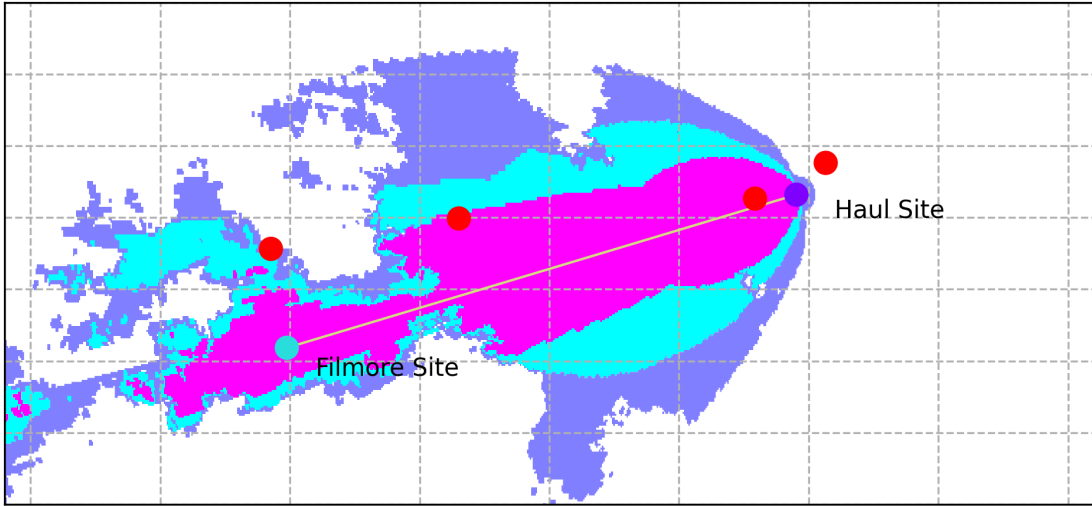


Figure 7.9: Sensitivity of Mid-Rate Link Received at Haul to Wi-Fi at 30 ft

7.3.3 High-Rate Paradigm

This section discusses the impact regions associated with the high-rate P2P paradigm. Again, we focus on the impact regions for interferers at 30 ft for the sake of comparison.

Figure 7.10 displays the impact region for a 5G interferer with the P2P receiver at Filmore. Figure 7.11 displays the impact region for an AWGN interferer with the P2P receiver at Filmore. Figure 7.12 displays the impact region for a CW interferer with the P2P receiver at Filmore. Figure 7.13 displays the impact region for a Wi-Fi interferer with the P2P receiver at Filmore. Among these figures, the significance of the CW interferer is clear. Further these results demonstrate the relative fragility of the high-rate P2P paradigm.

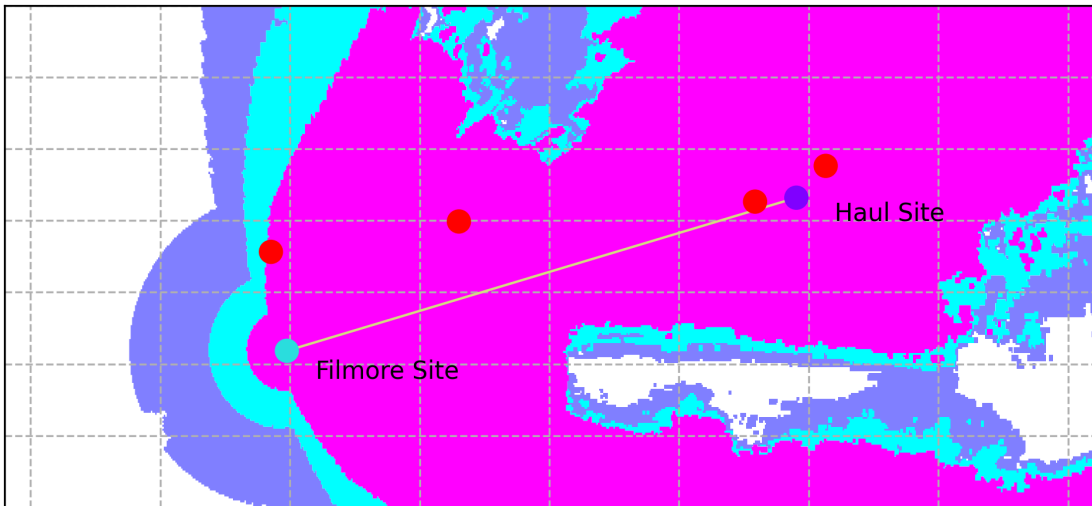


Figure 7.10: Sensitivity of High-Rate Link Received at Filmore to 5G at 30 ft

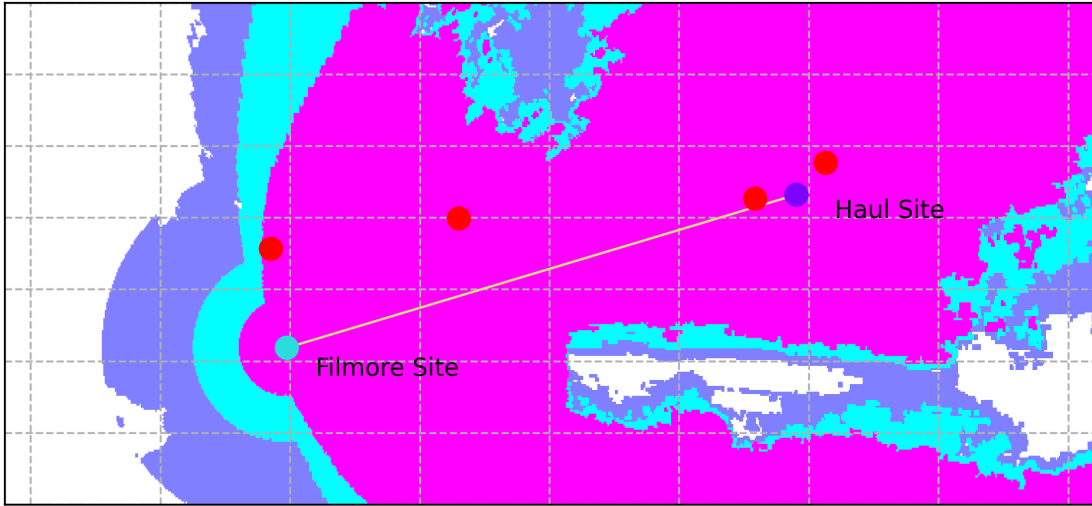


Figure 7.11: Sensitivity of High-Rate Link Received at Filmore to AWGN at 30 ft

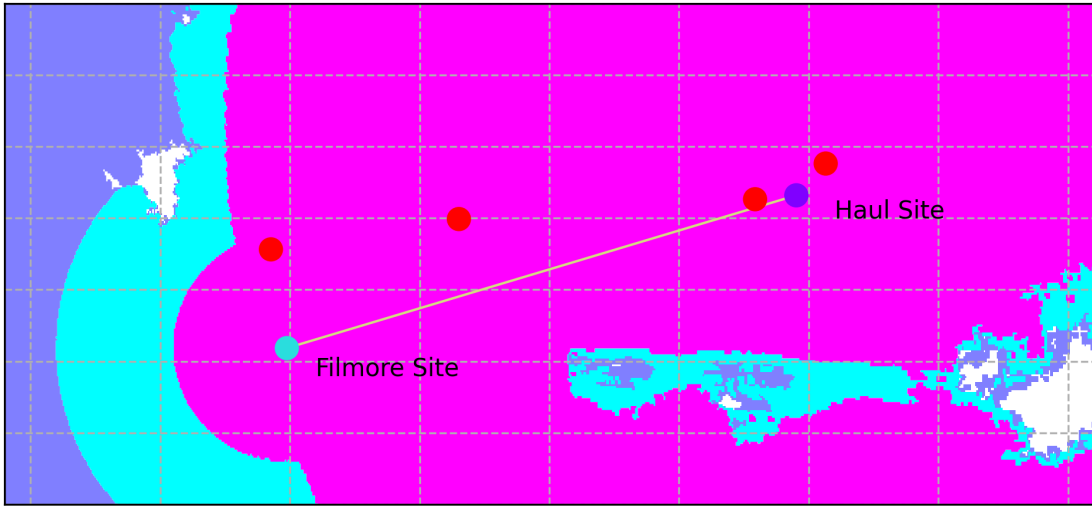


Figure 7.12: Sensitivity of High-Rate Link Received at Filmore to CW at 30 ft

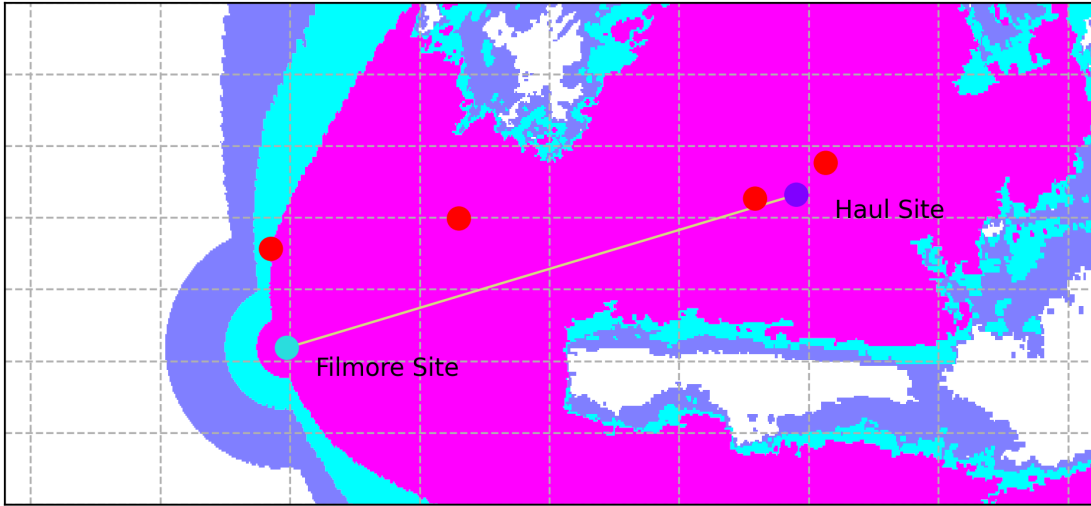


Figure 7.13: Sensitivity of High-Rate Link Received at Filmore to Wi-Fi at 30 ft

7.4 Conclusions

The simulation study demonstrates an approach to applying test results to expanded planning uses. Here, we show the impact regions implied by the open-range test results, per interferer type and P2P paradigm combination. These maps highlight the variable impact of interferers on different P2P paradigms (e.g., the high resilience of the low-rate paradigm or the significant impact of CW on the high rate paradigm). Further, these maps account for both antenna patterns and terrain effects to illustrate the geographic regions of concern for P2P protection. Here, we have shown that the vulnerability of P2P links exhibits a strong dependence on these geographic features.

8 Discussion of Results

This section collects the major themes of the results from this project. As foundation for this, we briefly summarize the major results of the studies that comprise this project. Additionally, we also summarize the technical limitations of our approach to provide the necessary context of the results. With that foundation we identify the major trends in the results. We finish this section with an examination of the major lessons learned during the course of this project.

8.1 Summary of Results

Here we briefly summarize the major results of the studies that comprise this project. Recall that this project includes three simulation studies: (1) site selection (see Section 3), (2) parameter exploration (see Section 4), and (3) results interpolation (see Section 7). Additionally, this project includes two over-the-air test events: (1) initial testing (see Section 5) and (2) open-range testing (see Section 6).

The site selection simulation study examines locations for testing to ensure that: (1) our P2P link configuration is feasible and representative of typical links and (2) we have a diversity of feasible interferer locations. This simulation study provides four types of results:

- Candidate locations for subsequent consideration (see Section 3.3.1)
- Final P2P locations for use in the rest of the project (see Section 3.3.2)
- Final interferer locations for use in the rest of the project (see Section 3.3.3)
- Confirmation that selected locations support a diversity of beam injection (see Section 3.3.3.2)

Overall the site selection simulation study provides a set of locations that allow realizing a typical P2P link and injecting interference from a diversity of angles. We list these locations in Section 2.4.

The parameter exploration simulation study examines the meaningful parameter ranges for both the P2P link and interferers. Additionally, this study provides a simulation-based prediction of the impact of interference on the P2P link. In the course of achieving this, this simulation study provides four types of results:

- The path loss for the P2P link (see Section 4.3.1.1)
- The expected operating margins for each P2P paradigm for a range of powers (see Section 4.3.1.2)
- The path loss and sidelobe attenuation for each pair of interferer location and P2P receiver locations (see Section 4.3.2.1)
- The range of interferer transmit powers that could feasibly impact the P2P link from each interferer location (see Section 4.3.2.2)
- Estimated Receive ISR thresholds, where the P2P link should start to be degraded by the interference (see Section 4.4)

The parameter exploration simulation study estimates both the range of meaningful link and interferer parameters as well as the impact of interference on the P2P link. Thus, this study provides both a starting point and a comparison point for subsequent studies.

The initial testing proves out our approach to managing the P2P link, collecting data, and injecting interference. Thus, this test provides three types of results:

- Validation of P2P operation (see Section 5.5.1)
- Validation of data collection (see Section 5.5.2)
- Validation of interferer injection (see Section 5.5.3)

Overall the initial test is a small scale validation of the rest of the project.

The open-range testing is the core of this project in that this test provides empirical data about the impact of interference on our P2P link. This test provides three types of results:

- Baseline characterization of P2P link performance with no interference signals present (see Section 6.3.1)
- Determination of the threshold Receive ISR values for each interferer type (see Section 6.3.2)
- Characterization of the influence of interferer location on the impact of interference on the P2P link (see Section 6.3.3)
- Capture of unexpected P2P link behaviors (see Section 6.3.4)

This open-range testing is the core source of data for this effort and provides a direct comparison point for the estimations of the parameter exploration study.

The interpolation simulation extends the empirical produced by the open-range testing to estimate the geographic regions from which different interferers could impact the P2P link. Thus, this study produces on type of result:

- Characterization of impact regions for each pair of interferer type and P2P paradigm (see Section 7.3)

This simulation study provides an example of how over-the-air, empirical can be used as the foundation of simulation to determine a strategy to protect P2P links. In this, we determine geographic regions where a co-mingled sharer should be prevented from using certain signal types at certain power levels.

8.2 Technical Limitations

This section summarizes the primary technical limitations of this project with the intention of putting our results in the appropriate context. For the most part, these limitations are driven by the practical limitations of conducting over-the-air testing.

Our testing only examined a signal instance of a P2P link. That is we only tested on set of P2P equipment, P2P antennas, and link distance. While we selected these to be typical of P2P links that support electric utilities, there are certainly several configurations that are not well represented by our configuration. Thus, the primary impact of this limitation is limiting the generalizability of our results. While this effect is partially mitigated by our examination of ratios, the response of different P2P equipment is likely to vary from the equipment that we examine here. Determining the magnitude of this variation would require subsequent testing.

Our consideration of the use for the P2P link is coarse relative to specific implementations of P2P links for electric utilities. Our purpose here is to broadly characterize the impact of interference on general electric utility use of P2P links. In pursuit of this, we have defined broad P2P paradigms that generally outline electric utility use of P2P links, but do not necessarily capture the particular concerns of any specific use case. This effect limits the applicability of our results for determining the operation impacts of interference for specific uses of P2P links. Instead our focus here is to broadly outline the communication impacts of interference.

We considered a limited scope in the variation of parameters for each interference. For example, while our full set of interferers display good variability of duty cycle each individual interference type only utilizes one duty cycle setting. Additionally, we only consider one variant for both 5G and Wi-Fi and do not examine the other variations or modulations that would be observed in practice. Together, these factors limit the extent to which we can identify signal characteristic that are more or less harmful to P2P links. This information would be particularly useful for designing spectrum sharing rules that maximally utilize the potential of the spectrum while maintaining the operation of critical links.

Similarly to the previous limitation, our investigation here conjectures that existing forms of 5G and Wi-Fi would be directly applied in 7 GHz. Given the precedent seen in the past, it seems likely that new variations of these signals would be designed for use in 7 GHz. While such new variations would certainly have some relationship to the variations that we consider here, they are likely to exhibit features that may alter the impact on P2P links. This seems especially likely for the 7 GHz band which currently lacks significant hardware support.

Our examination here does not consider any mechanisms to protect the P2P links. Given the approach seen for co-mingled sharing previously, it seems likely that there would some protection mechanism put in place to protect P2P links in the case that the 7 GHz band was opened to co-mingled sharing. These protection mechanisms are likely to significantly influence the impact of interference on P2P links. Currently, however, the nature of the protection mechanism that may be deployed in the 7 GHz band is entirely unclear. Further the enforcement of any given spectrum mechanism remains a largely open question. Therefore, we believe ignoring protection mechanisms to be the most appropriate choice at this point, even if such mechanisms are significant factors for our topic of interest.

8.3 Major Trends

This section identifies the major trends across the results of this project. These trends begin to outline the overall impact of interference on P2P, of course subject to the limitations discussed in Section 8.2.

Looking across the interference results, we see some clear relationships between interferer type and impact to the P2P link. These relationships vary with P2P paradigm as well. In our results we only observed impact to the P2P link from multiple interferer types for the mid-rate and high-rate paradigms; therefore, we focus on these paradigms here. Considering first the mid-rate paradigm, we see that the impact appears to be related to the total interference power delivered. We see that the AWGN interferer impacts the mid-rate link at the lowest Receive ISR value (see Table 6.8 in Section 6.3.2). This is followed by Wi-Fi and then CW. This order directly corresponds to the power of the interference signal as influenced by duty cycle and bandwidth. Considering the high-rate paradigm, we see a particular sensitivity to the narrow band CW signals. This is notable because it goes against the power based trend observed for the mid-rate case. Together these variable impacts highlights the fact that factors beyond raw power must be considered when determining the impact of interference. Unfortunately, these factors depend on the specific characteristics of the interfering signal and the implementation of the P2P receiver. Additional testing is required to fully characterize the sensitivities beyond raw interference power.

Interferer power is certainly a significant factor in the impact to P2P links, even if other factors occasionally supersede its influence. It is important to recognize that the relationship between interferer power and impact to the P2P link is highly nonlinear, however. There is, in fact only a narrow transition between a completely unaffected link and a completely inoperable one. Thus the major impact of interference is often pushing a P2P link closer to the proverbial cliff rather than directly causing noticeable degradation. This is especially problematic for critical P2P links that demand a high reliability and can not afford additional vulnerability to other fades.

Importantly, our results here show that simulation can under estimate the impact of interference. While part of this effect is related to the sensitivities beyond interference power that we discussed above, some amount of under estimation persists even without these additional sensitivities. We discuss the details of the under-estimation of interference impacts by simulation in Section 6.4. Here, we further note that this result is particularly troubling when we see spectrum policy decision made by nearly exclusive consideration of simulations [6] [7].

8.4 Lessons Learned

This section summarizes the major lessons learned about the interaction of interference and P2P links during the course of this project. These lessons push beyond the trends in the technical results discussed in Section 8.3 to highlight some of the practical implications of co-mingled interference for P2P links.

The communication performance of a P2P link depends on several factors and the causal relationships are not always clear. For example, in Section 6.3.4.2 we discussed a stratification in jitter values that appeared to be independent of the interference applied to the link. This result highlights a variability in the communication performance of the P2P link with a cause beyond interference. While this is certainly not necessarily a novel result, it serves as a clear reminder of the multiple competing factors that affect P2P link performance. These direct communication impacts range from specific implementation quirks of the P2P modem through natural variation in the propagation channel between the P2P endpoints.

The interaction between the applications running on a P2P link and the configuration of the link itself influence the perceived performance of the link. For example, our testing showed that the perceived performance of the low-rate link was significantly degraded by minorly overloading the link capacity (see Section 6.2.4). Again this result is not necessarily novel but rather a clear indicator of the cross stack interactions that influence the perceived link performance. Importantly, our testing examined a statically configured application running over a statically configured P2P link. As we increasingly move toward dynamic control of applications and links, the synchronization of the different layers is clearly a critical factor for the correct operation of the overall system.

Beyond the factors influencing P2P link performance itself, the perception of link performance is limited by the metrics available for observation. This situation is perhaps best highlighted by our experience with BER (see Section 6.3.4), where we observed that BER reported by the modem depends on data actively following on the link. That is if the data stops, whether because the operation using the link stops sending data or because the link is rendered inoperable, the reported BER drops to zero. Taken in isolation, a BER of zero typically indicates a perfectly operational link. That is, an important metric for tracking P2P link performance introduces an overlap between a link that is simply not transferring data at the moment and a link that is incapable of transferring data.

As discussed here, there are a variety of factors that impact both the communications performance of the P2P link and the perception of that performance. Additionally recall that the transition between an unimpacted P2P link and an inoperable link is narrow. Together this means that positively identifying an interference event on a P2P link is a non-trivial task. Even for the statically configured P2P links examine during this project, with full knowledge of when interferers were active in an otherwise quiet environment, positively identifying interference based impacts to the P2P link largely required post analysis of the collected data. Real-time, high-confidence attribution of communication performance degradation on an operational P2P link in a dynamic environment to interference seems highly unlikely. As such, the notion that a lack of complaints indicates good health for a co-mingled sharing configuration seems dubious at best.

9 Conclusions

This section explores the relationship of this project to the broader use of P2P links by electric utilities. We begin here with a reexamination of the goals of this effort to provide a contextual frame for our results. We then summarize various operational considerations to help scope our results from the perspective the operational use of P2P links. From there, we will cover the major implications of our results for electric utilities as they determine how to navigate the expansion of spectrum sharing. Finally, we outline future steps to expand the understanding of interference impacts to support the continued operation of critical communications.

9.1 Project Goals

Recall from Section 1.5 that the overarching goal of this project is to characterize the conditions necessary for representative potential interference signals to impact electric utility P2P links operating in the 7-8 GHz band. In particular, this effort takes a scientifically rigorous approach to establishing foundational data on interference impacts to P2P links in the 7-8 GHz band. This data development takes a forward leaning approach as a means to inform emerging spectrum policy with empirical data about the impact of interference on critical electric sector links. Ensuring that spectrum policy considers this impact is increasingly important as electric sector P2P links must provide increasing levels of performance and resilience at the same time that spectrum policy is increasingly turning toward spectrum sharing to meet growing spectrum demand. The characterization of interference impacts to P2P links conducted here is ultimately intended to support the continued operational efficiency, reliability, and security of the electrical grid by informing the design of spectrum sharing approaches that can support the continued operation of critical communications.

9.2 Operational Considerations

This section examines operational considerations that shape the extent to which our results directly apply to the operations of any specific electric utility. Given our focus on developing broad foundational data on the impact of interference on electric sector P2P links, our efforts do not consider several important factors that contribute to the resilience of electric utility operations. Here, we highlight a few particularly impactful factors.

Recall from Section 1.5 that our approach here is to generally consider the full range of electric utility operations that rely on P2P links by grouping them into operational paradigms. Specifically, we consider the three operational paradigms low-rate, mid-rate, and high-rate to broadly outline classes of electric utility operations. While this approach enables us to broadly consider electric utility operations, it also limits the granularity of our consideration of any given operation. That is our results outline general operational impacts but do not address the particular characteristics of any given operation. This approach aligns with our goal to provide foundational data rather than performing a case study for any particular use case.

A second consideration that results from our foundational approach is the lack of examination of cascaded effects or broader tradeoffs that shape the breadth of interference impacts. As noted in [5], the overall resilience of the electric system depends on the interaction of communication links and the electric grid. Ultimately, this means that the impact of interference on electric utilities depends on the interaction between these two systems. Further, note that P2P links are only one, albeit important, option for supporting the communications of electric utilities [4]. Thus determining the complete impact to electric utilities also

requires considering potential tradeoffs between different technologies. As such, the results of our project must be considered as only a portion of the overall resilience for electric utilities.

9.3 Operational Implications

This section summarizes the operational implications of our efforts for the electric sector. Here we examine the results of our project through the lens of electric sector operations to provide major lessons from our investigation of interference. Additionally we identify some potential updates to P2P links to better equip electric utilities to cope with interference.

First and foremost, our efforts demonstrate that co-mingled spectrum sharing has the potential to significantly degrade the operation of electric utilities by rendering critical P2P links impossible. Importantly, the results presented here outline the conditions necessary for this degradation to occur in terms of power ratios at the input the P2P receiver, which can be more readily compared across scenarios than various other metrics. Further, we show that the degradation of P2P links depends on both the configuration of the link and the type of interferer interacting with the link. Additionally, we demonstrate that the directional nature of P2P antennas significantly impact the geographic regions from which interferers will impact the link. Together, our results show that the impact of interference on P2P links depends on a broad range of factors that if not managed appropriately lead co-mingled spectrum sharing to be detrimental to the operation of critical communications.

Additionally our results indicate that managing interference on the basis of reported degradation alone is not a feasible strategy. Recall from Section 8.3 that identifying interference is non-trivial in practice. Importantly, the metrics reported by P2P modems can be a significant contributing factors to the challenge of identifying interference. For example, our results show that the BER reported by the modem will reset to show no errors after a certain threshold of harm to the P2P link, see Section 6.3.4.1. Further, the narrow transition between a completely unaffected link and a completely inoperable one limits the time available to observe interference in the first place. That is the primary effect of interference is to invisibly push P2P links closer to the threshold of significant degradation. Considering that potential interferers often exhibit bursty transmission that reflect highly variable usage patterns, the presence of interference largely turns the operating margin of critical P2P links into a random variable. Therefore, even without producing observable impacts, interference from co-mingled spectrum sharing can certainly materially degrade the ability of P2P links to maintain the level of resilience required to support critical electric utility operations.

We note that one factor in the inability to effectively observe and report interference stems from the lack of information about the operation of the error correction mechanism of the P2P receiver. While every modern digital P2P receiver employs error correcting mechanisms to improve the resilience of the link, typically information about the amount of errors corrected by these mechanisms is not externally reported. The overall effect of this is the narrowing of the observability of link degradation. This negative aspect of error correcting can be erased by exposing metrics that provide information about the level of effort that the error correction is putting into maintaining a high quality link. Ideally, this metric would provide a direct indication of the signal quality before any error correction is applied¹. While this information would not necessarily be able to differentiate interference from other sources of signal degradation such as weather effects, the addition of an initial signal quality metric would provide expanded visibility to signal degradations. Monitoring signal degradation with this expanded visibility would better support the identification of potentially bursty interference events and the long term impacts thereof on the resilience of P2P links.

Finally, our efforts here show that simulation studies can miss important interactions that cause them to significantly under estimate the impact of interference for some situations. As noted in Section 6.4, open-range testing demonstrates that the CW interferer impacts P2P links operating under the high-rate paradigm at power levels significantly less than the threshold predicted by simulation. At the same time, open-range testing showed that the antenna effects limited the impact of off-axis interference sites more than predicted by simulation. That is, simulation also over-estimated the impact of interference for several cases. As shown throughout this project, the impact of interference on P2P links is the result of several factors that interact through complex relationships. As a result simulations that reduce these interactions to statistical

¹We note that error vector magnitudes might be a good candidate metric for this purpose

or analytical models are likely to miss several important interactions that can lead to important deviations from reality. Therefore, while simulations can certainly be useful for estimation, the results must be verified by some examination of real systems.

9.4 Next Steps

This section highlights several potential next steps for this work. These steps are intended to continue our broader goals of developing a science based understanding of the potential impacts of emerging spectrum policy on critical links for the U.S. electric system and shaping spectrum sharing approaches to ensure the continued resilient operation of these links.

Recall that this project focuses on developing foundational data to characterize interference impacts. As noted in Section 8.2, there are several technical limitations to the scope of effort that we have accomplished here. In large part, these limitations stem from limitations in the feasible capacity for testing interference. That is, additional testing would allow investigation of more P2P types, interferer types, and parameter settings to better characterize the range of potential interference impacts. Further, laboratory investigation of the P2P modems would allow a more complete characterization of the transition between completely unaffected link and a completely inoperable link for various interference types. Such a characterization would provide a more nuanced understanding of the way that each interferer impacts the P2P links. Moreover, a more detailed examination of the transition period would inform discussion of potential metrics that could be useful for increasing the visibility of interference. Together these steps are based on filling gaps in the understanding of interference that remain in the foundational work presented here.

Beyond the direct augmentation of the technical understanding of interference, there are several clear steps to improve the utility of this work for informing electric utility operations. As noted in Section 9.2, our focus on producing broad foundational data here naturally limits the extent to which we directly explore the vulnerabilities of specific electric utility use cases to interference. Based on the foundational work presented here, there is a natural series of next steps that revolve around examining the impact of interference on specific electric utility use cases. Alternatively, this work can expand the capability of electric utilities for monitoring P2P links for interference by developing tools and techniques to extract information about interference from the P2P receiver directly. One component of this centers on the development of potential new P2P modem metrics. Another component of this focuses on examining a range of P2P types to support approaches that span a range of P2P modems and vendors. Together these steps would help to improve the ability of electric utilities to maintain awareness of interference and participate in the existing interference management approaches based on interference reporting.

Finally a clear set of next steps for this work focuses on the engagement of stakeholders in the management of interference to electric sector P2P links. Clearly, this includes engagement with electric utilities to help end users quantify the amount interference they experience. For example, the methods explored in this project could provide the foundation for in-situ testing of electric sector links. On the other hand stakeholder engagement includes dialog with policy makers to shape spectrum sharing approaches that balance the need for supporting increased access to spectrum against the need to ensure the continued operation of critical electric sector links. For example, the technique discussed in Section 7 demonstrate one approach to leveraging empirical, over-the-air data to inform the definition of geographic regions that could be used to define a geographic approach to spectrum sharing. Together, these steps focus on ensuring that emerging spectrum policy jointly considers the needs of many spectrum users.

Ultimately, this work provides a foundation for the scientific characterization of interference impacts to P2P links operating in the 7-8 GHz band based on over-the-air testing. This work outlines several implications of potential co-mingled spectrum sharing to electric utilities including some considerations for the design of spectrum sharing systems that include electric utilities as incumbent users. Further, here we outline several potential next steps to build upon the foundation provided by this work.

A References

- [1] 3GPP. *Technical Specification Group Radio Access Network; Physical layer procedures for shared spectrum channel access*. Technical Specification (TS) 37.213. Version 18.0.0. Sept. 2023.
- [2] 3GPP. *Technical Specification Group Radio Access Network; Study on NR-based access to unlicensed spectrum*. Technical Report (TR) 38.889. Version 16.0.0. Dec. 2018.
- [3] Office of Electricity. *Communications in the Electric Grid*. Tech. rep. Department of Energy, 2023.
- [4] Office of Electricity. *Grid Communications Technologies*. Tech. rep. Department of Energy, 2024.
- [5] Office of Electricity. *Power Grid and Communications Interdependencies*. Tech. rep. Department of Energy, 2023.
- [6] *FCC 20-51: Report and Order and Further Notice of Proposed Rulemaking*. Tech. rep. Federal Communications Commission, 2020.
- [7] *FCC CIRC2310-04: Second Report and Order, Second Further Notice of Proposed Rulemaking, and Memorandum Opinion and Order on Remand*. Tech. rep. Federal Communications Commission, 2023.
- [8] Wout Joseph et al. “Determination of the duty cycle of WLAN for realistic radio frequency electromagnetic field exposure assessment”. In: *Progress in Biophysics and Molecular Biology* 111.1 (2013), pp. 30–36. ISSN: 0079-6107. DOI: <https://doi.org/10.1016/j.pbiomolbio.2012.10.002>. URL: <https://www.sciencedirect.com/science/article/pii/S0079610712001083>.
- [9] Roshan Kumar and Mala De. “Power system resilience quantification and enhancement strategy for real-time operation”. In: *Electrical Engineering* (2024). ISSN: 1432-0487. DOI: 10.1007/s00202-024-02350-7. URL: <https://doi.org/10.1007/s00202-024-02350-7>.
- [10] *National Spectrum Strategy*. Tech. rep. The White House, 2023.
- [11] Md Ohirul Qays et al. “Key communication technologies, applications, protocols and future guides for IoT-assisted smart grid systems: A review”. In: *Energy Reports* 9 (2023), pp. 2440–2452. ISSN: 2352-4847. DOI: <https://doi.org/10.1016/j.egy.2023.01.085>. URL: <https://www.sciencedirect.com/science/article/pii/S2352484723000938>.
- [12] Günter Vermeeren et al. “In Situ Assessment of Uplink Duty Cycles for 4G and 5G Wireless Communications”. In: *Sensors* 24.10 (2024), p. 3012. ISSN: 1424-8220. URL: <https://www.mdpi.com/1424-8220/24/10/3012>.

B Mathematical Notation

Table B.1: Mathematical Symbols

Name	Symbol	Units	Description
P2P Noise Floor	N_{P2P}	dBm	Noise floor of P2P link
P2P Bandwidth	B_{P2P}	MHz	Receive bandwidth of P2P link
P2P Noise Figure	F_{P2P}	dB	Noise figure of P2P link
P2P SNR Threshold	S_{thres}	dB	Minimum received SNR to achieve a BER of 1×10^{-6}
P2P Received Power Threshold	$P_{P2P Rx Thres}$	dBm	Minimum received power to achieve a BER of 1×10^{-6}
P2P EIRP	$P_{P2P EIRP}$	dBm	Transmission power plus antenna gain of P2P link
P2P Transmit Power	$P_{P2P Tx}$	dBm	Transmission power of P2P link
P2P Antenna Gain	G_{P2P}	dB	Gain of P2P antenna
P2P Received Power	$P_{P2P Rx}$	dBm	Received power of P2P link
Path loss	$L_{P:i,j}$	dB	Path loss between location i and location j
P2P Achieved SNR	$S_{achieved}$	dB	SNR achieved on the P2P link
P2P Margin	M_{P2P}	dB	The amount of received signal level about the P2P SNR threshold
Received Interference Power Threshold	$P_{Int Rx thres}$	dBm	Interference power that must be received at the P2P receiver to impact the P2P link
Transmit Interference Power Threshold	$P_{Int Tx thres;i,j}$	dBm	Interference power that must be transmitted from location i to impact a P2P receiver at location j
Sidelobe loss	$L_{S:i,j}$	dB	Sidelobe loss between location i and location j
Interferer Antenna Gain	G_{Int}	dB	Antenna gain for the interferer
Interference EIRP Threshold	$P_{Int EIRP thres;i,j}$	dBm	Interference EIRP that must be emitted from location i to impact a P2P receiver at location j
Interference Transmit Power	$P_{Int Tx}$	dBm	Transmission power of the interferer
Interference EIRP	$P_{Int EIRP}$	dBm	Transmission power plus antenna gain of interferer
Transmit ISR	I_{Tx}	dB	Ratio of interference EIRP to the P2P EIRP

C Procedures

C.1 Data Collection

C.1.1 Sequences

C.1.1.1 P2P Link Setup

The following is the sequence to setup the P2P link:

1. Connect the -48 V Power supply to the PWR port of the Aviat modem.
2. Connect Ethernet to the GE2 port of the Aviat modem and to the driver laptop controller.
3. Wait for the Aviat modem to fully boot, which takes a few minutes, then test the connection to the data driver laptop by doing the following:
 - (a) Open a web-browser.
 - (b) Navigate to Aviat management webpage.
 - If the webpage loads, you have confirmed the connection.
 - If the webpage doesn't load, wait for a few minutes or ping the modem.
 - (c) Repeat this process for both ends of the P2P link.

Below we capture some notes about the P2P link setup:

- The modem positioned at Filmore is configured with an address of 192.168.1.2 and the modem positioned at Haul has an address of 192.168.1.1.
- We experienced an issue with powering the modem associated with the use of Eco Mode on the supporting generators. We found that the Eco Mode option limited the power draw of the Aviat modems below the required level.
- The maintenance port of the Aviat modems contains LEDs that indicate the status of the modem. The user guide and installation guides can provide more information.
- While the modem can be powered using power over Ethernet (PoE) or a direct DC power connection. We selected to use a 48 V power supply.

C.1.1.2 Continuous Capture of Terminal Data

This following is the sequence to start the continuous capture of terminal data:

1. Run the script for continuous terminal data collection (see Section C.1.2.2) by doing the following:
 - (a) Modify the test name parameters.
 - (b) Start the script.

Below we capture some notes about running the continuous capture of terminal data:

- The continuous capture script should be run after the P2P link is setup (see Section C.1.1.1).
- This script should run throughout all testing.
- The continuous capture script should run on the data driver laptop connected to the P2P receiver. In this case, the `location_name` parameter corresponds to the receive location.
- The `power_name` parameter corresponds to the P2P transmission power setting.
- The `modulation_name` parameter corresponds to the P2P modulation setting.
- Here, we save data into an SQL database. These databases should be checked periodically and/or backed up.

C.1.1.3 Running Tests

The following is the sequence to run a test case:

1. The data driver laptop connected to the P2P transmitter should run the test control script (see Section C.1.2.1) by doing the following:
 - (a) Modify the test name parameters.
 - (b) Start the script.

Below we capture some notes about running tests:

- The test control script should be run after the P2P link is setup (see Section C.1.1.1).
- The test control script should run on the data driver laptop connected to the P2P transmitter. In this case, the `location_name` parameter corresponds to the P2P transmitter location.
- The `power_name` parameter corresponds to the P2P transmission power setting.
- The `modulation_name` parameter corresponds to the P2P modulation setting.
- The `jammer_name` parameter corresponds to the type of interferer being used for the current test. If this is a P2P baseline test, this parameter should be "baseline".
- Here, we save data into an SQL database. These databases should be checked periodically and/or backed up.

C.1.1.4 5G Interferer Operation

The following is the sequence to operate the 5G interferer:

1. Set the signal generator to the appropriate frequency (see the notes below for information on signal generators)
2. Connect the USRP to the interferer controller laptop by doing the following:
 - (a) Connect the USB cable between the USRP and laptop.
 - (b) Run `sudo uhd_find_devices`
 - (c) Connect the USRP power cable.
3. Run 5Ghoul, by doing the following:
 - (a) Navigate to the directory containing the 5Ghoul material
 - (b) Run `./container.sh run release-5g`

- (c) Run
- ```
sudo bin/5g_fuzzer --MCC==001 --MNC=070 --GlobalTimeout=false \
--EnableMutation=false --BaseStationConfigFile n41.106.conf
```
- (d) Wait for the message "[Main] eNB/gNB started!" to confirm that the 5G network is operational.
- (e) Connect the UE to the 5G network by manually selecting the "Open5gs" network in the UE settings. The interferer controller terminal should display the message "[!] 1/2 UE connected to eNB/gNB" when the UE is connected.
4. Start an iPerf3 server on the UE, by doing the following:
    - (a) Open the HE Network Tools app on the UE.
    - (b) Open the settings menu (the bars button on the top left).
    - (c) Choose iperf3.
    - (d) Type `-s` into the main text box.
    - (e) Click go.
  5. Start a UDP iPerf session between the UE and the interferer controller laptop, by doing the following:
    - (a) Open a terminal.
    - (b) Type `iperf3 -c 45.45.0.2 -t 4000 -u -b 2000000`
    - (c) Press enter.
  6. Set the signal power with the programmable attenuator by doing the following:
    - (a) Open the Mini-Circuits control GUI on the control laptop connected to the programmable attenuator.
    - (b) Click USB in the GUI.
    - (c) Change the attenuator value as desired.

Below we capture some notes about running the 5G interferer:

- The USRP is the signal source for the 5G interferer.
- The default frequency of the 5G source is centered at 2533.350 MHz. The following settings should be applied to adjust the frequency:
  - To reach the 7390 MHz test frequency, the signal generator should be set to 4856.65 MHz.
  - To reach the 7690 MHz test frequency, the signal generator should be set to 5156.65 MHz.
- The signal generator power should be 10 dBm.
- Sometimes the laptop won't be able to connect to the USRP if both the power and the USB are connected at the same time.
- An orange light should appear on the USRP after connecting to the AC adapter.
- The iPerf session usually lasts for 200 seconds before crashing. When it crashes, do the following:
  1. Exit the 5G network on the interferer controller laptop by pressing Ctrl+C.
  2. Close the iperf3 session in the terminal on the laptop.
  3. Close the iperf3 session on the app on the UE.
  4. Restart everything and try again.
- The programmable attenuator can control several channels.
- The default value for the programmable attenuator is maximum attenuation for each channel.

### C.1.1.5 Wi-Fi Interferer Operation

The following is the sequence to operate the Wi-Fi interferer:

1. Set the signal generator to the appropriate frequency (see the notes below for information on signal generators)
2. Power on the Cambium AP by connecting it to a PoE.
3. Connect the Cambium AP to an externally hosted DHCP server.
4. Wait for the Cambium AP to boot (see notes below for information on Cambium AP status)
5. Connect the UE to the Wi-Fi network.
6. Start an iPerf3 server on the UE, by doing the following:
  - (a) Open the HE Network Tools app on the UE.
  - (b) Open the settings menu (the bars button on the top left).
  - (c) Choose iperf3.
  - (d) Type `-s` into the main text box.
  - (e) Click go.
7. Start a TCP iPerf session between the UE and the interferer controller laptop, by doing the following:
  - (a) Open a terminal.
  - (b) Type `iperf3 -c 192.168.0.101 -t 4000`
  - (c) Press enter.
8. Set the signal power with the programmable attenuator by doing the following:
  - (a) Open the Mini-Circuits control GUI on the control laptop connected to the programmable attenuator.
  - (b) Click USB in the GUI.
  - (c) Change the attenuator value as desired.

Below we capture some notes about running the Wi-Fi interferer:

- The default frequency of the Wi-Fi access point is centered at 2437 MHz. The following settings should be applied to adjust the frequency:
  - To reach the 7390 MHz test frequency, the signal generator should be set to 4953 MHz.
  - To reach the 7690 MHz test frequency, the signal generator should be set to 5253 MHz.
- The signal generator power should be 10 dBm.
- The Cambium AP doesn't have a built-in DHCP server and it won't work without one.
- The Cambium AP should show a steady green light once the Wi-Fi network is ready. It takes a few minutes for the Wi-Fi network to show up.
- The Wi-Fi network SSID is "Cambium1".
- The iPerf session might crash after running for a long and should therefore be checked periodically. This session can simply be restarted as necessary.
- The programmable attenuator can control several channels.
- The default value for the programmable attenuator is maximum attenuation for each channel.

### C.1.1.6 AWGN and CW Interferer Operation

The following is the sequence to operate for the AWGN and CW interferers:

1. Set the signal generator to the appropriate frequency (see the notes below for information on signal generators)
2. Connect the USRP to the interferer controller laptop by doing the following:
  - (a) Connect the USB cable between the USRP and laptop.
  - (b) Run `sudo uhd_find_devices`
  - (c) Connect the USRP power cable.
3. Start the script for the desired interferer (see notes below for information about the scripts)
4. Set the signal power with the programmable attenuator by doing the following:
  - (a) Open the Mini-Circuits control GUI on the control laptop connected to the programmable attenuator.
  - (b) Click USB in the GUI.
  - (c) Change the attenuator value as desired.

Below we capture some notes about running the AWGN and CW interferers:

- The USRP is the signal source for the AWGN and CW interferers.
- The default frequency of the AWGN and CW source is centered at 3000 MHz. The following settings should be applied to adjust the frequency:
  - To reach the 7390 MHz test frequency, the signal generator should be set to 4390 MHz.
  - To reach the 7690 MHz test frequency, the signal generator should be set to 4690 MHz.
- Sometimes the laptop won't be able to connect to the USRP if both the power and the USB are connected at the same time.
- An orange light should appear on the USRP after connecting to the AC adapter.
- See Section C.1.2.3 for the AWGN script.
- See Section C.1.2.4 for the CW script.

## C.1.2 Scripts

### C.1.2.1 Test Control

```
1 import mysql.connector
2 from mysql.connector import errorcode
3 from datetime import datetime
4 import iperf3
5 import time
6 import subprocess
7
8 def get_database_connection():
9 # This function returns a object configured to access the sql database
10 mysql_username = "[USERNAME]" # Change to match local configuration
11 mysql_password = "[PASSWORD]" # Change to match local configuration
12 mysql_host = "[CONNECTION_IP]" # Change to match local configuration
13 mysql_database = "aviat_data"
14 return mysql.connector.connect(user=mysql_username, password=mysql_password,
15 host=mysql_host,
16 database=mysql_database,
```



```

17 autocommit=True)
18
19 def iperf_mysql_table(power_name, modulation_name, location_name, jammer_name):
20 # This function creates a table in an SQL database to hold data from iPerf tools
21 current_datetime = datetime.now()
22 print("Current Datetime:", current_datetime)
23
24 cnx = get_database_connection()
25 cursor = cnx.cursor()
26
27 TABLES = {}
28 table_name = "iperf_" + "_".join([power_name, modulation_name, location_name,
29 jammer_name])
30 TABLES[table_name] = (
31 "CREATE TABLE " + table_name + " ("
32 " 'line' int AUTO_INCREMENT,"
33 " 'seconds' double NOT NULL,"
34 " 'bytes' double NOT NULL,"
35 " 'bits_per_second' double NOT NULL,"
36 " 'jitter_ms' double NOT NULL,"
37 " 'lost_packets' double NOT NULL,"
38 " 'packets' double NOT NULL,"
39 " 'lost_percent' double NOT NULL,"
40 " 'timestamp' timestamp NOT NULL,"
41 " PRIMARY KEY ('line')"
42 ") ENGINE=InnoDB")
43 table_description = TABLES[table_name]
44 print("Creating table {}:".format(table_name), end='')
45 cursor.execute(table_description)
46 cnx.close()
47
48 def aviat_data_mysql_table(power_name, modulation_name, location_name, jammer_name):
49 # This function creates a table in an SQL database to hold data from terminals
50 current_datetime = datetime.now()
51 print("Current Datetime:", current_datetime)
52
53 cnx = get_database_connection()
54 cursor = cnx.cursor()
55
56 TABLES = {}
57
58 table_name = "aviat_" + "_".join([power_name, modulation_name, location_name,
59 jammer_name])
60 TABLES[table_name] = (
61 "CREATE TABLE " + table_name + " ("
62 " 'line' int AUTO_INCREMENT,"
63 " 'bw' double NOT NULL,"
64 " 'txfreq' double NOT NULL,"
65 " 'rxfreq' double NOT NULL,"
66 " 'txmod' varchar(8) NOT NULL,"
67 " 'rxmod' varchar(8) NOT NULL,"
68 " 'txpow' double NOT NULL,"
69 " 'snr' double NOT NULL,"
70 " 'rem_snr' double NOT NULL,"
71 " 'rsl' double NOT NULL,"
72 " 'rem_rsl' double NOT NULL,"
73 " 'fade_margin' double NOT NULL,"
74 " 'rem_fade_margin' double NOT NULL,"
75 " 'ber' double NOT NULL,"
76 " 'rxtime' double NOT NULL,"
77 " 'rxsync' double NOT NULL,"
78 " 'timestamp' timestamp NOT NULL,"
79 " PRIMARY KEY ('line')"
80 ") ENGINE=InnoDB")
81 table_description = TABLES[table_name]
82 print("Creating table {}:".format(table_name), end='')
83 cursor.execute(table_description)
84 cnx.close()

```

```

85
86 def data_collect(power_name, modulation_name, location_name, jammer_name):
87 # This function runs the data collection
88
89 # Part 1: Setup parameters for test
90 rate_table = {"qpsk": 52,
91 "16qam": 121,
92 "32qam": 137,
93 "64qam": 179,
94 "128qam": 211,
95 "256qam": 241,
96 "512qam": 276,
97 "1024qam": 311,
98 "2048qam": 343,
99 "4096qam": 368}
100
101 data_rateMbps = rate_table[modulation_name]
102
103 ip_table = {"p2p_filmore": "192.168.1.2",
104 "p2p_haul": "192.168.1.1"}
105
106 modem_ip = ip_table[location_name]
107
108 cnx = get_database_connection()
109 cursor = cnx.cursor()
110
111 table_name = "iperf_" + "_".join([power_name, modulation_name, location_name,
112 jammer_name])
113 aviat_table_name = "aviat_" + "_".join([power_name, modulation_name, location_name,
114 jammer_name])
115
116 # Part 2: Iterate through tests
117 for i in range(1, 11):
118 # iPerf: setup test instance
119 client = iperf3.Client()
120 client.duration = 10
121 client.bandwidth = data_rateMbps * 1000000 # bits
122 client.server_hostname = '192.168.1.24'
123 client.port = 5201
124 client.protocol = 'udp'
125
126 # iPerf: run instance
127 result = client.run()
128
129 # iPerf: collect results
130 if result.error:
131 print(result.error)
132 else:
133 print(result)
134 print("/n")
135 print(' bytes transmitted {0}'.format(result.bytes))
136 print(' jitter (ms) {0}'.format(result.jitter_ms))
137 print(' lost packets {0}'.format(result.lost_packets))
138 print(' packets {0}'.format(result.packets))
139 print(' lost percent {0}'.format(result.lost_percent))
140 print(' bps {0}'.format(result.bps))
141 print(' seconds {0}'.format(result.seconds))
142
143 current_datetime = datetime.now()
144
145 add_data = ("INSERT INTO " + table_name + " "
146 "(seconds, bytes, bits_per_second,
147 jitter_ms, lost_packets, packets, lost_percent, timestamp) "
148 "VALUES (%s, %s, %s, %s, %s, %s, %s, %s, %s)")
149
150 data_vals = (float(result.seconds), float(result.bytes), float(result.bps),
151 float(result.jitter_ms),

```

```

150 float(result.lost_packets), float(result.packets), float(result.
lost_percent), current_datetime)
151 cursor.execute(add_data, data_vals)
152
153 # iPerf: clean up
154 del client
155
156 # Terminal: data collect
157 cmd = "sshpass -p admin ssh admin@" + modem_ip + " 'show radio-carrier status
Carrier1/1' << EOF | tee test_tmp.log\nshow radio-carrier status Carrier1/1\nEOF\n"
158 # returns output as byte string
159
160 returned_output = subprocess.check_output(cmd, shell=True)
161
162 file1 = open("test_tmp.log", "r")
163 data_read = file1.read()
164 print(data_read)
165
166 data_split = data_read.split()
167
168 len_data = len(data_split)
169
170 for i in range(0, len_data):
171 entry = data_split[i]
172
173 if 'bandwidth' == entry:
174 entry_bw = data_split[i + 1]
175 if 'tx-modulation' == entry:
176 entry_txmod = data_split[i + 1]
177 if 'rx-modulation' == entry:
178 entry_rxmod = data_split[i + 1]
179 if 'tx-frequency' == entry:
180 entry_txfreq = data_split[i + 1]
181 if 'rx-frequency' == entry:
182 entry_rxfreq = data_split[i + 1]
183 if 'current-tx-power' == entry:
184 entry_txpow = data_split[i + 1]
185 if 'snr' == entry:
186 entry_snr = data_split[i + 1]
187 if 'remote-snr' == entry:
188 entry_rem_snr = data_split[i + 1]
189 if 'rsl' == entry:
190 entry_rsl = data_split[i + 1]
191 if 'remote-rsl' == entry:
192 entry_rem_rsl = data_split[i + 1]
193 if 'fade-margin' == entry:
194 entry_fade_margin = data_split[i + 1]
195 if 'remote-fade-margin' == entry:
196 entry_rem_fade_mar = data_split[i + 1]
197 if 'ber' == entry:
198 entry_ber = data_split[i + 1]
199 if 'active-rx-time' == entry:
200 entry_rxtime = data_split[i + 1]
201 if 'rx-sync-loss-time' == entry:
202 entry_rxsync = data_split[i + 1]
203
204 current_datetime = datetime.now()
205
206 add_data = ("INSERT INTO " + aviat_table_name + " "
207 "(bw, txfreq, rxfreq, txmod, rxmod,
txpow, snr, rem_snr, rsl, rem_rsl, fade_margin, rem_fade_margin, ber, rxtime, rxsync,
timestamp) "
208 "VALUES (%s, %s, %s, %s, %s, %s, %s, %s,
%s, %s, %s, %s, %s, %s, %s, %s)")
209
210 data_vals = (float(entry_bw), float(entry_txfreq), float(entry_rxfreq), entry_txmod,
entry_rxmod, float(entry_txpow),

```

```

211 float(entry_snr), float(entry_rem_snr), float(entry_rsl), float(entry_rem_rsl),
float(entry_fade_margin),
212 float(entry_rem_fade_mar), float(entry_ber), float(entry_rxtime), float(entry_rxsync
), current_datetime)
213
214 cursor.execute(add_data, data_vals)
215
216 print("Done")
217
218 cnx.close()
219
220 if __name__ == "__main__":
221 power_name = "11_5"
222 modulation_name = "4096qam"
223 location_name = "p2p_filmore"
224 jammer_name = "loc4_cw_atten00"
225
226
227 iperf_mysql_table(power_name, modulation_name, location_name, jammer_name)
228 aviat_data_mysql_table(power_name, modulation_name, location_name, jammer_name)
229
230 data_collect(power_name, modulation_name, location_name, jammer_name)

```

### C.1.2.2 Continuous Capture of Terminal Data

```

1 # Datacollection Aviat Script
2 # The purpose of this script is to collect data from the aviat modems and put it into a
mysql database.
3 #
4
5 import mysql.connector
6 from mysql.connector import errorcode
7 from datetime import datetime
8 import iperf3
9 import time
10 import subprocess
11
12 mysql_username = "[USERNAME]" # Change to match local configuration
13 mysql_password = "[PASSWORD]" # Change to match local configuration
14 mysql_host = "[CONNECTION_IP]" # Change to match local configuration
15 mysql_database = "aviat_data"
16
17 def iperf_mysql_table(power_name, modulation_name, location_name, jammer_name):
18 current_datetime = datetime.now()
19 print("Current Datetime:", current_datetime)
20
21 cnx = mysql.connector.connect(user=mysql_username, password=mysql_password,
22 host=mysql_host,
23 database=mysql_database,
24 autocommit=True)
25
26 cursor = cnx.cursor()
27
28 DB_NAME = 'aviat_data'
29
30 TABLES = {}
31 table_name = "iperf_" + power_name + "_" + modulation_name + "_" + location_name + "_" +
jammer_name
32 TABLES[table_name] = (
33 "CREATE TABLE " + table_name + " ("
34 " 'line' int AUTO_INCREMENT,"
35 " 'seconds' double NOT NULL,"
36 " 'bytes' double NOT NULL,"
37 " 'bits_per_second' double NOT NULL,"
38 " 'jitter_ms' double NOT NULL,"
39 " 'lost_packets' double NOT NULL,"
40 " 'packets' double NOT NULL,"

```

```

40 " 'lost_percent' double NOT NULL,"
41 " 'timestamp' timestamp NOT NULL,"
42 " PRIMARY KEY ('line')"
43 ") ENGINE=InnoDB")
44 table_description = TABLES[table_name]
45 print("Creating table {}:".format(table_name), end='')
46 cursor.execute(table_description)
47 cnx.close()
48
49 def aviat_data_mysql_table(power_name, modulation_name, location_name, jammer_name):
50 current_datetime = datetime.now()
51 print("Current Datetime:", current_datetime)
52
53 cnx = mysql.connector.connect(user=mysql_username, password=mysql_password,
54 host=mysql_host,
55 database=mysql_database,
56 autocommit=True)
57
58 cursor = cnx.cursor()
59
60 DB_NAME = 'aviat_data'
61
62 TABLES = {}
63
64 table_name = "aviat_" + power_name + "_" + modulation_name + "_" + location_name + "_" +
65 jammer_name
66 TABLES[table_name] = (
67 "CREATE TABLE " + table_name + " ("
68 " 'line' int AUTO_INCREMENT,"
69 " 'bw' double NOT NULL,"
70 " 'txfreq' double NOT NULL,"
71 " 'rxfreq' double NOT NULL,"
72 " 'txmod' varchar(8) NOT NULL,"
73 " 'rxmod' varchar(8) NOT NULL,"
74 " 'txpow' double NOT NULL,"
75 " 'snr' double NOT NULL,"
76 " 'rem_snr' double NOT NULL,"
77 " 'rsl' double NOT NULL,"
78 " 'rem_rsl' double NOT NULL,"
79 " 'fade_margin' double NOT NULL,"
80 " 'rem_fade_margin' double NOT NULL,"
81 " 'ber' double NOT NULL,"
82 " 'rxtime' double NOT NULL,"
83 " 'rxsync' double NOT NULL,"
84 " 'timestamp' timestamp NOT NULL,"
85 " PRIMARY KEY ('line')"
86 ") ENGINE=InnoDB")
87
88 table_description = TABLES[table_name]
89 print("Creating table {}:".format(table_name), end='')
90 cursor.execute(table_description)
91 cnx.close()
92
93 def data_collect(power_name, modulation_name, location_name, jammer_name):
94 rate_table = {"qpsk": 50,
95 "16qam": 121,
96 "32qam": 137,
97 "64qam": 179,
98 "128qam": 211,
99 "256qam": 241,
100 "512qam": 276,
101 "1024qam": 311,
102 "2048qam": 343,
103 "4096qam": 368}
104
105 data_rateMbps = rate_table[modulation_name]
106
107 ip_table = {"day2_p2p_filmore": "192.168.1.2",
108 "day2_p2p_haul": "192.168.1.1"}

```

```

107 modem_ip = ip_table[location_name]
108
109 cnx = mysql.connector.connect(user=mysql_username, password=mysql_password,
110 host=mysql_host,
111 database=mysql_database,
112 autocommit=True)
113
114 cursor = cnx.cursor()
115
116 table_name = "iperf_" + power_name + "_" + modulation_name + "_" + location_name + "_" +
117 jammer_name
118
119 aviat_table_name = "aviat_" + power_name + "_" + modulation_name + "_" + location_name +
120 "_" + jammer_name
121
122 while True:
123 time.sleep(4) # Sleep for seconds
124 # Aviat data collect via SSH
125 cmd = "sshpass -p admin ssh admin@" + modem_ip + " 'show radio-carrier status
126 Carrier1/1' << EOF | tee test_tmp.log\nshow radio-carrier status Carrier1/1\nEOF\n"
127 # returns output as byte string
128
129 returned_output = subprocess.check_output(cmd, shell=True)
130
131 file1 = open("test_tmp.log", "r")
132 data_read = file1.read()
133 print(data_read)
134
135 data_split = data_read.split()
136
137 len_data = len(data_split)
138
139 for i in range(0, len_data):
140 entry = data_split[i]
141
142 if 'bandwidth' == entry:
143 entry_bw = data_split[i + 1]
144 if 'tx-modulation' == entry:
145 entry_txmod = data_split[i + 1]
146 if 'rx-modulation' == entry:
147 entry_rxmod = data_split[i + 1]
148 if 'tx-frequency' == entry:
149 entry_txfreq = data_split[i + 1]
150 if 'rx-frequency' == entry:
151 entry_rxfreq = data_split[i + 1]
152 if 'current-tx-power' == entry:
153 entry_txpow = data_split[i + 1]
154 if 'snr' == entry:
155 entry_snr = data_split[i + 1]
156 if 'remote-snr' == entry:
157 entry_rem_snr = data_split[i + 1]
158 if 'rsl' == entry:
159 entry_rsl = data_split[i + 1]
160 if 'remote-rsl' == entry:
161 entry_rem_rsl = data_split[i + 1]
162 if 'fade-margin' == entry:
163 entry_fade_margin = data_split[i + 1]
164 if 'remote-fade-margin' == entry:
165 entry_rem_fade_mar = data_split[i + 1]
166 if 'ber' == entry:
167 entry_ber = data_split[i + 1]
168 if 'active-rx-time' == entry:
169 entry_rxtime = data_split[i + 1]
170 if 'rx-sync-loss-time' == entry:
171 entry_rxsync = data_split[i + 1]
172
173 current_datetime = datetime.now()
174
175 add_data = ("INSERT INTO " + aviat_table_name + " "

```

```

172 "(bw, txfreq, rxfreq, txmod, rxmod, txpow, snr, rem_snr, rsl, rem_rsl,
173 fade_margin, rem_fade_margin, ber, rxtime, rxsync, timestamp) "
174 "VALUES (%s, %s, %s, %s, %s, %s, %s, %s, %s, %s, %s, %s, %s, %s, %s, %s)"
175
176 data_vals = (float(entry_bw), float(entry_txfreq), float(entry_rxfreq), entry_txmod,
177 entry_rxmod, float(entry_txpow),
178 float(entry_snr), float(entry_rem_snr), float(entry_rsl), float(entry_rem_rsl),
179 float(entry_fade_margin),
180 float(entry_rem_fade_mar), float(entry_ber), float(entry_rxtime), float(entry_rxsync
181), current_datetime)
182
183 cursor.execute(add_data, data_vals)
184
185 print("Done")
186
187 cnx.close()
188
189 if __name__ == "__main__":
190 power_name = "11_5"
191 modulation_name = "qpsk"
192 location_name = "day2_p2p_haul"
193 jammer_name = "cont_cap"
194
195 #iperf_mysql_table(power_name, modulation_name, location_name, jammer_name)
196 aviat_data_mysql_table(power_name, modulation_name, location_name, jammer_name)
197
198 data_collect(power_name, modulation_name, location_name, jammer_name)

```

### C.1.2.3 AWGN Interferer

```

1 import uhd
2 import numpy as np
3 import matplotlib.pyplot as plt
4
5 usrp = uhd.usrp.MultiUSRP()
6 num_samps = 10000
7 fc = 3e9
8 bw = 40e6
9 dB = 50
10
11
12 samples = 0.1*np.random.randn(10000) + 0.1j*np.random.randn(10000) # create random signal
13 duration = 14000 # seconds
14 center_freq = 3e9
15 sample_rate = 50e6
16 gain = 90 # [dB] start low then work your way up
17 usrp.send_waveform(samples, duration, center_freq, sample_rate, [0], gain)

```

### C.1.2.4 CW Interferer

```

1 import uhd
2 import numpy as np
3 import matplotlib.pyplot as plt
4
5 usrp = uhd.usrp.MultiUSRP()
6 num_samps = 10000
7 fc = 3e9
8 bw = 40e6
9 dB = 50
10
11
12 samples = 0.1*np.ones(10000) + 0.1j*np.ones(10000) # create random signal
13 duration = 14000 # seconds

```

```
14 center_freq = 3e9
15 sample_rate = 50e6
16 gain = 90 # [dB] start low then work your way up
17 usrp.send_waveform(samples, duration, center_freq, sample_rate, [0], gain)
```